UNIVERSITÀ DEGLI STUDI DI MILANO

Dipartimento di Biotecnologie Mediche e Medicina Traslazionale

Dottorato in Scienze Biochimiche – Ciclo XIXX – BIO/10

IDENTIFICATION OF THE ANTIGEN RECOGNIZED BY rHIgM22, A REMYELINATION-PROMOTING HUMAN MONOCLONAL ANTIBODY

Docente guida: Prof. Alessandro Prinetti
Direttore del corso di dottorato: Prof. Sandro Sonnino

Tesi di Dottorato di:
SARA GRASSI
Matricola n. R10417

Anno Accademico 2015/2016

Index

ABSTRACT

Oligodendrocytes (OLs) are the myelin-forming cells of the central nervous system (CNS). They synthesize large amounts of plasma membrane and extends multiple processes that individually wrap around axons generating a multilayered stack of membranes tightly attached at their cytosolic and external surfaces [1], *i.e.* myelin. The myelin membrane provides electric insulation of axons and dictates the clustering of the sodium channels at the nodes of Ranvier and the organization of the node itself, allowing saltatory nerve conduction [2, 3]. A number of neurological diseases of the CNS are characterized by destruction of oligodendrocytes with consequent damage or loss of the myelin sheath. In most experimental models, the normal response to this is remyelination, a process mediated by oligodendrocyte precursor cells (OPC) that ultimately leads to functional recovery. However in human diseases, and in specific in multiple sclerosis (MS), this process is inefficient and fails to successfully counteract the accumulation of lasting axonal damage and increasing brain atrophy, thus resulting in motor and neurological deficits [4, 5]. The development of strategies aimed to increase the efficiency of the remyelination process is therefore an important therapeutic goal. One of these strategies involves the use of CNS reactive antibodies to promote remyelination [6]. One of these antibodies, rHIgM22, is able to bind to oligodendrocytes and myelin *in vitro*. Moreover, rHIgM22 is able to enter the CNS, accumulate at lesion site and promote remyelination in mouse models of chronical demyelination [7, 8]. As a matter of fact, this antibody has recently passed a phase I clinical trial for treatment of MS.

rHIgM22 binds to CNS tissues with a pattern very similar to that of the anti-sulfatide antibody O4 [9], and binding of rHIgM22 is abolished in CNS tissue slices from CST (-/-) mice [10], suggesting that rHIgM22 binding to myelin requires the presence of a product of cerebroside sulfotransferase, possibly sulfatide. However the exact identity of the antigen recognized by this antibody remains to be elucidated. The binding of rHIgM22 to purified lipids and to lipid extracts from various sources, including wild type, ASM (-/-), CST (+/-) and CST (-/-) mice brains, mouse mixed glial cells (MGC), mouse astrocytes, rat rHIgM22^{+} oligodendrocytes (OL), rat microglia, and mouse myelin, has been tested using TLC immunostaining assays and SPR experiments with lipid monolayers with different composition.

The results obtained show that rHIgM22 binds to sulfatide, and, to a lesser extent, to lysosulfatide *in vitro*, while it does not bind to other myelin sphingolipids, including galactosylceramide and sphingomyelin, suggesting that sulfatide at the oligodendrocyte

surface might be important for the binding of rHIgM22 to the surface of these cells and to myelin. The binding affinity for both sulfatide and its deacylated derivate is low, even if the binding is specific. On the other hand, our data shows that the binding affinity of rHIgM22 for sulfatide can be modulated by the presence of other lipids suggesting a possible role of the membrane microenvironment in the recognition of the antigen by rHIgM22. In addition, rHIgM22 also reacts with phosphatidic acid, and with an unknown molecule present in lipid extracts from various sources, including CST knock-out mice brains, MGC, and isolated astrocytes and microglia. The exact identity of this antigen has yet to be confirmed but preliminary data suggests it might be a form of phosphatidylethanolamine with a free amino group and multiple hydroxylation in the fatty acid residues. Remarkably, this antigen is also present in the extracts from mixed glial cultures, which do not contain mature O4-positive oligodendrocytes, and also in isolated astrocytes and microglia suggesting that other glial cells in addition to oligodendrocytes might be important in the response to rHIgM22. All this suggests that not only sulfatide, but also other membrane lipids might play a role in the binding of rHIgM22 to oligodendrocytes and other cell types. Moreover, binding of rHIgM22 to intact cells might require a complex molecular arrangement, and, in particular, sulfatide might be part of the functional rHIgM22 antigen localized at the cell surface.

INTRODUCTION

Glycosphingolipids

Overview

Eukaryotic cell membranes, whose basic role is that of a physical barrier between the extracellular milieu and the intracellular environment, are composed of a lipid bilayer. It is known that, in eukaryotic cells, there are three major classes of lipids: sterols, glycerolipids, and sphingolipids. All these classes have biochemical and biophysical properties that vary considerably and impact upon their function [11]. An accurate regulation of their composition is crucial for proper growth, division, and responses to environmental stimuli leading to a correct maintenance of the cellular homeostasis [12].
The most abundant lipids in eukaryotic cell membranes are by far glycerophospholipids, a family of amphipathic molecules distributed asymmetrically across the plasma membrane. They do not only constitute the backbone of cellular membranes, but also provide the membrane with a suitable environment, fluidity, and ion permeability [13]. In neural membranes, it is possible to find three major classes of glycerophospholipids. These three, 1,2-diacyl glycerophospholipid, 1-alk-1-enyl-2-acyl glycerophospholipid or plasmalogen, and 1-alkyl-2-acyl glycerophospholipids, all have a glycerol backbone with a fatty acid, and a phosphobase (ethanolamine, inositol, choline, serine) [14].
The most enriched glycerophospholipids in mammal tissues are phosphatidylethanolamine (PE) phosphatidylcholine (PC), phosphatidylserine (PS), and phosphatidylinositol (PI; PtdIns). Phosphatidic acid (PA; PtdOH) is also present in all cell membranes and has a role as precursor of all neural membrane glycerophospholipids. PA also acts as an intracellular second messenger regulating different signaling proteins [15, 16], including kinases, phosphatases, and also the transcription factor mTOR. Phosphatidic acid however is not the only glycerophospholipid able to act as a second messenger. For example, diacylglycerol (DAG), arachidonic acid, and phosphoinositides have also been implicated as messengers for Ca^{2+} homeostasis and protein phosphorylation [17-19].
Sphingolipids (SLs), first identified in the 19th century as major constituents of brain tissue by J. L. W. Thudichum [20], are minor amphipathic cell components, mainly residing in the outer layer of the plasma membrane with their hydrophilic head group facing out toward the extracellular milieu [21, 22]. They are universal components of eukaryotic cell membranes and are involved in various and important biological

functions [23]. Ceramide, the simplest sphingolipid, is the backbone of all complex sphingolipids which are characterized by the presence of a charged group linked to the hydroxylated group in position 1 of the sphingoid base [24], the most common base being sphingosine (2S,3R-D-erythro-2-amino-1,3-dihydroxy-octadec-4-ene), linked to a fatty acid through an amide bond. Homologous lipids with a different length of the carbon chain or with a saturated chain, sphinganine or 4-hydroxy-sphinganine, are present in cells in minor amount [25]. The polar head group, which defines the sphingolipid class, is a phosphate group in ceramide-1-phosphate, phosphorylcholine in sphingomyelin, monosaccharides in cerebrosides, and one or more sugar residues linked with a β-glycosidic bond in complex glycosphingolipids. The latter, are the most structurally diverse class of complex sphingolipids, and are normally classified as acidic, neutral or basic [11, 26]. They are ubiquitous components of mammalian cell membranes, but are particularly abundant in the nervous system where they are not merely structural components of the membranes, but also play other essential roles, especially in signaling. Of the simple SLs, ceramide, ceramide-1-phosphate, sphingosine and sphingosine-1-phosphate have been shown to be involved in several cellular events, like proliferation, motility, growth, differentiation, and apoptosis. Complex glycosphingolipids (GSLs) are involved in cell physiology by acting as antigens, mediators of cell adhesion, binding agents for growth factors, and as modulators of signal transduction [11]. Gangliosides, sialic acid-containing GSLs, have been shown to be involved in the development, differentiation, and function of nervous system in vertebrates [27]. Galactosylceramide (GalCer) and sulfatide, instead, are involved in the formation and maintenance of a myelin with a correct structure [28, 29], and deeply affect the survival, proliferation and differentiation of oligodendrocytes [30, 31].

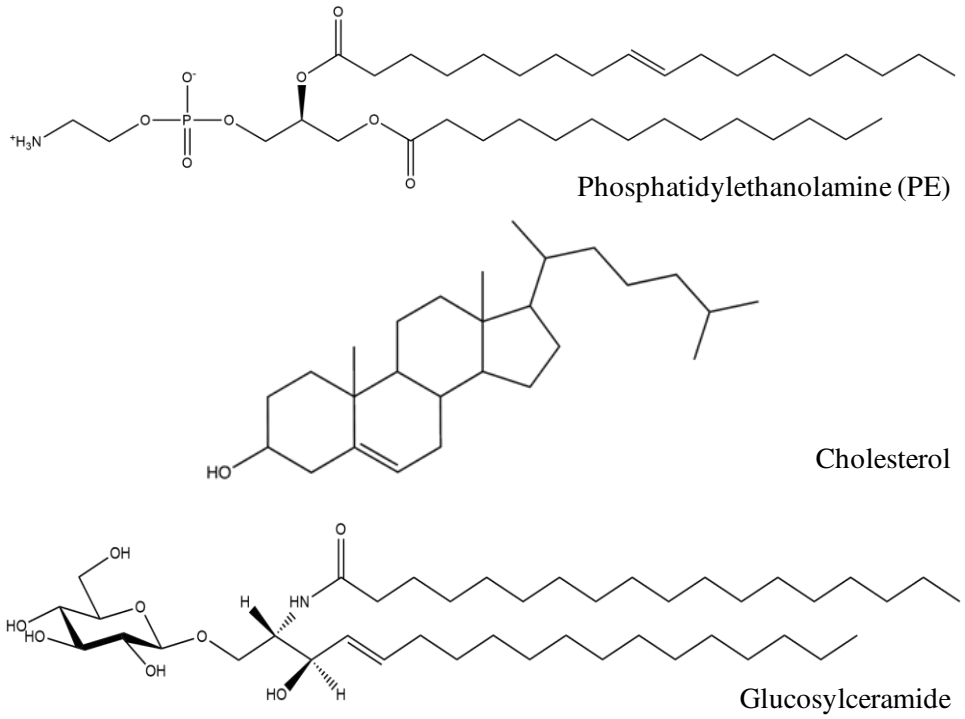

Figure 1. Representatives of the major lipid classes of eukaryotic cell membranes.

Glycosphingolipids biosynthesis, trafficking and degradation

Over the past few decades, the biochemical pathways of glycosphingolipids metabolism and the intracellular sites of synthesis and degradation, respectively in the endoplasmic reticulum/Golgi apparatus and lysosomes, have been extensively characterized [32, 33]. Glycosphingolipids synthesis is set in motion by a sequence of three enzyme-catalyzed reactions that, at the cytosolic leaflet of the membranes of the endoplasmic reticulum (ER), lead to the formation of ceramide starting from L-Serine and palmitoyl-CoA [21]. Ceramide acts as precursor of at least five different products, namely ceramide-1-phosphate, sphingosine, sphingomyelin (SM), glucosylceramide (GlcCer), and galactosylceramide (GalCer). After its synthesis, ceramide equilibrates to the luminal side of the ER where the ceramide galactosyltransferase (CGT) can convert it into galactosylceramide (GalCer), through the transfer of galactose from a UDP-galactose donor [34, 35]. GalCer then traffics through the Golgi apparatus where it can be sulfated or glycosylated [36, 37]. Ceramide is also transported from the ER to the Golgi complex via two alternative pathways. Ceramides with relatively short acyl chain length (C16-C20) can be delivered by the ceramide transfer protein CERT to the *trans*-Golgi network where, after translocation across the membrane bilayer, it is used for the synthesis of SM, by transfer of phosphorylcholine from phosphatidylcholine to

ceramide [38-40]. Alternatively, ceramide is transported from the ER to the cytosolic side of the *cis*-Golgi apparatus membrane through a CERT-independent mechanism [41, 42]. There, the glucosylceramide synthase, a transmembrane glycosyl transferase, catalyzes the glycosylation of the primary hydroxyl group in ceramide using UDP-glucose as a donor [43]. After its synthesis, GlcCer can either be transported across the Golgi complex via vescicular trafficking [44], or it can be picked up by the lipid transport protein FAPP2, which mediates the non-vescicular transport of GlcCer to the distal Golgi compartments [45, 46]. GalCer and GlcCer are precursors of the hundreds of known glycosphingolipids, which are formed via sequential transfer of sugars by galactosyltransferases, sialyltransferases, GalNAc transferases and GalCer sulfotransferases, all located in the Golgi apparatus [11, 47]. After GlcCer flips into the Golgi lumen, the addition of the next sugar residue leads to the formation of lactosylceramide (LacCer) that, once produced, cannot be translocated back to the cytosolic leaflet [44]. The final orientation of GSLs during their biosynthesis is consistent with their nearly exclusive appearance on the outer leaflet of the plasma membrane. While ceramide resides on intracellular organelles such as mitochondria, glycosphingolipids beyond GlcCer are not known to exist on membranes facing the cytoplasm [48, 49]. The biosynthesis of glycosphingolipids in the brain provides an example of how competing biosynthetic pathways can lead to glycan structural diversity [48]. Stepwise biosynthesis of GalCer and sulfatide occurs, in the brain, in oligodendrocytes, the myelinating cells of the central nervous system (CNS). Synthesis of GalCer and sulfatide, in the brain, is switched on at the onset of the terminal differentiation, and remains constant in mature oligodendrocytes [50]. Moreover, in rat brain, their synthesis is maximal at the developmental stage of most rapid myelination [51]. All this suggests that GalCer and sulfatide might represent not only structural components of the myelin sheath but also active players in myelin formation and maintenance [36]. Gangliosides, in contrast, are synthesized by all cells, with concentration of the different forms varying according to cell type. It is well known that during brain development there are marked changes in expression of glycoconjugates ranging from complex proteoglycans to gangliosides. The expression pattern shifts from simple gangliosides, like GM3 and GD3, to complex gangliosides, such as GM1, GD1a, GD1b, and GT1b, and this shift is mainly regulated by the differential expression and intracellular distribution of the enzymes required for the biosynthesis of these glycosphingolipids [52, 53]. Moreover, multiple glycosyltransferases can compete for

the same precursor. LacCer, for example, can act as a substrate for sialyltransferase I, which forms GM3, or for GalNAc transferase, which forms GA2 [54]. GM3, in turn, can be acted on by N-acetylgalactosaminyltransferase, forming GM2, or by sialyltransferase II, thereby forming GD3, the simplest “b-series” ganglioside [55, 56]. Due to the branch exclusivity, since sialyltransferases cannot convert a-series gangliosides to their b-series correspondent, the relative expression level of the final GSL products is determined by enzyme competition at each branch. The transfer of *N*-acetylgalactosamine to a-, b-, and c-series gangliosides, converting GM3 into GM2, GD3 into GD2, or GT3 into GT2, is catalyzed by the same N-acetylgalactosaminyltransferase. Likewise, the transfer of galactose to GM2 to form GM1, to GD2 to from GD1b, or to GT2 to form GT1c is accomplished by a single galactosyltransferase [57]. An additional level of regulation may occur via stable association of different glycosphingolipid glycosyltransferases into functional “multiglycosyltransferase” complexes. The enzymes involved are thought to act concertedly on the growing glycosphingolipid without releasing intermediate structures, ensuring progression to the preferred end product [58].

While sphingolipid synthesis occurs in membranes of the secretory pathway, their catabolism occurs predominantly in endosomes and lysosomes. After internalization, GSL-rich membrane portions fuse with early endosomes, where the GSLs destined for degradation are sorted through the formation of multivescicular bodies which reach the lysosomes. Following the fusion, glycosphingolipids are exposed to lysosomal hydrolases and, *in vivo*, they are eventually broken down to their individual components, which are available for reuse [59, 60].

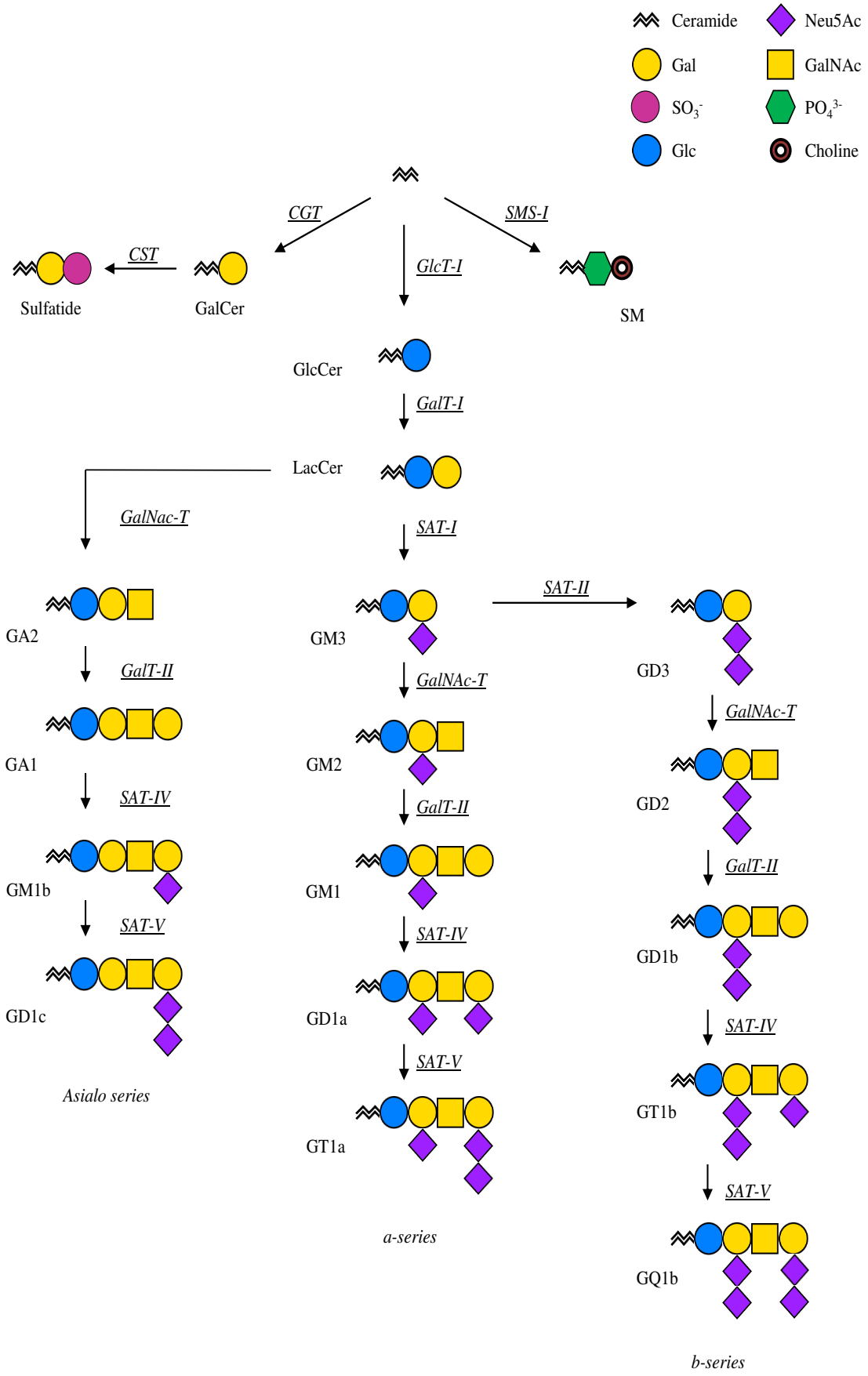

Figure 2. Schematic biosynthetic pathway of glycosphingolipids.

Biological functions glycosphingolipids

Studies on the role of glycosphingolipids using genetic, biophysical, biochemical and cell biology approaches led to establish that GSLs are essential for the proliferation, survival, and differentiation of eukaryotic cells within complex multicellular systems. Various studies involving the analysis of genetically engineered mice provided a general framework for the understanding of the roles of glycosphingolipids in mammals and their vital importance in the life of cells that are dealing with a multifaceted extracellular reality. These studies revealed that ablation of either GlcCer synthase or of B4GALT-V, responsible for the synthesis of LacCer, leads to embryonic lethality [61, 62]. Moreover, mice lacking all ganglioside, as a result of the knockout of both GalNAcT and SAT-I genes, suffer severe lethality. These mice show enhanced cell apoptosis, perturbed axon-glia interactions and axonal degeneration [63], though, it still remains to be elucidated whether these phenotypes are the result of a functional deficiency or a consequence of the accumulation of substrate precursors.

Glycosphingolipids are not randomly distributed along the membrane surface; moreover, they are highly segregated, together with cholesterol, in lipid domains with specialized signaling functions [64]. Within the cell, they are highly asymmetrically enriched in the external leaflet of plasma membranes, with the oligosaccharide chain protruding toward the extracellular space, where the sugar residues can engage *cis* and *trans* interactions with a wide variety of cell surface and extracellular molecules [65]. The local concentration of GSLs in the membrane affects these interactions. Direct lateral interactions (*cis* interactions) with plasma membrane proteins are strongly favored within a sphingolipid-enriched membrane domain [66], whereas in the case of *trans* interactions, it has been shown that recognition of lipid-bound oligosaccharides by soluble ligands (for example antibodies or toxins) or by complementary carbohydrates and by carbohydrate binding proteins (such as selectins or lectins) belonging to the interfacing membrane of adjacent cells is strongly affected by their degree of segregation (or dispersion) [67].

This variety of interactions is reflected in the variety of roles of glycosphingolipids. GSLs, for example, act as receptors for bacteria and viruses. As a matter of fact, GM1 acts as a receptor for cholera toxin B subunit [68, 69], Gb3 acts as a receptor for verotoxins [70, 71], whereas two of the surface proteins of influenza virus are aimed against the terminal Neu5Ac group on glycosphingolipids and glycoproteins of the

human host [72]. Some pieces of evidence also suggest a receptor role for glycosphingolipids in HIV infections. The HIV adhesin gp120, in fact, binds to several GSLs, including GalCer, sulfatide [73, 74], GM3, GD3 and also Gb3 [75, 76].

Glycosphingolipids also have a role in the modulation of the immune response. For example, the interdigitation of the acyl chains of long chain LacCer with the cytosolic leaflet of the bilayer, leading to Lyn kinase activation, has been strongly implicated in ligand activation of human neutrophils phagocytosis [77]. Moreover, LacCer has also been found to play a role in the induction of proinflammatory cytokines in both glial cells and neutrophils [78, 79], while gangliosides play a role in the modulation of the cytotoxicity of natural killer cells [80].

Glycosphingolipids are also known to interact with growth factor receptors, to modulate cell growth, and, in many cases, to inhibit receptor-associated tyrosine kinases. An example of this is the interaction of ganglioside GM3 with the insulin receptor (IR). Accumulation of GM3 upon acquisition of insulin resistance leads not only to the displacement of IR from caveolin-1 complexes, required for insulin signaling leading to the translocation of GLUT4 at the surface of normal adipocytes [81], but also to its sequestration in a complex with GM3 [82]. Another example is the epidermal growth factor receptor (EGFR) interaction with GM3. GM3 negatively regulates ligand-stimulated autophosphorylation and dimerization of EGFR [83-85], and cross-talk of EGFR with integrin receptors [86] and PKCα [87], inhibiting EGFR-dependent cell proliferation and survival.

Glycosphingolipids also play important roles in modulating several properties of tumor cells. Most tumor cells show altered glycosphingolipid patterns on their surface as well as abnormal sphingolipid signaling and increased glycosphingolipid biosynthesis, which together play a major role in tumor growth, angiogenesis, and metastasis [88, 89].

Glycosphingolipids are also known to play a role in the regulation of axonal growth. For example, gangliosides GD1a and GT1b, enriched in axonal rafts, act as MAG receptors in MAG-induced inhibition of axonal growth [90, 91].

Glial cells in the central nervous system

Glial cells, neuroglia, or simply glia, in the mammalian adult central nervous system (CNS), comprise astrocytes, oligodendrocytes, and microglia. These cells, together, are by far the most abundant cells in the nervous system, comprising about 60-90% of all cells in the human brain [92, 93]. Rudolf Virchow, in 1856, named these cells glia, from the Greek word meaning glue, reflecting his view that these cells had the function to hold together the nervous system and, for a long time, they were thought only to support neurons passively. However, in the past few decades, evidence has shown that glia function as master regulators of the nervous system, providing valuable support in synaptic plasticity, axonal function, and acting as integral mediators of neuronal connectivity. Moreover, in addition to development and aging, these cells also play important roles in repair and remyelination in CNS disease [94-98].

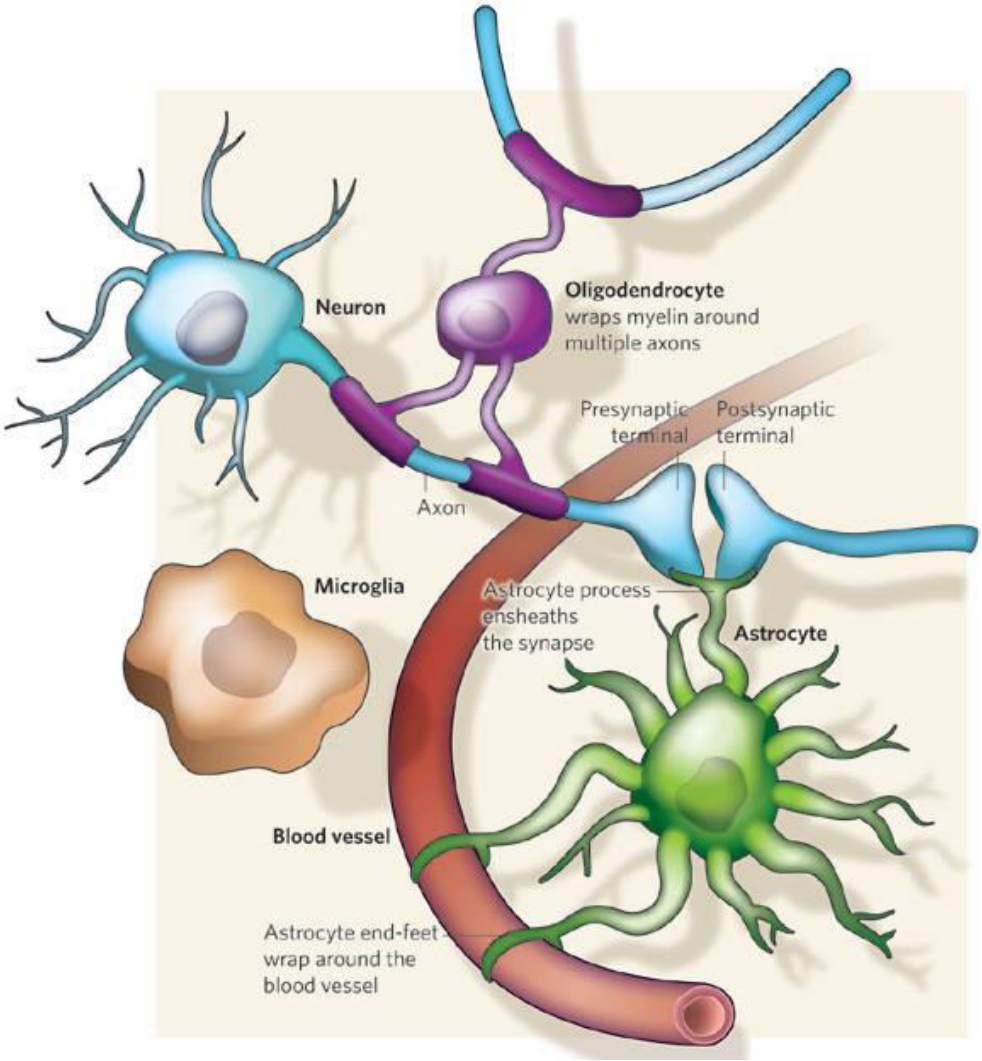

Figure 3. The major types of glia interacting with a neuron.
Adapted from Allen and Barres 2009 [92].

Oligodendrocytes

Oligodendrocytes (OLs) are the myelinating cells of the CNS, and they are the last major neural phenotype to form during development. They arise from oligodendrocytes progenitor cells (OPCs), which can form either oligodendrocytes or astrocytes depending on the context [99, 100]. Once an OPC is committed to an oligodendroglial fate, it synthesizes large amounts of plasma membrane and extends multiple processes that individually wrap around axons generating a multilayered stack of membranes tightly attached at their cytosolic and external surfaces [1]. The thus formed myelin membrane provides electric insulation of axons and dictates the clustering of the sodium channels at the nodes of Ranvier and the organization of the node itself, allowing saltatory nerve conduction [2, 3]. In addition to these contributions to neuronal signaling, OLs also provide trophic support to neurons, and to long axons that may not receive adequate support from intra-axonal trafficking alone [97]. As such, oligodendrocytes are essential not only for the maintenance of neural transmission, but also of neurons themselves.

Oligodendrocytes originate from neuroectodermal cells within the subventricular zone and, to be able to produce myelin, they go through highly regulated differentiation steps, that can be defined according to their migratory capacity, the increase in morphological complexity and the expression of specific markers, several of which are glycosphingolipids [101].

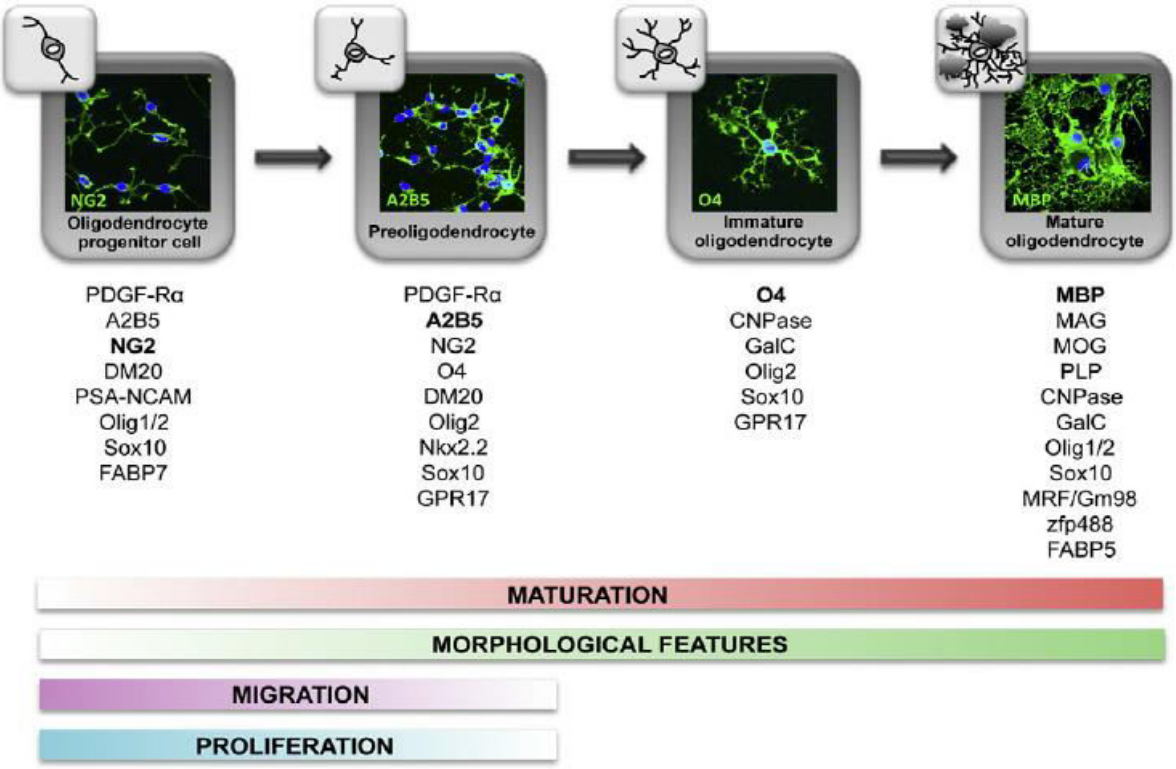

Figure 4. Oligodendrocyte maturation toward oligodendroglial lineage.
Each stage is identifiable according to the increasing complexity in morphology, the ability to proliferate, migrate and differentiate, and the expression of specific antigens. *Adapted from Barateiro et al, 2014 [101].*

During the main phase of myelination, oligodendrocytes generate about 5,000-50,000 μm^2 of myelin surface area per cell per day [102], and this is accomplished by a remarkable synthesis and transport of myelin lipids. Moreover, by the time myelination is completed, oligodendrocytes have synthesized about 40% of the total lipids in the human brain [103]. The myelin membrane has a unique composition, characterized by an high lipid content, ranging between 73 and 81% of its total dry weight [104]. Moreover, studies have shown that the ratio of protein to lipid is around 1 to 186 [105]. All the major lipid classes are found in myelin, like in other membranes, however myelin still has a remarkably characteristic composition. In fact, while in most cell membranes the molar ratio of cholesterol, phospholipids and glycosphingolipids is 25:65:10, these ratios in myelin are in the range of 40:40:20 [106] which allows the close packing and tight organization of molecules within the membrane.

The myelin membrane has a high level of cholesterol, at least 26% by weight [104, 107, 108], which, in contrast with other cell types, is synthesized using mainly ketone bodies as precursors instead of glucose [109]. The high level of cholesterol not only is necessary for myelin growth and compaction, but also provides stability to this

membrane through the regulation of fluidity and permeability [108, 110]. Cholesterol is also necessary for correct myelin assembly, and the supply/synthesis of this molecule dictates this process, suggesting that upstream signaling systems which drive myelin biogenesis could be coupled to cholesterol metabolism [110].

The myelin membrane also has a high amount of ethanolamine plasmalogens, whose levels correlate with the degree of myelination and reach the highest point between 30 and 40 years of age, when myelination is complete [111, 112]. The structural features of these ethanolamine plasmalogens, like the perpendicular orientation of the *sn*-2 acyl chain instead of the bent orientation it has in phosphatidylethanolamine, favors a closer alignment of both acyl chains in plasmalogens, thus decreasing the fluidity of the membrane. Moreover, the absence of a carbonyl oxygen at the *sn*-1 position determines an increased hydrophilicity, resulting in stronger intermolecular hydrogen bonding between the head groups [113, 114]. Considering this, one of the function of the high level of plasmalogens in myelin could be to increase the packing density and with it the stability of the membrane. There is also evidence suggesting that plasmalogens could have a role in protecting unsaturated membrane lipids against oxidation by singlet oxygen [115] and in providing lipid mediators for inflammatory reactions [116].

Gangliosides, brain-enriched sialic acid-containing glycosphingolipids, increase not only in amounts but also in complexity as the brain develops [53]. The most prominent shift in gangliosides levels occurs in the late stages of fetal development and extends into the first two years of human development, a period that coincides with the most active phase of myelination, and, while only small amounts of gangliosides are present in myelin (~1% of total lipids), they represent a major fraction of the neuronal membrane [111]. It is known that gangliosides are able to interact with several growth factor tyrosine kinase receptors, thus regulating their activity [117]. For example, GM3 binding to EGFR determines the inhibition of the receptor tyrosine kinase activity [83-85], and several gangliosides inhibit the dimerization of PDGFR [118]. In addition, FGF-2 is able to interact with several gangliosides [119]. Specific gangliosides in the local environment could therefore modulate the activity of receptors such as PDGFR and FGFR, which are known to influence proliferation and differentiation of oligodendrocyte progenitors [102, 120]. Moreover, there is evidence that the addition of GM3, but not of other GM or GD gangliosides, determines an enhanced differentiation of OLs in culture [121]. Furthermore, two of the major axonal gangliosides, GD1a and GT1b, are involved in long term myelin stability via their *trans* interaction with the

myelin-associated glycoprotein (MAG), leading to MAG-induced inhibition of axon outgrowth [90, 91, 122]. Studies using mutants lacking a combination of gangliosides have further elucidated the role of gangliosides in myelination. Some mutations lead to the development of a severe phenotype, others do not affect myelination. For example, GD3 synthase null mice, lacking both b- and c-series gangliosides, do not exhibit demyelination in the brain [123]. In contrast, mice with disruption of the GM2/GD2 synthase gene exhibit axonal degeneration, increased presence of unmyelinated, redundant myelin loops, disrupted paranodal junctions, and dysfunction of ion channels coupled with their erroneous localization [107, 124]. Taken together, these studies suggest a role of gangliosides in axon-glial interaction.

Another distinguishing feature of myelin lipid composition, perhaps the most striking, is the enrichment in galactolipids. Galactosylceramide and 3-*O*-sulfogalactosylceramide (sulfatide), with long chain fatty acids, account for approximately 20% and 5% of myelin lipids respectively [30, 125]. Their biosynthesis involves two sequential steps. The enzyme UDP-galactose:ceramide galactosyltransferase (CGT), localized in the luminal side of the ER, catalyzes the transfer of a galactose from UDP-galactose to ceramide, thus forming GalCer [35]. A subpopulation of GalCer is then transported to the Golgi apparatus where the 3'-phosphoadenosine-5'-phosphosulfate:cerebroside sulfotransferase (CST) enzyme catalyzes the addition of the sulfate group, to obtain sulfatide [36, 125, 126].

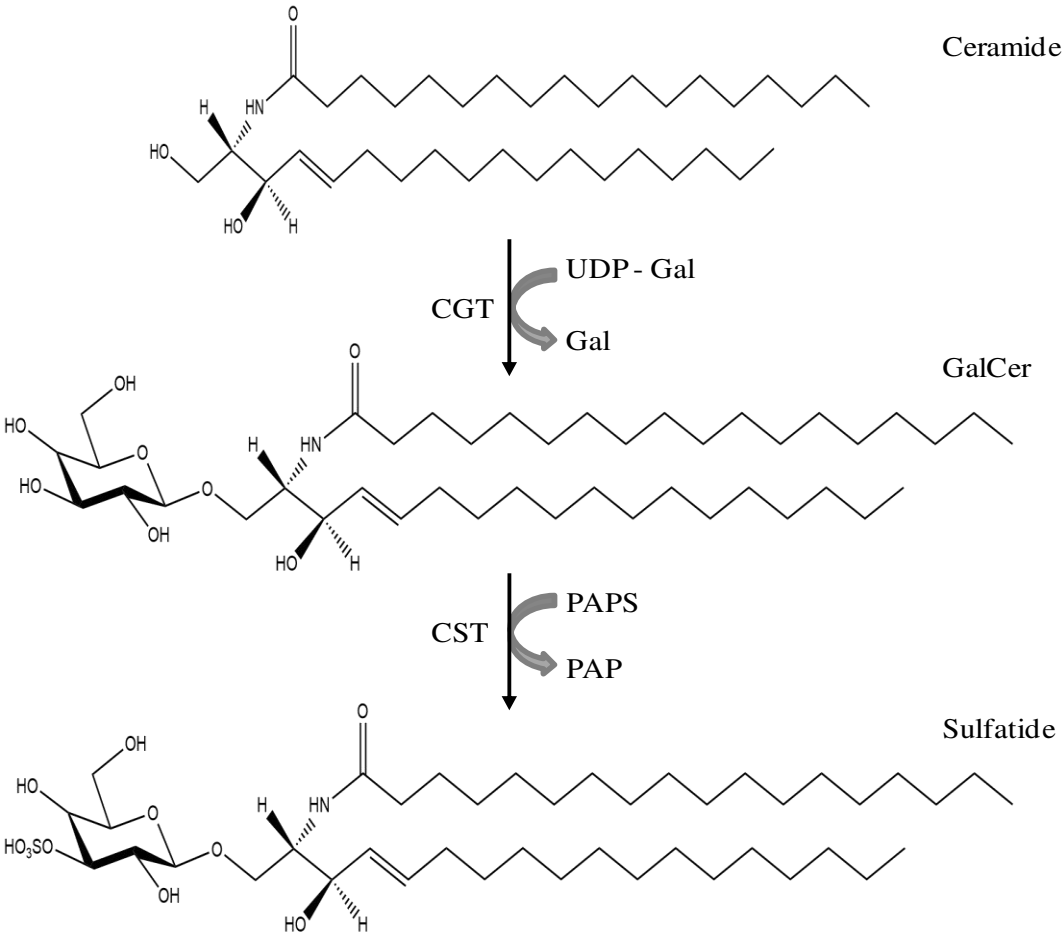

Figure 5. Structure and biosynthetic pathway of sulfatide, the major sulfoglycolipid in the nervous system.
3-O-sulfogalactosylceramide is highly heterogeneous in its fatty acid composition. The main fatty acids found in mature CNS myelin are long chain fatty acids (24:0 and 24:1), including a significant amount of 2-hydroxylated fatty acids. Sulfatide synthesis requires the addition of galactose from UDP-galactose (UDP-Gal) to ceramide, catalyzed by the UDP-galactose:ceramide galactosyltransferase (CGT, EC 2.4.1.45, encoded by the ugt8 gene), and the subsequent addition of the sulfate group by the enzyme 3'-phosphoadenosine-5'-phosphosulfate:cerebroside sulfotransferase (CST, EC 2.8.2.11, encoded by the gal3st1 gene).

Following their synthesis, both lipids are transported to the outer leaflet of the plasma membrane [107], and, although they are not myelin-specific lipids, their enrichment in myelin, which is common feature of both CNS and peripheral nervous system (PNS) across species, is much higher than in any other tissue [36]. The abundance of galactosylceramide and sulfatide has led to the hypothesis that they could be involved in myelin formation and stabilization, and in oligodendrocyte development [29]. Therefore, to gain a better understanding of the role of GalCer and sulfatide, genetically altered models have been established and analyzed. The animal models lacking the

enzymes responsible for the synthesis of GalCer and sulfatide, CGT knock-out and CST knock-out respectively, will be described in the following paragraphs.

The CGT enzyme, responsible for the synthesis of galactosylceramide, is highly expressed in the actively myelinating CNS ad PNS [127, 128]. Even though the CGT knock-out mice cannot synthesize GalCer and sulfatide, they are still able to form myelin with an apparently normal structure, which could be due to a partial compensation of the loss of these galactolipids by synthesizing 2-hydroxylated glucosylceramide, usually not present in myelin. Moreover, in the myelin of this model, the level of hydroxy-fatty acid-containing sphingomyelin (HFA-SM) is also higher, which suggests that the α-hydroxy ceramide, normally destined for HFA-GalCer production, is most likely used for the synthesis of HFA-GlcCer and HFA-SM [29]. On the other hand, the deletion of glucosylceramide synthase in oligodendrocytes from CGT (-/-) mice did not alter the severity of the myelin defects, indicating that synthesis of GlcCer and GlcCer-based glycolipids is not essential for proper myelin formation, and suggesting that the levels of HFA-GlcCer are not sufficient to functionally compensate for the loss of GalCer in the CGT (-/-) model [129]. Nevertheless, even though this compensatory mechanism is not efficient enough, the CGT knock-out mice can form apparently normal myelin with a normal major dense and intraperiod line periodicity [130]. These animals, however, display a neuropathological phenotype, characterized by splaying of the hind limbs, tremors, and ataxic locomotion that progressively worsens, leading to death of most animals by the third month of age [29, 131]. This phenotype is consistent with nerve conduction disruption despite the presence of compact myelin and, as a matter of fact, the action potential measured in the spinal cord of these mice is smaller and has a longer latency respect to wild type animals [29]. Moreover, while CGT (-/-) myelin is apparently normal, several ultrastructural abnormalities associated with myelination in the CNS have been identified. CNS myelin thickness is reduced, while nodal length is increased and lateral loops are widely spaced. The disorganization of the lateral loops suggests a disruption in the formation of the tight junctions, unsurprisingly since sulfatide is a prominent constituent of myelin tight junctions and the formation of these junctions may be dependent on the presence of sulfatide. These loops, loosely opposed to the axolemma, facilitate the entrance of cellular and non cellular material into the paranodal periaxonal space [132]. Additionally, in mutant mice, myelin sheaths also show a widespread, progressive vacuolation between the sheaths and the axolemma [29, 132]. Furthermore,

at least one-third of the myelin processes in CGT knock-out mice retains oligodendrocyte cytoplasm, indicating presence of immature myelin in regions that appear as structurally mature myelin, and profiles of compact myelin frequently show more than two oligodendrocytic loops in a single internodal segment [130, 133]. Despite the presence of all these anomalies in CNS myelin, PNS myelin appears normal suggesting that galactolipids, less abundant in the PNS, might not be as essential in the formation and maintenance of the PNS myelin sheath structure [130, 132, 134].

The CGT (-/-) model, however, does not allow discrimination between the specific functions of GalCer and sulfatide, considering that in these mice they are both absent. To overcome this limitation, thus opening the way to the understanding of the specific functions of these two glycolipids, a new model, the CST knock-out mice, was developed [135]. The CST knock-out mice are completely devoid of sulfatide, whereas other glycolipids in the brain, galactosylceramide included, are not significantly altered [136]. CST-deficient mice are born healthy but, around 6 weeks of age, they start exhibiting hind limb weakness, followed by pronounced tremor and progressive ataxia. The phenotype of these mice is in fact similar to that of CGT knock-out mice, even though it is milder in terms of age of onset, life span and severity of symptoms which allows these mice to survive for more than one year [135]. CST knock-out mice produce compact myelin, even though its thickness is reduced, compared to that of wild type mice, and paranodal structure displays alterations similar to those of the CGT (-/-) mice. Whereas in young mice the myelin sheaths are rather stable, the node/paranode structure only moderately altered, and axon size is comparable to that of wild type mice, as they age these mice show nodal structure deterioration, myelin vacuolar degeneration and also reduction of axon caliber [137]. Furthermore, electron microscopy analysis of myelinated nerve fiber revealed disorganized termination of the lateral loops at the node of Ranvier [138]. CST (-/-) mice also exhibit a deterioration in the clustering of Na^+ and K^+ channels at the node [139]. In mutant mice Na^+ channels concentrate in small regions, presumptive nodes of Ranvier, and the lengths of the clusters are occasionally higher than the ones present in the wild type mice. The K^+ channels clusters instead accumulate in regions adjacent to the Na^+ channels clusters in presumptive paranodal regions, whereas in normal CNS axons Na^+ channels cluster at the node of Ranvier and the K^+ channels concentrate in juxtaparanodal regions [139]. These alterations in localization and clustering of ion channels are present in both PNS and CNS and are accompanied by an altered distribution of axonal proteins such as Caspr, contactin and

NF155. Moreover, CST null mice show low levels of axonal paranodal Caspr and contactin, whereas paranodal NF155 is absent, even though its total cellular levels are unaltered, suggesting that sulfatide might play a role in the trafficking or stabilization of this protein at paranodal level [139-141].

The loss of GalCer and sulfatide affects the proliferation and survival rate of oligodendrocyte precursors. CGT knock-out mice show a significant increase in cellularity in the spinal cord [134], while CST (-/-) mice exhibit an increased number of oligodendrocytes, which mature earlier and in higher number [142]. In CGT (-/-) mice this increase seems to be due to an increased terminal differentiation [142], and this is supported by experiments showing that perturbation, either immunological or chemical, of GalCer and sulfatide leads to a dramatically altered maturation process in myelin forming cells [132]. This is in contrast with the observation that in CST (-/-) mice the increase in oligodendrocyte population seems to be determined by an increased proliferation and by a reduced apoptosis [143]. Interestingly, in CST null optic nerves the increase in cell numbers involves mostly mature oligodendrocytes, whereas astrocytes and microglia show no significant variation. In wild type mice the number of oligodendrocytes is strictly regulated by axons during development, and in fact the number of myelinating cells that survive seems to be precisely matched to the number and length of axons requiring myelination. In young CST knock-out mice, oligodendrocytes have fewer processes indicating that axons might need a greater number of oligodendrocytes to compensate for the fewer processes. However, it is still unknown if the same is true for adult CST null oligodendrocytes [144]. Taken together, the discrepancy in phenotype between CST- and CGT-null mice suggests that GalCer does not only act as a precursor for sulfatide synthesis, but also has a distinct function. GalCer appears to be primarily involved in myelin formation and maturation, while sulfatide contributes to the long term stability of myelin structure, in particular affecting the integrity and stability of the nodal and paranodal regions.

GalCer and sulfatide, or more precisely, GalCer- and sulfatide-rich domains in the oligodendrocyte membrane also regulate the co-clustering and lateral distribution of several myelin proteins, thus affecting the proliferation, differentiation and survival of oligodendrocytes [31]. In the early stages of myelin formation, only a few typical myelin proteins are associated with lipid rafts. However, by the mid-myelination stage, when GalCer and sulfatide are synthesized at detectable levels, the myelin/oligodendrocyte glycoprotein (MOG) and the proteolipid protein (PLP) tend to

localize in lipid rafts, and subsequently, in the final stages of myelination MAG and myelin basic protein (MBP) are also translocated into lipid rafts[145-147]. In particular, sulfatide seems to be essential for the transport of PLP to myelin membranes, which is consistent with the observation that association of PLP is reduced in CGT (-/-) mice [148]. In addition, oligosaccharide-oligosaccharide trans interactions between GalCer and sulfatide present in the extracellular surfaces of the multilayered myelin membrane form a specialized "glycosynapse" which stabilizes the myelin sheath [149-152].

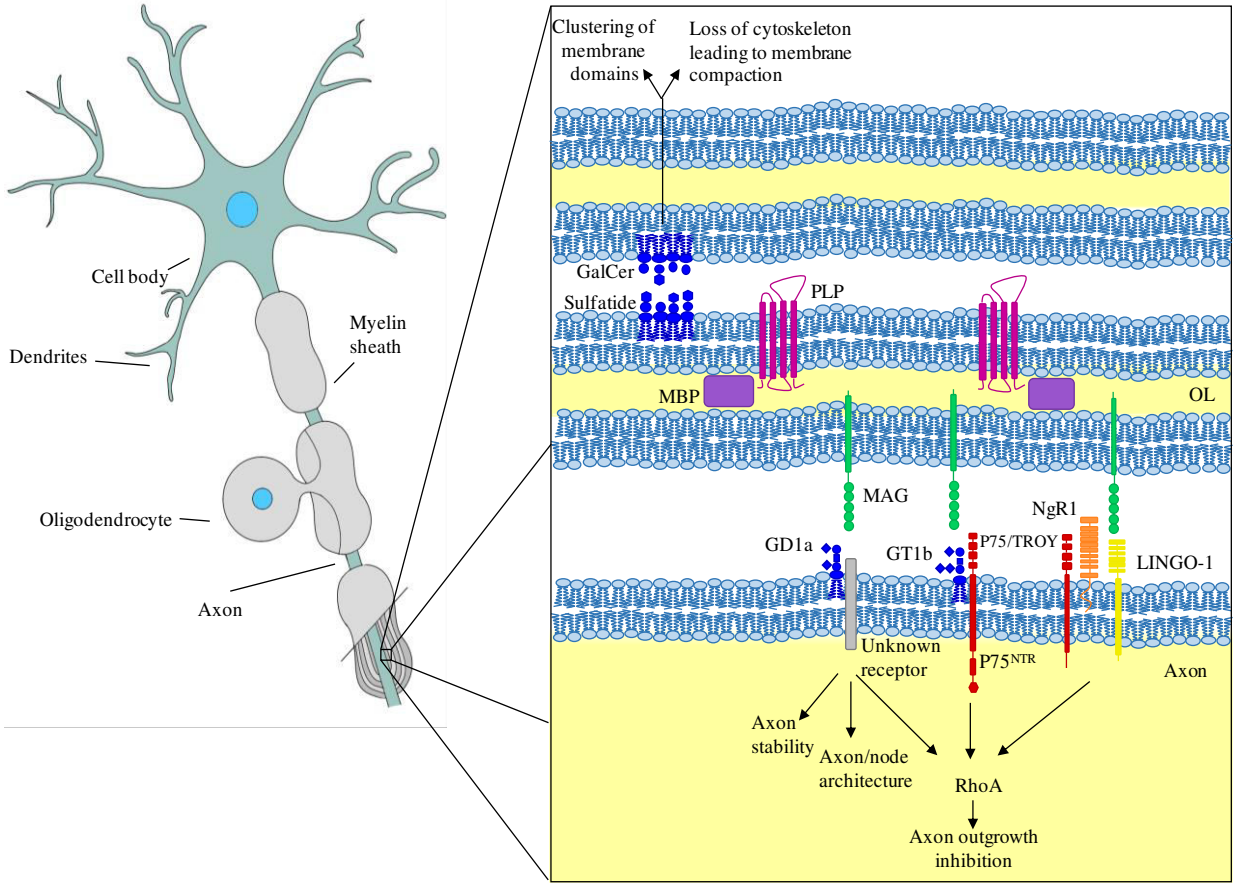

Figure 6. Glycolipid-enriched membrane domains in myelin. Glycolipid–glycolipid and glycolipid–protein interactions play multiple roles in myelin formation, maintenance and functioning but also in axon-myelin stability and communication. GalCer and sulfatide on opposing surfaces of the myelin wrap interact with each other through *trans* carbohydrate–carbohydrate interactions forming a "glycosynapse" causing transmembrane signaling which results in clustering of membrane domains and loss of cytoskeleton integrity, leading to compaction and formation of mature myelin. On the other hand, GD1a and GT1b gangliosides, enriched in axonal lipid rafts, interact with MAG resulting in transmembrane signaling. MAG can also interact with Nogo-R1 (NgR1) which in turn interacts with signaling molecules p75/TROY and LINGO-1, leading to RhoA activation and axon outgrowth inhibition. Lateral interaction of GD1a and GT1b with p75 is important for the organization of NgR1 complex. *Adapted from Aureli et al, 2015 [153].*

Astrocytes

Astrocytes, or astroglia, are the most abundant and heterogeneous glial population in the central nervous system. In fact they outnumber neurons by over five fold [154]. Astrocytes have a plethora of functions, comprising roles as regulators of CNS homeostasis, through control of ion, pH, and neurotransmitter metabolism, and roles in the development and maintenance of the BBB, and in synaptogenesis and myelination [155, 156]. They originate from the neural embryonic progenitor cells that line the lumen of embryonic neural tube, although they can also be formed indirectly via radial glia [157]. Though the heterogeneity of these cells is quite complex, the classification by Cajal, based on morphological differences, is still in use. Based on this classification, two main subtypes of astrocytes exist. Type 1 astrocytes, also named protoplasmic astrocytes, are localized in the gray matter where they ensheath blood vessels and synapses to promote blood brain barrier (BBB) and synapses functions [94]. Type 2 astrocytes, defined fibrous astrocytes, are found in the white matter and have small cell bodies and processes aligned with myelinated fibers, which gives them an elongated morphology. They also contact the nodes of Ranvier and the blood vessels [94,155, 158]. In addition to this, other morphologically distinct populations of astrocytes have been described [159]. Moreover, astrocytes can also be diverse in their ability, ranging from inactive (quiescent), which exist in the normal resting CNS, to active (reactive). Astrocytes become activated in response to all form of CNS insults (infection, trauma, ischemia, etc.) through a process defined as reactive astrogliosis [160].

Recent evidence suggests a correlation between astroglial differentiation, during fetal cortical development, and lipid rafts, in particular phosphatidylglucoside-enriched lipid rafts (PGLRs). Phosphatidylglucoside (PtdGlc) is a glycoglycerolipid localized in the outer leaflet of the plasma membrane of several mammalian cell types, in particular in the brain, where it is highly expressed in the two neurogenic regions of the adult brain [161]. Its localization in the external leaflet of the membrane and its fatty acid composition, consisting solely of saturated fatty acyl chains, $C_{18:0}$ at *sn*-1 and $C_{20:0}$ at *sn*-2 of the glycerol backbone, favor its segregation into PtdGlc enriched lipid rafts [162, 163]. PGLRs are enriched in cells of astroglial lineage in developing mouse CNS [164] and they are potentially involved in astrogliogenesis, by physiologically coupling to EGFRs during late-embryonic stages of development. In fact, evidence shows that in multipotent neural progenitor cells treatment with DIM21, a mouse monoclonal that

recognizes preferentially PtdGlc, induced rapid recruitment and activation of EGFRs followed by the enhanced expression of the astrocyte marker GFAP (glial fibrillary acidic protein) [165].

Lipid rafts are also involved in the astrocytic inflammatory signaling. Recent evidence suggests a role of DJ-1 in the regulation of the inflammatory response to lipopolysaccharide (LPS) by modulating the lipid raft-dependent LPS/TLR4 pathway [166]. DJ-1 is a ubiquitous protein, highly expressed in both brain and peripheral tissues, that was initially described as an oncogene and whose mutations are associated with autosomal recessive forms and some sporadic cases of Parkinson disease [167]. Recent evidence suggests that DJ-1 is a multifunctional protein that has potent antioxidant properties and protects neurons against oxidative stress-induced cell injury [168]. Moreover, alterations in the expression levels of DJ-1 have been observed in various neurodegenerative diseases, including sporadic Parkinson disease, amyotrophic lateral sclerosis (ALS), and Alzheimer disease [169, 170]. Furthermore, recent findings suggest a role of DJ-1 in the pathogenesis of multiple sclerosis (MS), as DJ-1 mRNA and protein expression is enhanced in brain tissue of animal suffering from experimental autoimmune encephalomyelitis (EAE), a validated animal model for MS [168]. DJ-1, in the brain, is expressed in glial cells and neurons. Moreover, its expression is higher in astrocytes, where it associates with lipid rafts through palmitoylation, than in neurons [166]. LPS treatment and serum treatment of astrocytes increases DJ-1 association with lipid rafts, and, in turn, raft-associated DJ-1 seems to be able to regulate LPS signaling through the control of TLR4 endocytosis. As a matter of fact, in DJ-1 knock-out astrocytes, TLR4 is retained on the plasma membrane following LPS stimulation, leading to an enhanced LPS/TLR4 signaling suggesting a role of DJ-1 in the regulation of the LPS/TLR4 pathway [166].

In addition to roles of lipid rafts on the astrocytic inflammatory signaling, it has been shown that lipid rafts are involved in the signaling leading to ganglioside-induced astrocyte death [171] and in homeostatic roles of astrocytes such as glutamate clearance through EAAT2 modulation [172], and potassium buffering through the modulation of Kir4.1 [173].

Microglia

Microglial cells are widely regarded as the resident immune cells of the brain, constantly scanning through the microenvironment with their long protrusions, readily sensing alterations in tissue homeostasis and integrity [174]. These cells, representing around 10% of the total glial cells in the nervous tissue, are present ubiquitously in the CNS, even though they are more enriched in the grey matter than in the white matter [175]. Under non-pathological conditions, microglia cells are highly ramified. In the diseased brain however their morphology changes, becoming more amoeboid. Upon activation, microglia progressively changes aspect, increasing the size of the cell body, retracting protrusions, and expressing *de novo* or up-regulating distinct profiles of surface phenotypic antigens, leading to an increased motility and to the adoption of immune effectors functions. Moreover, reactive microglia produces pro-inflammatory mediators including nitric oxide, reactive oxygen species (ROS), tumor necrosis factor α (TNFα) and a wide variety of other inflammatory cytokines [176]. Under pathological conditions, microglial functions depend on the stimuli that led to their activation; moderate CNS damage elicits protection by microglia [177-179], while following an intensive acute activation (for example stroke) or chronic activation (typical of neurodegenerative diseases) these cells tend to become neurotoxic, thus impairing neuronal activity [180-182].

The morphology and functions of microglia are highly affected by lipids, and changes in the composition of lipid rafts can lead to a decrease in the release of microparticles, which in turn leads to altered cell-cell communications [183]. Moreover, there is evidence showing that high levels of cholesterol increase the expression of pro-inflammatory genes in microglia [184], while polyunsaturated fatty acids seem to have an anti inflammatory effect on these cells [185]. Sulfatide is also able to induce a rapid activation of microglia. As a matter of fact, sulfatide released at brain lesions sites, following myelin damage, determines not only an increase in the activation of intracellular signaling pathways, including MAPKs and inflammation-associated transcription factors, but also an increase in the production of inflammatory cytokines and chemokines [186].

Lipid rafts, in these cells, are involved in several processes. For example, it has been shown that in microglial cells lipid rafts are involved in lysophosphatidylcholine (LysoPC) induction of ROS production, which leads to caspase-1 activation and to the

subsequent IL-1β processing. They are also involved in the internalization of α-synuclein (α-syn), a key player in the pathogenesis of Parkinson's disease (PD), through the interaction between ganglioside GM1, an unknown receptor, and the α-syn protein [187]. Moreover, caveolins, membrane adaptor proteins associated with lipid rafts, have been identified as structural and metabolic regulators of microglia. In particular, it has been observed that the switch between a resting phenotype and an immunoinflammatory one is associated with a switch in the caveolin isoform expression. When cells are in the inactive state, Caveolin-1 (Cav-1) levels are low and the protein is localized in cytoplasmic vescicles and at plasma membrane level. Caveolin-3 (Cav-3) instead is highly expressed and localizes in cellular processes and perinuclear regions. Upon microglia activation, concomitantly with the changes in cell morphology, Cav-3 expression lowers, whereas Cav-1 expression increases. Cav-1 in these cells enhances mitochondrial function and acts as a negative regulator of microtubule stability, and, since lipid raft marker flotillin-1 levels increase alongside Cav-1 levels, it has been hypothesized that lipid rafts might be involved in the regulation of the morphology changes associated with the inactive-active state transition [188].

In addition to contributing to the maintenance of the normal CNS functions and to their role as sensors of altered homeostatic conditions, microglia also regulates apoptosis and survival of developing neurons [189]. Moreover, microglia provides trophic support and promotes differentiation of astrocytes and oligodendrocytes. Furthermore, recent evidence suggests a possible role of microglia as multipotent stem cells able to differentiate into neurons, astrocytes and oligodendrocytes [190].

Myelin development, damage and repair

Glial cells interaction in CNS (re)myelination and demyelination

In the central nervous system, myelination is carried out by oligodendrocytes. The synthesis of myelin and the consequent ensheathment of axons by this multilamellar membrane restrict action potentials to short unmyelinated segments, namely the nodes of Ranvier. This provides the structural basis for saltatory action potential propagation, which in turn speeds up nerve conduction 10-20 times compared to non myelinated axons [191]. Myelin however is also important for axon maintenance and function [192]. Moreover, the cross talk between oligodendrocytes and axons is necessary to maintain metabolic function of axons, cytoskeletal arrangement, axonal transport, trophic support, and ion channel organization [97, 192-196].

Whereas the early postnatal human brain is mostly non-myelinated, central nervous system myelination increases progressively in a defined temporal and topographic sequence within the first two decades of life [197]. During development, oligodendrocytes progenitor cells (OPCs), highly proliferative, motile, bipolar cells, are the main source for mature oligodendrocytes and myelin. These cells originate in sequential waves in specific regions of the ventral and dorsal neuroepithelium of the spinal cord and brain before migrating and dispersing into the CNS [198, 199]. The majority of these cells undergo a series of changes triggered by first contact with the axonal membrane and characterized by a rapid increase in morphological complexity and expansion of uncompacted myelin membrane, ultimately leading to their differentiation into myelinating oligodendrocytes [200]. A small pool of OPCs, characterized by the expression of the surface antigens platelet derived growth factor α receptor (PDGFαR) and neural/glial antigen 2 (NG2), instead, remains undifferentiated and quiescent in the adult CNS [199] where they are involved in myelin repair in the injured or diseased CNS [201]. A number of CNS diseases damage or destroy myelin and oligodendrocytes, leading to demyelination. This pathological process is typically a consequence of either a direct insult aimed at the oligodendrocytes, or of primary axonal loss. The first, commonly referred to as primary demyelination, can be further divided in two categories from a clinical point of view: genetic abnormalities affecting glia (leukodystrophies), and inflammatory damage to myelin and oligodendrocytes (multiple sclerosis being the most representative) [202]. Following the loss of the myelin sheath,

axons undergo several molecular reorganizations and physiological changes that ultimately result in axonal dysfunction, degeneration, and loss of sensory and motor function [203] and, regardless of causes or underlying mechanisms, the adult CNS has only a limited capability to repair damaged tissue. This limitation does not only involve neurons and their axons but also mature oligodendrocytes, unable to compensate for the myelin loss as they usually degenerate [204, 205]. However, demyelination often triggers a spontaneous myelin repair process, defined remyelination [202]. This process, mediated by OPCs that are recruited to differentiate and replace the lost oligodendrocytes [206], leads to myelin sheath restoration, reinstatement of saltatory conduction and functional recovery, and, ideally, it should recapitulate developmental myelination and tissue reconstruction should be complete. The myelin sheaths generated during this process however are thinner and exhibit shorter internodes than the developmental ones [207, 208]. On the other hand, recent data suggests that at late time points of recovery newly remyelinated fibers have comparable internode length and thickness compared to their developmental counterparts [209].

As previously stated, the remyelination process is mediated by OPCs. In particular, NG2/PDGFαR-expressing adult progenitors are recruited to lesion sites and differentiate into mature oligodendrocytes able to remyelinate axons, thus restoring nerve conduction [210]. The efficacy of this process however is compromised and limited by the inflammatory and activated milieu surrounding the demyelinated lesions [211]. In multiple sclerosis, for example, changes in the CNS microenvironment during the progression of the pathology cause OPCs to gradually lose their ability to respond to myelin damage, thus limiting their remyelination capacity [212]. All the steps of the remyelination process (OPC activation, recruitment, differentiation and myelination) are tightly regulated by a plethora of extrinsic and intrinsic factors acting either as activators or inhibitors [213, 214]. In response to injury, adult OPCs undergo a switch from a quiescent state to an active one, corresponding to a regenerative phenotype. During this activation step, the progenitor cells become responsive to growth factors, cytokines and chemokines, enhancing their proliferation and recruitment to the demyelinated area. Moreover, several genes involved in oligodendrocyte development and differentiation are upregulated [215-218]. Astrocytes and microglia, both activated by injury, are the main source of the factors that induce the rapid activation of OPCs during demyelination. Astrocytes, for example, secret several soluble factors implicated in enhancing myelination, including platelet derived growth factor (PDGF) and basic

fibroblast growth factor (FGF2) [200, 219-221], whereas microglia is able to induce chemotaxis of OPCs through the secretion of hepatocyte growth factor [222]. Following activation, OPCs, in addition to the ongoing proliferation, migrate to demyelinated areas. Concomitantly, macrophages and microglia begin the removal of the myelin debris, whose presence impairs remyelination [223, 224]. Astrocytes also play a role in this clearance, by inducing the recruitment of microglia to the lesion site, a process regulated by the chemokine CXCL10 [225]. Once OPCs reach the demyelinated area, they must differentiate into remyelinating oligodendrocytes. To do so, they need to establish contact with the demyelinated axon, synthesize the myelin membrane and subsequently form the myelin sheath, a process that presents many similarities with the developmental myelination.

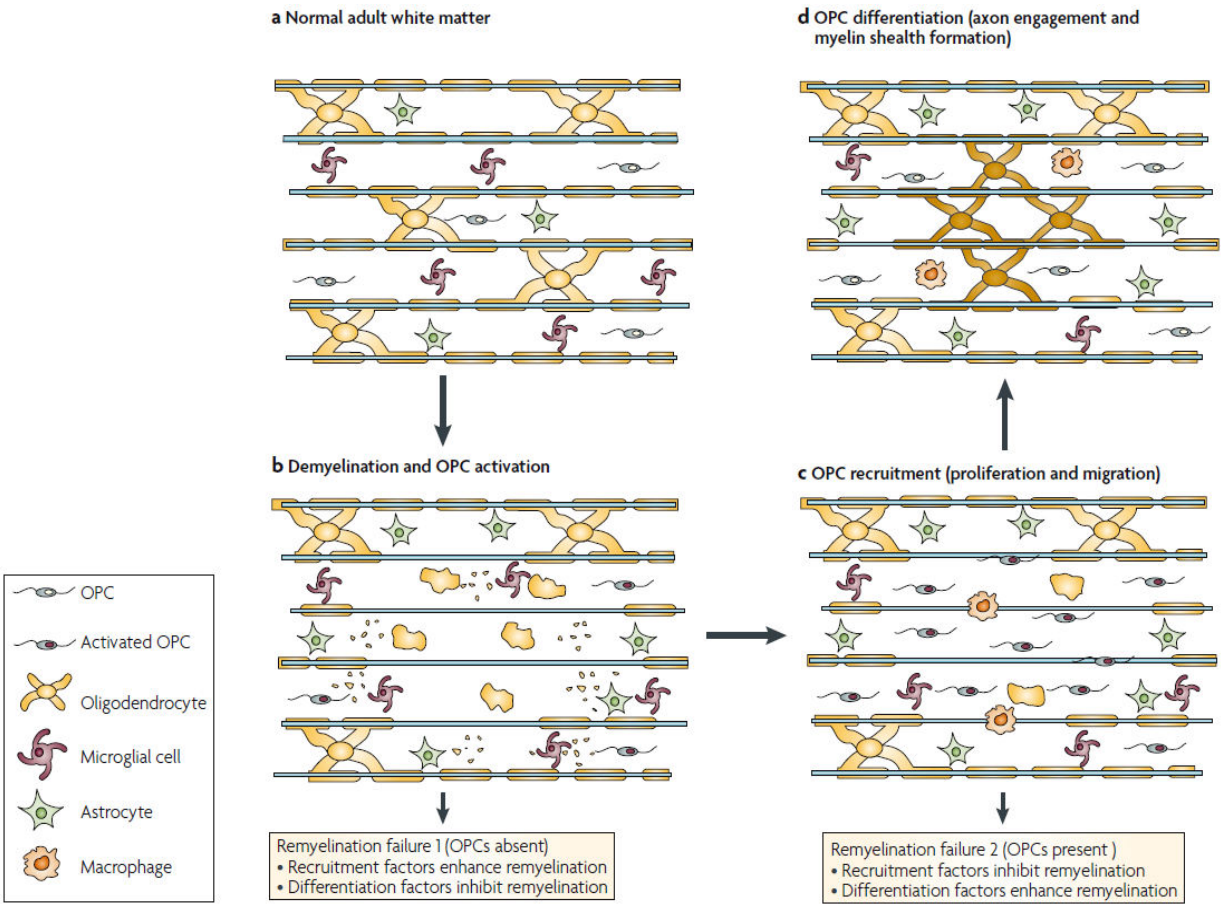

Figure 7. Phases of remyelination. Following demyelination, astrocytes and microglia activate, consequently leading to OPC activation. These activated OPC are then recruited and migrate toward the lesion area, while macrophages and microglia start to remove the myelin debris. In the final phase of remyelination, the recruited OPCs differentiate into mature oligodendrocytes, leading to the formation of a new myelin sheath. *Adapted from Franklin et al, 2008 [202].*

FGF and IGF, secreted respectively by astrocytes and microglia, play a role both in developmental myelination and in remyelination [226, 227]. However, differences between the regulation of development and regeneration of myelin do occur. OLIG1, for example, which is essential for developmental myelination, has a less redundant role during remyelination [228]. Another example is represented by the Notch signaling pathway, which is redundant during remyelination [229]. While remyelination can be quite efficient in experimental models, its efficiency remains generally low, leading to permanent deficits and dysfunctions. To a certain degree this decline is due to failure to the recruit OPC and to the failure of these cells to differentiate [202]. The underlying reasons for this are not completely understood but several pieces of evidence suggest the involvement of different factors, including age [230], gender [231], genetic background [232], and also the presence of a variety of differentiation inhibitors that affect the glial regeneration potential [214, 233].

Myelin damage in multiple sclerosis

Several neurological diseases are characterized by loss of myelin sheath and destruction of oligodendrocytes. As previously stated, primary demyelination in the CNS can be caused by genetic abnormalities affecting glial cells. The diseases associated with this kind of abnormalities, though rare, usually present during childhood with generalized neurological symptoms. They can be divided into those due to defects of lysosomal function, like metachromatic leukodystrophy, those resulting from defects in astrocytes providing trophic support for myelinating cells, like Alexander's disease, and those due to deficiencies or misfolding of myelin proteins which in turn lead to abnormal myelinogenesis, like hypomyelinating leukodystrophies [234]. Primary CNS demyelination can also be caused by inflammation damage. The diseases associated with this kind of damage, characterized by myelin loss that occurs on a background of inflammation, include pathologies such as multiple sclerosis (MS), Marburg disease, neuromyelitis optica (NMO), Balo's concentric sclerosis, acute disseminated encephalomyelitis (ADEM) and its hyperacute variant, acute hemorrhagic leukoencephalitis (AHL) [235].

Among these, MS has been considered the lead disease featuring demyelination as a result of the scientific effort invested into its description and of its high prevalence. Multiple sclerosis is the most common cause of non traumatic disability in young

people, with an onset usually between 20-40 years of age [236], affecting 2.5 million people throughout the world [237]. MS is characterized by inflammation, progressive demyelination and gliosis, axonal injury and loss. The pathological hallmarks of all the subtypes of this disease are focal areas, called plaques, of demyelination in the CNS, with surrounding inflammation and neurodegeneration [238, 239]. MS etiology however remains to be defined. Currently the most widely accepted hypothesis concerning MS pathogenesis is the autoimmune hypothesis. This hypothesis proposes autoimmune inflammation as the cause of demyelination, and auto-reactive leukocytes as disease initiators. The process begins when naïve myelin specific $CD4^+$ T cells are primed in the lymph nodes by dendritic cells presenting either myelin or myelin cross-reactive epitopes. These cells differentiate into Th17 cells following stimulation by interleukin 23 (IL-23), likely to play a central role in CNS autoimmunity [240, 241]. As these cells enter the CNS via subarachnoid space (SAS), together with activated macrophages, microglia and astrocytes, they secrete cytotoxic cytokines leading to demyelination [242-244]. A second hypothesis regarding MS onset is that the disease might be triggered by viral infection. This hypothesis does not exclude the autoimmune hypothesis, considering that virus could trigger the autoimmunity. Moreover, the viral infection might occur several years before the development of the MS lesions [245, 246]. A large amount of evidence supporting these hypothesis however was obtained using the most frequently used MS animal model, experimental autoimmune encephalomyelitis (EAE) and, while there are similarities between EAE and MS, there are still major differences between the two [247]. Therefore, EAE, while useful and suitable to study CNS-immune relationships and to test drugs targeting the CNS, might not represent a complete model of MS and the autoimmune hypothesis remains unproven.

There is, however, a third hypothesis, defined as the oligodendrogliopathy hypothesis, which is based on neuropathological studies on MS. Through histopathological examination of MS lesions Lucchinetti et al. defined four major immunopatterns, on the basis of specific myelin protein loss, plaque extent and topography, immunoglobulin deposition, oligodendrocyte destruction, and complement activation [235, 248], each possibly reflecting a different pathogenesis. Whereas in the first two types, type 1 (T cell-mediated autoimmune encephalomyelitis) and type 2 (T cell plus antibody-mediated autoimmune encephalomyelitis), demyelinated lesions are associated with inflammation consisting mainly of T cells and macrophages, in the other two types, type

3 (primary oligodendroglial apoptosis) and type 4 (primary oligodendroglial dystrophy), oligodendroglial death is a prominent feature in active and inactive lesions. The four types of patterns identified by Lucchinetti were further analyzed first by Barnett and Prineas [249] and later on by Henderson [250]. These studies, based on a thorough analysis of oligodendroglial apoptosis and inflammatory cell distribution in the various lesions, provided evidence suggesting that oligodendrocyte death and microglial activation are the initial event in MS lesion formation, followed by immune responses to scavenge dead myelin. Moreover, these immune responses seem to be permissive for oligodendroglial regeneration and remyelination, consistently with the observation that removal of myelin debris is necessary for remyelination [223]. The pathological heterogeneity observed in the four patterns is reflected in the clinical spectrum of MS. MS extends from an asymptomatic phase, of unknown duration starting at an unknown age, to clinically symptomatic phases commonly known as radiologically isolated syndrome, clinically isolated syndrome (CIS), single-attack MS (SAMS), relapsing–remitting MS (RRMS), single-attack progressive MS (SAPMS), secondary progressive MS (SPMS), and primary progressive MS (PPMS) [235]. These different phases of MS are characterized by an interplay between different levels of inflammation-demyelination, remyelination and axonal loss[251]. Moreover, remission of the disease symptoms in the initial stages is most likely due to a combination of resolution of inflammation, axonal plasticity, and remyelination. Furthermore, in early MS lesions remyelination is a frequent phenomenon while the majority of chronic MS lesions is characterized by limited remyelination [252]. The efficiency of this remyelination process seems to be influenced by factors such as anatomical localization, disease course, lesion size, and other patient dependent factors [252-255]. Astrocytes also seem to play a role. Following injury, these cells are activated and form a glial scar, composed of a dense network of hypertrophic cells, whose formation is crucial for restoring the blood brain barrier (BBB) normal function and integrity. In demyelinating conditions, however, the glial scar also represents a physical barrier hindering OPC entry into the demyelinated area to interact with neurons [192, 256-258]. Moreover, the scar also poses a biochemical obstacle for remyelination. The reactive astrocytes have marked changes in the expression levels of several molecules, including adhesion molecules, antigen presentation molecules, growth factors, receptor, cytokines, and protease inhibitors able to modify the composition of the extracellular matrix and to directly affect remyelination[259].

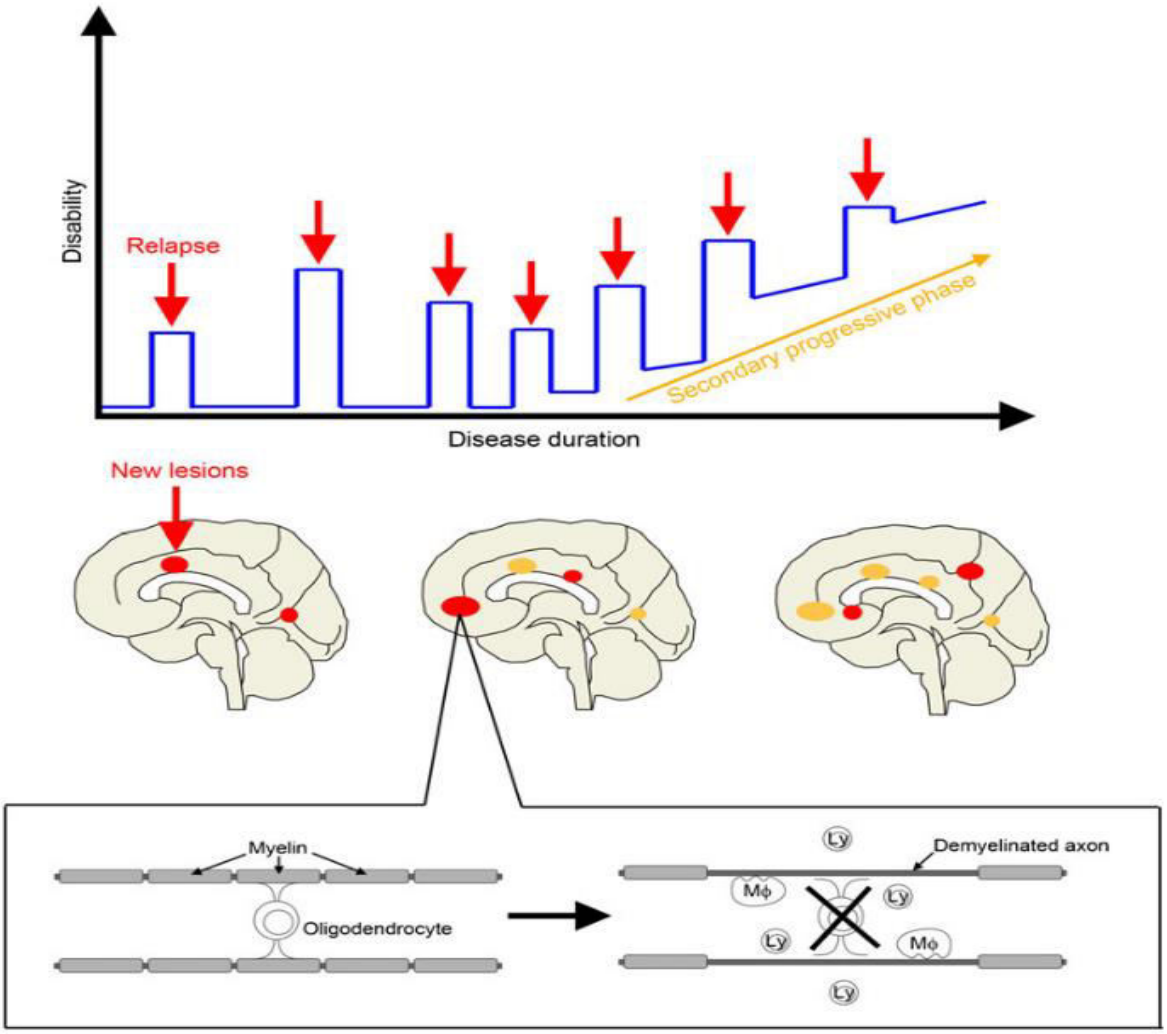

Figure 8. Clinical course of multiple sclerosis. The majority of MS patients initially develop RRMS and, usually, during the remittance there is a spontaneous neurological recovery. Later, these patients progress to SPMS, and the functional recovery is abolished. The hallmark of MS lesions is inflammatory demyelination. Loss of mature oligodendrocytes is often associated with this demyelinating process. *Adapted from Nakahara et al, 2012 [244].*

Whether the immune response is the cause of the pathogenesis or simply a consequence of the oligodendroglial cell death, the failure of the immune system to discriminate myelin components from foreign antigens plays a critical role in the pathophysiology of MS. Several CNS myelin proteins, including MBP, PLP, MAG and MOG, have been described as targets for autoantibodies in MS [260-266]. Recent evidence however also suggests possible roles for myelin lipids in MS. In fact, in MS patients increased serum levels of glycolipids and anti glycolipid antibodies have been reported [267-271]. For example, it has been hypothesized that anti GD1a antibodies, increased in sera of MS patients, could have a role in the impairment of OPC maturation [272]. Moreover, it has been observed that MS patients exhibit an enhanced antibody response against

sulfatides [273, 274]. Furthermore, recent evidence has shown that increased levels of serum and CSF sulfatides are found in MS patients and in their healthy siblings, with stage-specific accumulation of different molecular species [275-277], suggesting that the presence of sulfatide in these biological fluids could represent a risk/prognostic factor for the onset and progression of MS.

Studies have also shown how anti-sulfatide antibodies can interact with the surface of cultured oligodendrocytes and affect the lateral organization of sulfatide with myelin proteins with opposite consequences (demyelination versus stimulation of myelin formation), depending on the type of ECM protein prevalent in the culture environment [145]. Hence, these antibodies might play a role in the onset of the disease, but they might also represent an important immunological tool for the treatment of demyelinating diseases [278].

Therapeutic approaches and remyelination promotion

The adult mammalian CNS is usually regarded as a regeneration incompetent organ, as opposed to the PNS, where axonal connections and myelin sheaths can be restored more easily [279]. The development of therapies aimed to promote remyelination within the demyelinated lesion in the CNS is an important therapeutic goal. In MS, naturally occurring remyelination is an overall inefficient process that fails to successfully counteract the accumulation of lasting axonal damage and increasing brain atrophy, thus resulting in motor and neurological deficits [4, 5]. Considering OPCs have been detected in chronic MS lesions [280], other determinants such as factors affecting migration and differentiation of these cells might be involved in the failure to remyelinate. Treatment able to modulate these factors could be clinically valuable. One of the FDA approved immunomodulatory drugs for MS, Fingolimod, is a sphingosine-1-phosphate (S1P) receptor modulator able to control lymphocyte trafficking [281]. However, it was also found to modulate resident glial cells, including oligodendrocytes, and to increase remyelination efficiency [282-285]. It is however still unclear whether this remyelination-promoting effect is simply due to a modulation of the inflammatory microenvironment or if it is due to a direct modulation of oligodendrocytes. Currently two major approaches involving a more direct stimulation of the remyelination process are being tested in animal models of demyelination. The first approach involves the transplantation of cells capable of remyelination and is based on the evidence, gathered

from multiple studies, that transplanted glial cells myelinate in the CNS following their introduction in the developing CNS of rodents with myelin mutations or with toxin-induced demyelination [286, 287]. This approach however has limitations. There is little benefit to be gained by transplanting OPCs into lesions that already contain abundant cells with the ability to generate new oligodendrocyte. In these lesions the environment is inhibiting differentiation and regeneration and it would likely do the same for the exogenous cells. Moreover, the method of delivery also represents a problem. In fact, while for focal lesions a single injection might be enough, for diffuse disease multiple injections at different sites, each carrying a risk of intracerebral hemorrhage, would be necessary [288]. The second approach being tested in animal models of demyelination involves the promotion of repair by the resident stem- and precursor-cell populations in the adult CNS, through the administration of growth, trophic, and neuroprotective factors [289]. This approach is based on the idea that if the mechanisms of remyelination can be understood, and non-redundant pathways described, the causes of remyelination failure and consequently possible therapeutic targets, will be identified. As discussed in previous sections, remyelination failure is likely associated with either failed recruitment or differentiation of OPCs. However, different and mutually exclusive biologies underlie these two phases or remyelination. For example, PDGF promotes OPCs proliferation and migration but there is also evidence showing its inhibitory effect in the final stages of differentiation when the myelin sheath is formed [290]. Therefore, therapies aimed to recruit OPCs might not promote remyelination in situations where the main problem is OPC differentiation, and vice versa [291, 292].

An alternative therapeutic approach is the use of CNS reactive antibodies to promote remyelination [6]. So far, all identified remyelination promoting antibodies have natural autoreactive antibodies (NAbs) features and are of the IgM isotype, with one exception. This exception is represented by the high affinity anti-LINGO IgG antibodies, which are able to promote remyelination but do not have NAb features. One of these anti-LINGO antibodies, BIIB033, a monoclonal antibody, is currently being tested for its efficiency as a remyelinating drug. Neutralization of LINGO-1, an axonal protein involved in the regulation of axonal growth and in OPC differentiation, has been found to promote remyelination in several animal models [293], and has fueled high expectations regarding its potential effect in MS. While a study investigating the effect of BIIB033 in optic neuritis (ClinicalTrial.gov: NCT01721161) has not reached its endpoint, a Phase II study in RRMS is still underway (ClinicalTrial.gov: NCT01864148).

Excluding the anti-LINGO IgGs, all remyelination promoting antibodies have NAbs features and are of the IgM isotype. These antibodies react to self antigens and, compared to conventional antibodies, they have a relatively low affinity. In addition, all remyelination promoting antibodies with identified antigens are polyreactive, as a result of their flexible antigen-binding site. Several of these monoclonal antibodies (mAbs) recognize not only protein antigens but also multiple sphingolipids. For example, the ganglioside-binding antibody A2B5 is able to recognize several GSLs due to their similar carbohydrate epitope [294, 295]. O4 recognizes sulfatide, seminolipid and also the unknown proligodendroblast antigen (POA) [296, 297], while HNK-1 targets MAG and also 3-sulfoglucuronyl paragloboside (SGPG) [298, 299]. All remyelination promoting IgMs produce a calcium influx in astrocytes, oligodendrocytes precursor cells, and immature oligodendrocytes [300]. The α-amino-3-hydroxy-5-methyl-4-isoxazolepropionic acid glutamate receptor has been shown to mediate the calcium influx into oligodendrocytes (both OPC and immature OL), while this influx, after antibody stimulation, in astrocytes is mediated by inositol triphosphate-sensitive channels [300]. Another feature common to all remyelination promoting IgMs is their ability to access demyelinated lesions within the CNS. Direct evidence of this was obtained through a magnetic resonance imaging-based study, however, accumulation seems to occur only in models in which the BBB integrity is compromised, and not in animals without demyelination [7].

One of these remyelination promoting IgMs, recombinant human IgM22 (rHIgM22), is able to bind to myelin and to the surface of oligodendrocytes *in vitro* and has successfully completed a phase I clinical trial, aimed to evaluate safety, tolerability, pharmacokinetics and immunogenicity of a single intravenous dose of rHIgM22 in patients with MS (ClinicalTrial.gov: NCT01803867). In addition, a second phase I trial aimed to evaluate safety and tolerability in relapsing MS patients is now recruiting (ClinicalTrial.gov: NCT02398461). This antibody was first identified through the screening of human serum of a patient with Waldenström macroglobulinemia, a rare, low grade malignancy, characterized by the presence of IgM-secreting clonal cells in the bone marrow [301]. The serum of this patient was screened to identify antibodies able to bind to myelin, and, out of the six antibodies satisfying this criteria, two IgMs (sHIgM22 and sHIgM46) promoted significant remyelination *in vivo* [8]. sHIgM22, in particular, was able to bind to the surface of rat, mouse, and human oligodendrocytes [8,

278]. Further characterization of sHIgM22 led to the production of its recombinantly expressed version, rHIgM22 [302], which was found able to promote myelin repair in Theiler's virus infection-induced (TMEV) and lysolecithin-demyelinated models of multiple sclerosis [303]. The actual target and mechanisms of rHIgM22 are still under investigation however several pieces of evidence suggest that the antigen recognized by this antibody might be a plasma membrane lipid, possibly sulfatide, and that lipid raft might be involved in the signaling associated with rHIgM22 remyelinating activity. This hypothesis is based on the observation that the well known anti-sulfatide antibody O4 and rHIgM22 have a similar binding pattern to CNS tissues [9], and that binding of rHIgM22 is abolished in CNS tissue sections from CST (-/-) mice [10]. Moreover, existing literature suggests that the binding target of rHIgM22 could be associated with detergent-resistant membranes (DRM)/lipid rafts and that rHIgM22 biological activity depends on lipid raft organization [9, 10]. rHIgM22 exerts its biological activity by inhibiting apoptotic signaling in OPCs and also by inhibiting the differentiation of these cells [9, 304]. The inhibition of the apoptotic signaling pathways is achieved via reduction of caspase-3 and caspase-9 cleavage and alteration of the caspase gene expressions in TMEV mice and in primary rat oligodendrocytes [9, 304], and this is dependent on calcium influx, through CNQX-sensitive AMPA channels [9]. Moreover, literature strongly suggests that rHIgM22 biological activity, responsible for its myelin-repair promoting activity, could require a multimolecular complex organizing Lyn and the cell surface molecules integrin αvβ3 and PDGFαR [304, 305]. Taken together, these observations have led to hypothesize that rHIgM22, through its pentameric structure, could mediate the clustering of a lipid antigen and stabilize lipid rafts domains. Moreover, it could determine the reorganization of Lyn, integrin αvβ3 and PDGFαR to form a signaling complex which, in turn, promotes OPC survival and proliferation [10, 304]. Signaling through this complex determines Lyn activation, and subsequent activation of the ERK 1/2 MAPK cascade, leading to the inhibition of caspase-3/9, to inhibition of OPCs differentiation and promotion of OPCs proliferation [305, 306].

In isolated OPCs, PDGF is required for rHIgM22-mediated inhibition of apoptotic signaling and differentiation. PDGF is produced by neurons and astrocytes and stimulates OPC proliferation and promotes OPC survival both *in vivo* and *in vitro*. Indeed, IgM-mediated OPC proliferation is detectable only in cultures containing substantial amounts of astrocytes, microglia and OPCs (mixed glial cultures) but not in highly enriched OPC population [305].

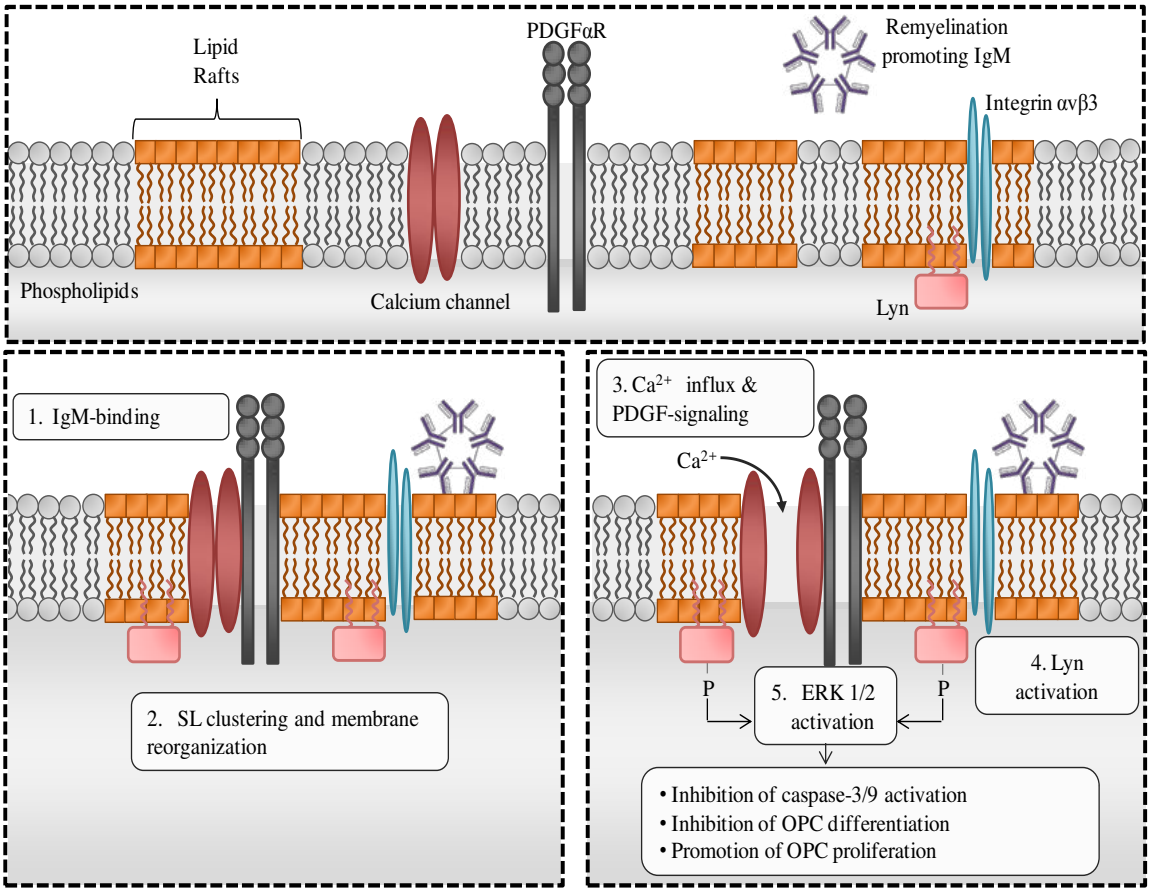

Figure 9. Proposed mechanism of action of rHIgM22. Binding of rHIgM22 to the surface of oligodendrocyte determines a reorganization of the membrane, favoring the interaction of Lyn, integrin αvβ3 and PDGFαR. IgM-stimulated activation of Lyn, with consequent activation of ERK 1/2 determines the inhibition of the apoptotic pathway and of OPC differentiation. Other factors (e.g. PDGF) might be required to promote the proliferation of these cells. *Adapted from Watzlawik et al, 2013 [306].*

AIM OF THE STUDY

A number of CNS diseases damage or destroy myelin and oligodendrocytes, leading to demyelination. This pathological process is typically a consequence of either a direct insult aimed at the oligodendrocytes, or of primary axonal loss, and ultimately leads to the loss of the myelin sheath. Following demyelination in the central nervous system, a demyelinated axon has two possible fates. The normal response to demyelination, at least in most experimental models, is spontaneous remyelination, a process mediated by oligodendrocyte precursor cells. These cells are activated and recruited by the other glial cells in response to CNS injury and their proliferation and differentiation leads to the formation of new myelin sheaths, typically thinner and shorter than their developmental counterparts but nevertheless associated with functional recovery. However, even though in experimental models this process is efficient, remyelination is often inadequate in demyelinating diseases such as multiple sclerosis. If remyelination fails, the axon, devoid of its myelin sheath, undergoes several molecular reorganizations and physiological changes that ultimately result in axonal dysfunction, degeneration, and loss of sensory and motor function [203]. For this reason, therapies that increase the chances of the regenerative outcome of demyelination are keenly sought.

One of the therapeutic approaches that is currently being developed to improve the regenerative outcome involves the use of CNS reactive antibodies to promote remyelination [6]. One of these antibodies, rHIgM22, is able to bind to myelin and to the surface of oligodendrocytes *in vitro* has successfully completed a phase I clinical trial for the treatment of MS (ClinicalTrial.gov: NCT01803867). Moreover, a second phase I trial aimed to evaluate safety and tolerability in relapsing MS patients is now recruiting (ClinicalTrial.gov: NCT02398461). This antibody is able to enter the CNS, accumulate at lesion site and promote remyelination in mouse models of chronical demyelination [7, 8]. The antigen recognized by this antibody and the molecular mechanism underlying the remyelinating activity of rHIgM22 however are yet to be elucidated. Evidence suggests that the binding target of rHIgM22 could be associated with plasma membrane lipid rafts, and that lipid rafts might be involved in the signaling associated with the biological activity of this antibody [9, 10]. Moreover, O4, an anti sulfatide antibody, and rHIgM22 have a similar binding pattern to CNS tissues [9], and binding of rHIgM22 is abolished in CNS tissue sections from CST knock-out mice [10], suggesting that the antigen recognized by rHIgM22 could be one or more CST-sulfated antigens present in myelin and on the surface of oligodendrocyte.

On the basis of these considerations, the aim of this study is to identify the molecular binding targets of rHIgM22, thus allowing a better understanding of the signaling mechanisms underlying the remyelination inducing activity of this antibody. The identification of the binding targets of this antibody, able to promote remyelination in validated mouse models of MS, and the characterization of their membrane microenvironment could significantly contribute to the reveal the signaling mechanisms underlying the biological activity of rHIgM22. This, in turn, would allow to gain a better knowledge regarding both the molecular mechanisms involved in the remyelination process, and the ones involved in MS aetiology thus allowing to define new potential therapeutic targets.

MATERIALS AND METHODS

Materials

Commercial chemicals were the purest available and, unless otherwise stated, were purchased from Sigma Aldrich Srl.
Ca^{2+} and Mg^{2+}-free HBSS, D-Glucose, BSA fraction V, HEPES, trypsin, sodium pyruvate, poly-D-lysine, poly-L-lysine, PBS, Na_3VO_4, KCl, NaOH, methanol, chloroform, polyisobuthylmethacrylate, O-phenylenediamine, H_2O_2, citric acid, Na_2HPO_4, and n-octyl-β-D-glucoside were purchased by Sigma Aldrich; penicillin/streptomycin, bovine fetal serum, DMEM high glucose, and glutamine from Euroclone Spa; $MgSO_4$, $CaCl_2$, and HPTLC plates from Merck; DNaseI from Roche Spa; acetic acid from Fluka; HCl from VWR International PBI Srl; HPA sensor chips and HBS-N buffer from GE Healthcare Srl.

Chrompure Human IgM (#009-000-012) has been purchased from *Jackson Immuno Research, Inc.*; anti-MAG L-20 (#sc-9543) was purchased from *Santa Cruz*; HRP-conjugated anti-human IgM μ-chain antibody (#31415) and HRP-conjugated anti-goat IgG (#31402) have been purchased from *Thermo Fisher Scientific, Inc.*
The rHIgM22 antibody has been kindly provided from *Acorda Therapeutics, Inc. (Ardsley, NY).*

Pure galactosylceramide (GalCer), sulfatides, and lyso PC were purchased from *Avanti Polar Lipids*; phosphatidylcholine (PC), DOPC, phosphatidylethanolamine (PE), phosphatidylinositol (PI), phosphatidylserine (PS), sphingomyelin (SM), and phosphatidic acid (PA) were purchased from *Sigma Aldrich*. Lysosulfatide was purchased from *Matreya*. Ceramide, gangliosides (GM3, GM2, GM1, GD3, GD1a, GD1b, GT1b), glucosylceramide (GlcCer), glucosylsphingosine (GlcSph), and lactosylceramide (LacCer) were synthesized or purified in our laboratories.
PtdGlc and four structurally related lipids were kindly given us by Dr. Yoshio Hirabayashi (RIKEN Brain Science Institute, Laboratory for Molecular Membrane Neuroscience, Wako, Japan).

Animal specimens

For the experiments reported in this thesis, the sources of animal specimens were:

- wild type (WT) C57BL/6N mice and acid sphingomyelinase knock-out (ASM(-/-)) mutant C57BL/6N mice [307], used for brain lipid extraction, myelin purification and preparation of mixed glial cultures, cultured oligodendrocytes and astrocytes;
- primary cultured rat oligodendrocytes positive for rHIgM22 staining (kindly prepared by Dr. Yana Zorina, Acorda Therapeutics, Ardsley, NY);
- primary cultured rat microglia [183], kindly provided by Dr. Michela Matteoli, Department of Medical Biotechnology and Translational Medicine, University of Milano;
- hemibrains from wild type and cerebroside sulfotransferase (CST) (+/-) and (-/-) mice [136], kindly provided by Dr. Xianlin Han, Sanford-Burnham Medical Research Institute, FL, USA.

Cell culture

Mixed glial cell (MGC) culture

A primary mixed glial culture, composed of astrocytes, oligodendrocytes, and microglia, is obtained when newborn disaggregated cerebral brain cells from rat or mouse are plated at high cell density in serum-supplemented medium [305, 308]. In this culture model, neurons fail to survive and, after one week, mixed glial cell cultures are free of neurons, meningeal cells, and fibroblasts. MGC cultures were prepared according to Watzlawik et al [305]. Briefly, the hemispheres from P3 mice brains were minced with a surgical blade and then incubated for 30’ at 37°C in 0.05% trypsin in modified HBSS (Ca^{2+} and Mg^{2+} free HBSS containing 5 g/L D-glucose, 3 g/L BSA fraction V, 20 mM HEPES, 100 U/mL penicillin and 100 µg/mL streptomycin). Following the addition of $MgSO_4$ and DNase I, the sample was centrifuged at 200 g at 8°C for 5 minutes and resuspended in modified HBSS. The tissue was then further dissociated by trituration through a sterile flame narrowed glass pipette, centrifuged at 200 g at 8°C for 10 minutes, resuspended in culture medium and plated on Petri dishes or T75 flasks coated with poly-D-lysine (25 µg/mL).

The cells were cultured in DMEM high glucose containing 10% heat inactivated FBS, 100 U/mL penicillin, 100 µg/mL streptomycin, 1 mM sodium pyruvate, and 2 mM glutamine and the culture medium is changed every 3/4 days.
With this protocol it is possible to obtain cultures with about 60-70% of astrocytes, 30-40% of OPCs, and less than 3% of microglial cells.

Glial cells (oligodendrocytes and astrocytes) isolation and differentiation

Oligodendrocytes were harvested, through shaking procedure, from 8-10 days old mixed glial cell cultures, when the cell were mostly immature, containing progenitor cells and immature oligodendrocytes. Briefly, microglia and dead cells are removed with a 30 minute shake at 37°C, 150 rpm in a HT Infors minitron shaker (orbit size:25 mm). After an 18-20 hour shaking to detach oligodendrocytes, the cell suspension was plated twice on untreated, non-TC, dishes to further remove microglia and astrocytes, before being centrifuged for 10 minutes at 8°C, 850 rpm. The surnatant was discarded and the pellet resuspended in OPC proliferative medium (DMEM:F12 1:1 containing 2 mM glutamine, 100 U/mL penicillin, 100 µg/mL streptomycin, 2% StemPro Neural Supplement, 10 ng/mL EGF, 10 ng/mL PDGF-AA, 10 ng/mL FGF-2). Media was replaced every 3/4 days and cells were carried using Accutase (Invitrogen). The cells obtained with this method are mostly immature oligodendrocytes.
Mixed glial cell culture that underwent a shaking procedure to isolate oligodendrocytes precursors were used maximum three times. After the third time, the adherent layer was represented mostly by astrocytes, thus allowing to collect these cells. The collected cells were then stored at -80°C, before being lyophilized and subjected to lipid extraction.

Lipid analysis

Purification of myelin from mouse brain

Myelin isolation was performed using an optimized version of the protocol described in [309]. Briefly, frozen brains from C57BL/6N wild type mice ranging from 2 to 4 months of age were thawed at room temperature (RT) before removing the cerebellum and the meningeal membranes. 50 mg of tissue were suspended in 500 µL of 0.25 M sucrose in 10 mM Tris-HCl, pH 7.4 and Dounce homogenized (10 strokes, tight) before

being centrifuged at 500 g, 4°C for 10 minutes. The supernatant was collected and further centrifuged at 21000 g, 4°C for 10 minutes with Ultra-centrifuge Beckman TL-100. The supernatant was discarded and the pellet was resuspended in 500 µL of 0.25 M sucrose in 10 mM Tris-HCl, pH 7.4 and then layered on top of 1250 µL of 0.88 M sucrose in 10 mM Tris-HCl, pH 7.4. After this, the samples were centrifuged at 21000 g, 4°C for 10 minutes to separate the mitochondria from the myelin vesicles. In fact, myelin will float on the surface whereas the denser mitochondria will pellet at the bottom of the tube.

The myelin vesicle layer was carefully recovered, resuspended in an equal volume of ice-cold water and then centrifuged at 21000 g, 4°C for 10 minutes. After discarding the supernatant, the pellet was resuspended in 500 µL of 0.25 M sucrose in 10 mM Tris-HCl, pH 7.4, layered on top of 1250 µL of 0.88 M sucrose in 10 mM Tris-HCl, pH 7.4 and centrifuged at 21000 g, 4°C for 10 minutes in order to separate myelin from membrane debris. The myelin layer was carefully recovered, resuspended in an equal volume of ice-cold water and then centrifuged at 21000 g, 4°C for 10 minutes. The supernatant was discarded and the pellet was resuspended in 120 µL of ice-cold water. Protein content was determined with DC protein assays (Bio-Rad).

Lipid extraction

Sample preparation

Frozen brains and cerebella from C57BL/6N wild type mice ranging from 2 to 5 months of age, and frozen brains from cerebroside sulfotransferase (CST) (+/-) and (-/-) 3.5 months old mice were thawed at room temperature (RT). Meninges were removed, the brains were minced with a surgical blade, resuspended in ice-cold water and subjected to sonication. The samples were then Dounce homogenized (10 strokes, tight) before being snap frozen and subsequently lyophilized.

Frozen rHIgM22-positive rat oligodendrocytes from Acorda, and frozen rat microglia were thawed at RT, resuspended in ice-cold water, snap frozen and then lyophilized.

Cultured mouse mixed glial cells, oligodendrocytes, and astrocytes were collected after washing the flasks and/or petri dishes twice with PBS containing 1 mM Na_3VO_4. The cells were scraped twice in PBS containing 1 mM Na_3VO_4 and centrifuged at 3000 rpm, 4°C for 5 minutes. The supernatant was discarded, the pellet was snap frozen and stored

at -80°C. Frozen samples were then thawed at RT, resuspended in ice-cold water, snap frozen and lyophilized.

Total lipid extraction, phase partitioning and alkali treatment

Lipids from the lyophilized samples were extracted with chloroform/methanol/water 20:10:1 (v/v/v) and subjected to a modified two-phase Folch's partitioning to obtain the aqueous (Aq. Ph.) and the organic phases (Or. Ph.) [310]. Briefly, 1550 µL of the solvent system were added to the lyophilized samples. The samples were then mixed at 1100 rpm, RT for 15 minutes and centrifuged at 13200 rpm, RT for 15 minutes. The supernatant was collected as Total lipid extract (TLE) and the extraction was repeated again twice by adding the 1550 µL of the solvent system to the pellets. The pellets were air dried and resuspended in 1N NaOH and incubated overnight at RT before being with water to 0.05N NaOH to allow the determination of the protein content with DC assay. Aliquots of the TLE were then subjected to phase partitioning adding either 20% of water by volume or 20% of 0.88% KCl in H_2O by volume. The samples were then mixed at 1100 rpm, RT for 15 minutes and centrifuged at 13200 rpm, RT for 15 minutes. The Aq. Ph. were recovered, and CH_3OH:H_2O 1:1 (v/v) or CH_3OH: 0.88% KCl 1:1 (v/v) were added to the organic phase before mixing the samples at 1100 rpm, RT for 15 minutes and centrifuging at 13200 rpm, RT for 15 minutes. The new aqueous phases were recovered and united to the ones previously collected. The aqueous phases were dried under N_2 flux, and resuspended in water before undergoing dialysis and lyophilization. The organic phases were dried under N_2 flux and resupended in a known volume of cholesterol/methanol 2:1. Aliquots of the organic phases were then subjected to alkali treatment to remove glycerophospholipids [310].

Thin layer chromatography

To determine endogenous lipid content, the various samples were analyzed by mono-dimensional silica gel HPTLC using different solvent systems. The total lipid extracts were analyzed using chloroform/methanol/0.2% aqueous 60:35:8 (v/v/v) as a solvent system, the aqueous phases were analyzed with chloroform/methanol/0.2% aqueous $CaCl_2$ 50:42:11 (v/v/v), whereas the organic phases and the methanolyzed organic phases were analyzed using chloroform/methanol/water 110:40:6 (v/v/v). The organic phases were also subjected to HPTLC separation with chloroform/methanol/acetic acid/water 30:20:2:1 (v/v/v/v) to analyze the glycerophospholipid content.

Aqueous phases from wild type mouse brain were also analyzed by two-dimensional HPTLC [310] using chloroform/methanol/0.2% aqueous $CaCl_2$ 50:42:11 (v/v/v) as a solvent system for both of the separations. Between the first and second chromatographic run, the HPTLC was exposed to NH_3 vapors for 3 hours at RT.
After separation, lipids were detected either by spraying the TLC plates with different colorimetric reagents (anisaldehyde, aniline, Ehrlich's reagent) or by TLC immunostaining. Identification of lipids after separation and chemical detection was assessed by co-migration with lipid standards.

TLC immunostaining and dot blot

rHIgM22 binding to individual purified lipids from commercial sources or to lipid extracts was assessed by TLC immunostaining following standard protocols [138, 139, 311]. Briefly, after chromatographic separation (as described above) the TLC plates were coated three times with a polyisobuthylmethacrylate solution [310], and air dried for 1 hour before being immersed in blocking solution (3% BSA in PBS) for 1 hour. The plates were then incubated with rHIgM22 or isotype human IgM (Chrompure Human IgM; Jackson Immunoreasearch; negative control) at 5 µg/mL in 1% BSA in PBS or 5 µg/mL in 1% BSA in PBS (with/without 1% inactive goat serum) for 2 hours at RT or overnight at 4°C. After the incubation with the primary antibody, the plates were incubated with an HRP-conjugated anti-Human IgM µ-chain antibody for 1 hour, RT, and developed using *o*-phenylenediamine (OPD)/H_2O_2 in 0.05 M citrate-phosphate buffer pH 5.0.
To allow a more quantitative evaluation, the binding of rHIgM22 to individual purified lipids was also assessed using a TLC dot blot system. In this case, different amounts of the lipids in analysis were applied as spots on silica gel plates. These plates were fixed with a polyisobuthylmethacrylate solution and the TLC immunostaining was carried out as described above.

Surface Plasmon resonance

The affinity of rHIgM22 for different purified lipids in supported lipid monolayers was assessed by SPR using a BIAcore 3000 analytical system (GE Healthcare, Uppsala, Sweden) with HPA sensor chips. Chips were incubated in the presence of DOPC liposomes containing different amounts of the target lipids. Liposomes containing the

target lipids were prepared following standard procedures. Briefly, different amounts of sulfatide (1 – 0.1 – 0.01 – 0.001 - 0.0005 μmol) in chloroform/methanol 2:1 were mixed with 1 μmol of DOPC, either alone or in presence of different amounts of a second lipid (cholesterol, GalCer, SM, lysosulfatide), and dried under N_2 flux. The residue was then suspended in 200 μL HBS-N buffer (20 mM 4-(2-hydroxyethyl)-1-piperizineethanesulfonic acid (HEPES) pH 7.4, 150 mM NaCl), mixed with a vortex mixer and sonicated for 15 minutes with a water bath sonicator. The solutions were then filtered using a 0.22 μm polyvinylidene difluoride (PVDF) syringe-driven filter unit. The sensor chip were pretreated with 40 mM n-octyl-β-D-glucoside and the liposome solutions were immobilized on the chip for 30 min at a flow rate of 2 μL/min, using HBS-N buffer without or with 1 mM $CaCl_2$ and 1 mM $MgSO_4$ as running buffer. The chip surface was then washed with 50 mM NaOH for 1 min at 5 μL/min, and blocked with 100 μg/ml bovine serum albumin (BSA) before proceeding with the analysis. For analysis, 5 μg/mL of rHIgM22 or control IgM were injected at a flow rate of 10 μL/min. Signals generated in a negative control cell without target lipid have been subtracted from the experimental values. Quantitative evaluation of the binding and dissociation reactions were performed using the software BIAevaluation version 3.1 [312].

Mass spectrometry

Following the chromatographic separation of the aqueous phases, the area corresponding to the unidentified band was scraped. The scraped gel was subjected to lipid extraction, dialyzed and lyophilized. The lyophilized samples were then resuspended in chloroform and analyzed by ESI mass spectrometry in negative mode. The analyses of the compound were carried out using a ThermoQuest Finnigan LCQ Deca ion-trap mass spectrometer (Finnigan MAT, San Jose, CA) equipped with an electrospray ionization (ESI) ion source, an Xcalibur data system, and a TSP P4000 quaternary pump. The conditions for MS analysis, in negative mode, were the following: sheath gas flow, 50 arbitrary units; spray voltage, 4 kV; capillary voltage, -47 V; capillary temperature, 260°C; and fragmentation voltage (used for collision-induced dissociation), 50%.

Protein analysis

Protein quantification

The protein quantification was performed through DC assay (Bio-Rad). The assay was performed in 96 well plates following the protocol supplied with the Bio-Rad DC assay kit. The samples were analyzed in triple, like the protein standard, bovine serum albumin (BSA), at different concentrations. 25 µL of reagent A and 200 µL of reagent B, both supplied with the kit, were added to each well. After 15 minutes of incubation, the absorbance at 750 nm was measured with the spectrophotometer. The samples reading were compared with the ones of the standard. The assay is linear between 1.5 and 7.5 µg of protein amount.

Electrophoresis and Western Blotting

The samples were analyzed using electrophoresis on a polyacrilamide gel with denaturing conditions. The samples were resuspended in *Laemmli buffer* (1x: 62.5 mM Tris-HCl pH 6.8, 2% SDS, 5% 2-mercaptoethanol, 0.01% Bromophenol blue, 10% glycerol) and boiled for 5 minutes at 100°C before being analyzed.
The electrophoresis run was performed using a Miniprotean II unit, produced by Bio-Rad. To obtain optimal resolution, a stacking gel is polymerized on top of the resolving gel. A solution of 25 mM Tris, 192 mM glycine, 0.1% SDS, pH 8.3 was used as *running buffer*. The proteins were separated using 10% polyacrylamide gels.
After electrophoresis separation, proteins were transferred to polyvinylidene difluoride (PVDF) membranes, at 200 mA for 3 hours at 4°C with a wet blotting (Mini Transblot Biorad). The transfer buffer used is *Blotting buffer* 1x (25 mM Tris-HCl, 192 mM glycine, 15 % methanol, pH 8.0-8.5).
After the transfer, the PVDF membranes were immunoblotted using either rHIgM22 (lot 09-0052), Chrompure Human IgM (Jackson Immunoresearch, #009-000-012), or MAG (L-20; Santa Cruz, #sc-9543).Briefly, after the transfer the membrane was incubated in 5% milk in TBS-T 0.05% (1 mM Tris-HCl pH 8, 150 mM NaCl, 0.05% Tween) to block the aspecific binding sites of the membrane. The membrane was then washed three times with TBS-T 0.05% and incubated with a specific antibody (primary antibody) 1 hour at room temperature, depending on the antibody used. The primary antibody was diluted in a solution of TBS-T 0.05% containing 1% bovine serum

albumin (BSA). The membrane was washed again with TBS-T 0.05% for four times, to get rid of the antibody excess, before being incubated with the secondary antibody conjugated with horseradish peroxidase (HPR) at room temperature for 45 minutes. For membranes previously incubated with either rHIgM22 or Human IgM, an anti human IgM (Thermo, #31415) was used. For membranes incubated with MAG, an anti goat IgG (Thermo, #31402) was used. The membrane was then washed again for six times and the peroxidase activity was assessed through incubation with a non-radioactive light emitting substrate for the detection of immobilized specific antigens conjugated with horseradish peroxidase-linked antibodies (LiteAbLot Plus, Euroclone) for 2 minutes. The luminescent compound generated following the reaction can be detected through exposition to a photographic film (Kodak BioMax MR Film, Sigma-Aldrich). The data acquisition was performed using a GS-700 Imaging Densitometer.

Statistical analysis

Experiments were run in triplicate, unless otherwise stated. Data are expressed as mean value ± SD and were analyzed by one-way analysis of variance followed by Student-Neuman-Keul's test. *p*-values are indicated in the legend of each figure.

RESULTS

Binding of rHIgM22 to purified lipids

Binding to sulfatide

The central nervous system (CNS) of vertebrates is characterized by the presence of myelin, a specialized multilamellar structure, produced by oligodendrocytes, which wraps around the axons and not only acts as an insulator, thus allowing saltatory transmission of the electric impulses, but also provides metabolic support to the axon itself [313]. The myelin membrane has a high lipid content and is enriched in glycolipids [107, 314]. In particular, galactosylceramide (GalCer) and sulfatide account, respectively, for about 20 and 5% of myelin lipids [30, 125]. It has been reported that rHIgM22 is able to bind to myelin and to the surface of oligodendrocytes *in vitro* [8, 10] and that it binds to CNS tissue sections with a pattern similar to that of O4, an anti-sulfatide antibody [9], suggesting that sulfatide could be one of the antigen recognized by this remyelination-promoting antibody.

Binding of rHIgM22 to different amounts of pure sulfatide from commercial sources (0.05 to 10 nmol) was assessed through TLC immunostaining following the protocol detailed in Materials and Methods. Different concentrations (0.5-5.0 µg/mL) of the two primary antibodies, rHIgM22 and Human IgM (negative control), were used in the assay. The analysis revealed that rHIgM22 was able to bind pure sulfatide with a signal detectable from 0.5 nmol of the target lipid, and that the binding was proportional to the amount of sulfatide. The binding decreased if the concentration of the antibody was lowered, however the intensity of the signals was not quantitatively proportional to rHIgM22 concentration, at least below 2.5 µg/mL. Binding of the control Human IgM was also observed, however it was significantly lower than that of rHIgM22 for all experimental points, except for the IgM concentration of 0.5 µg/mL (Figure 10).

On the basis of these results, surface plasmon resonance experiments were set up to allow a more quantitative analysis of rHIgM22 binding to sulfatide under experimental conditions where antigen presentation was closer to the one happening in a biological membrane, and also to verify the specificity of the binding. Binding of rHIgM22 to different amounts of sulfatide (0.0005 to 1 µmol), in monolayers of DOPC, was analyzed using sensor chips HPA and, as shown in Figure 11, it was significantly higher than the binding of the control IgM for all experimental points. Furthermore, the shape of the sensorgram was consistent with a specific binding for rHIgM22, and the binding

response increased with an increase of the amount of sulfatide present in the monolayers.

Taking into account the values of maximum response and the prompt return to the baseline upon antibody removal, the DOPC:sulfatide 1:0.01 molar ratio was selected for further experiments aimed to analyze the binding response of rHIgM22 for monolayers containing different lipids which will be detailed in the following pages. Under the experimental conditions selected (DOPC:sulfatide 1:0.01 molar ratio), the binding response of rHIgM22 to sulfatide containing monolayers was consistent and highly reproducible (Figure 12).

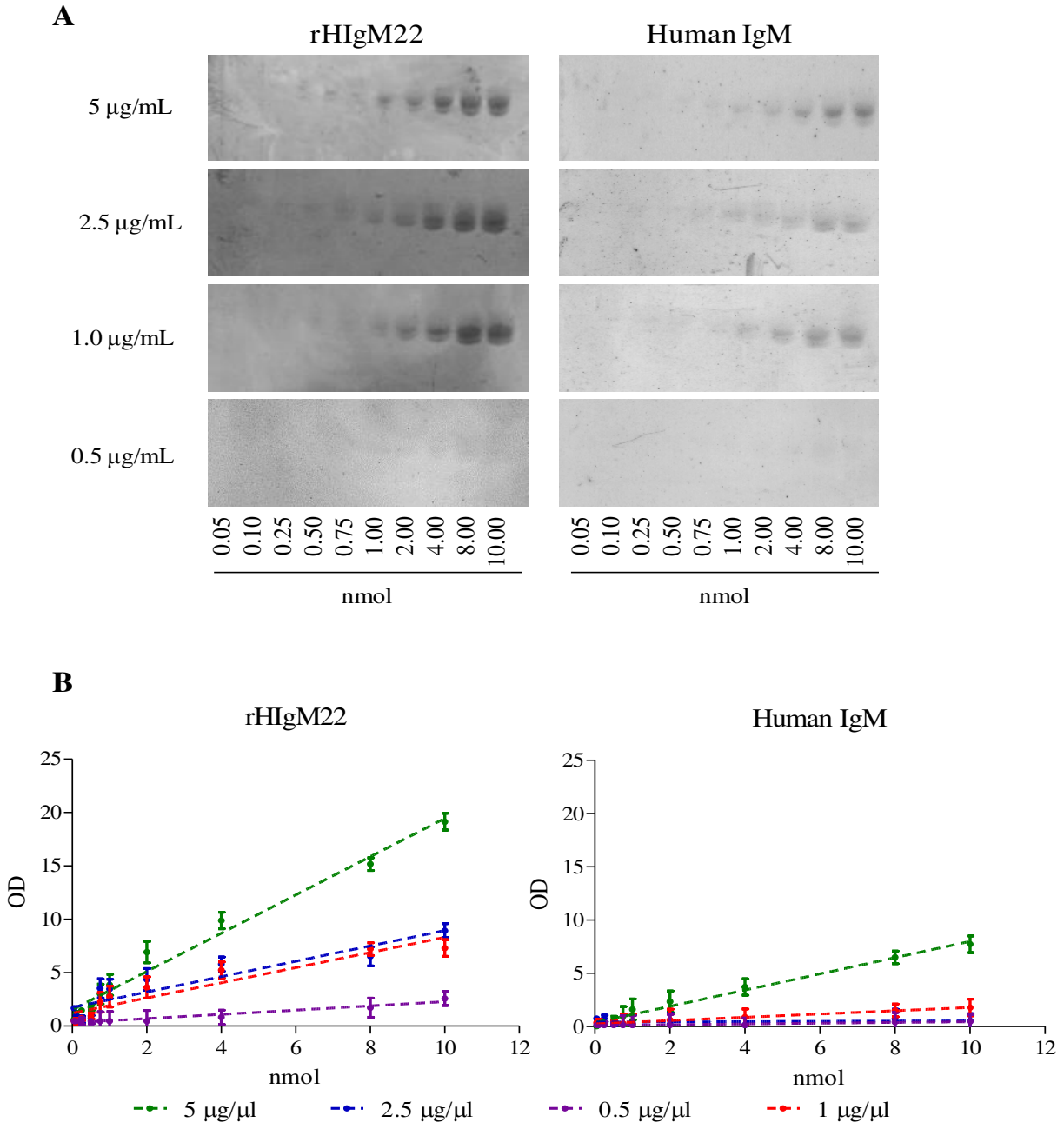

Figure 10. rHIgM22 binding to purified sulfatide in TLC immunostaining. rHIgM22 binding to different amounts of sulfatide (from 0.05 to 10 nmol) was assessed using TLC immunostaining. Briefly, after chromatographic separation (solvent system: $CHCl_3$:CH_3OH:H_2O 110:40:6), TLC plates were fixed with a polyisobuthylmethacrylate solution, air dried and incubated with 3% BSA in PBS for 1 hour. The plates were then incubated with either rHIgM22 or Human IgM (negative control) in 1% BSA in PBS for 2 hours at room temperature (RT). Different concentrations of the two primary antibodies (5-2.5-1-0.5 μg/mL) were used in this assay. The plates were then incubated with a HRP-conjugated anti-Human IgM μ-chain antibody for 1 hour at RT, and immunoreactive bands were revealed using *o*-phenylenediamine (OPD)/H_2O_2 in 0.05 M citrate-phosphate buffer pH 5.0. Optical density of each band was calculated by densitometry and the results are shown in *panel B*. Data in *panel B* is expressed as mean ± SD of three independent experiments.

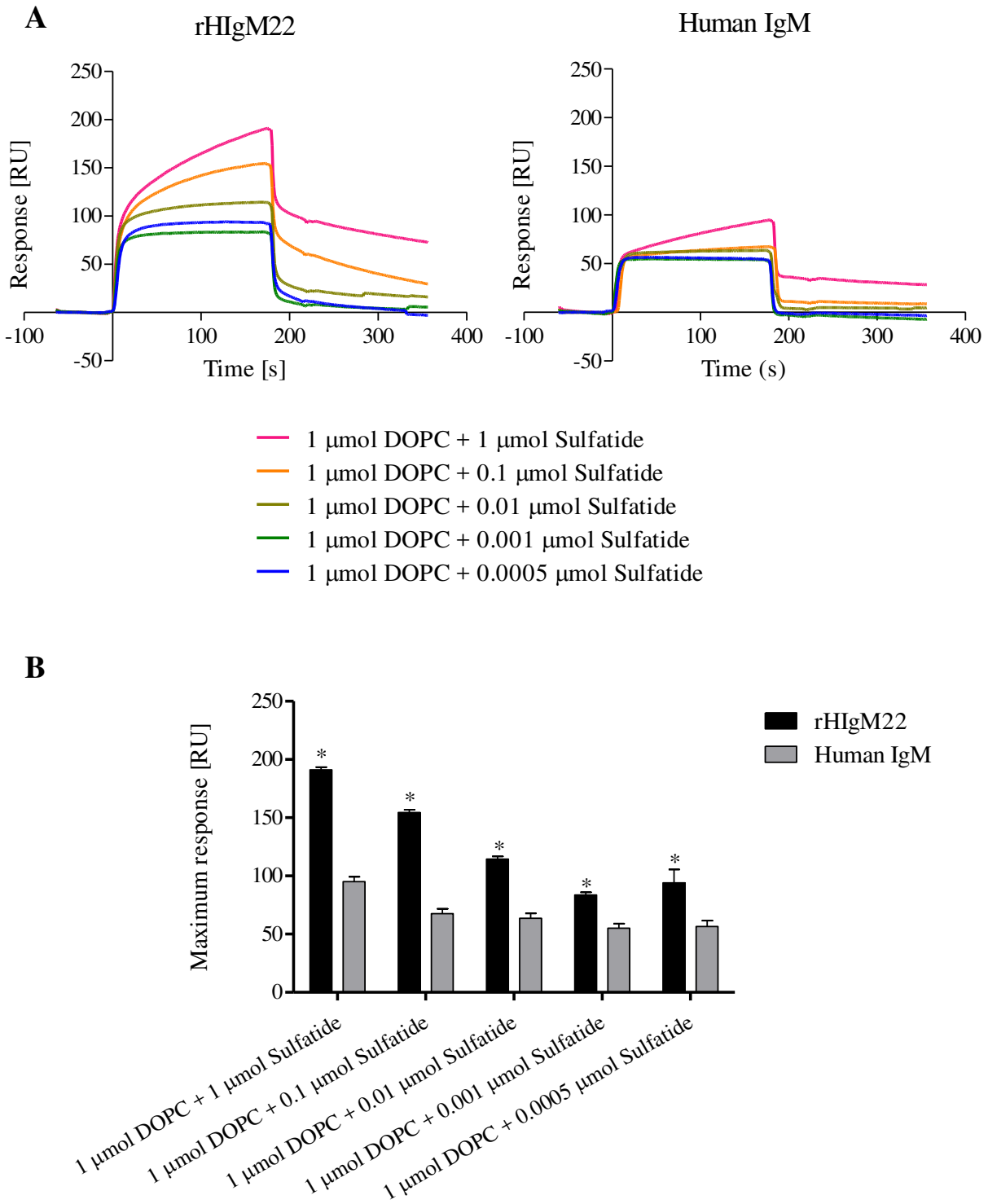

Figure 11. rHIgM22 binding to purified sulfatide. DOPC (1 µmol) was mixed with different amounts of sulfatide (from 0.0005 µmol to 1 µmol) and dried. The lipid mixture was resuspended in HBS-N buffer, mixed vigorously and sonicated. The liposome solutions were immobilized on an HPA sensor chip. The surface was washed briefly with 50mM NaOH and blocked with 100 µg/mL BSA. For analysis, 5 µg/mL rHIgM22 or Human IgM was injected. The binding of the two antibodies is represented as a sensorgram (*Panel A*) and also as maximum response (*Panel B*). Data in *panel B* are expressed as mean ± SD of three independent experiments; *, $p<0.05$ versus control.

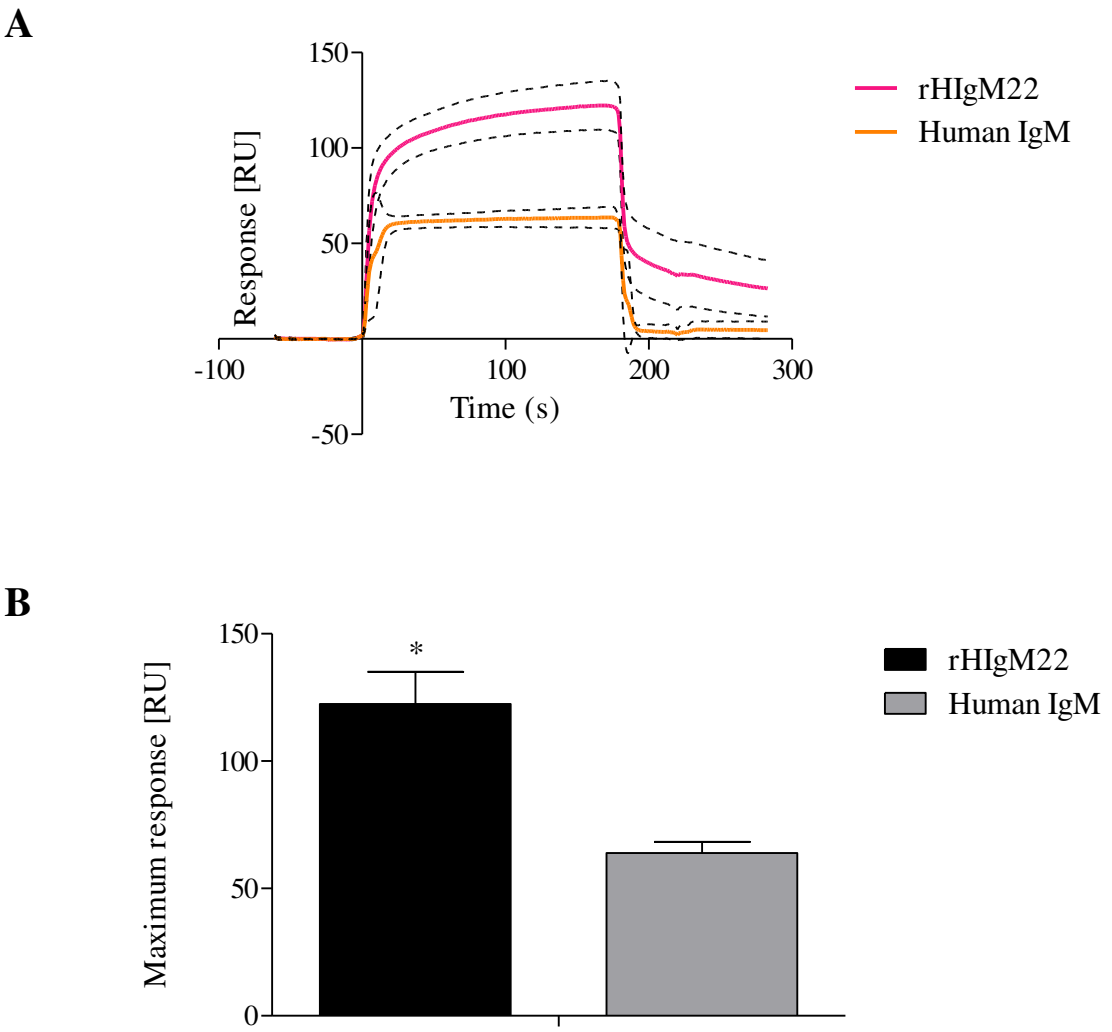

Figure 12. Sensorgram of rHIgM22 binding to purified sulfatide. DOPC (1 µmol) was mixed with sulfatide (0.01 µmol) and dried. The lipid mixture was resuspended in HBS-N buffer, mixed vigorously and sonicated. The liposome solutions were immobilized on an HPA sensor chip. The surface was washed briefly with 50mM NaOH and blocked with 100 µg/mL BSA. For analysis, 5 µg/mL rHIgM22 or Human IgM was injected. Data are the mean + SD of four experiments; the dashed lines indicate the SD; * *$p<0.05$ versus control.*

Binding to lysosulfatide

Lysosulfatide, the deacylated form of sulfatide, is present as a minor component in the normal CNS but its levels can be increased as a consequence of some pathological conditions, such as methachromatic leukodystrophy [315-317].

Considering that rHIgM22 was able to recognize sulfatide in a specific manner, and considering that sulfatide and lysosulfatide bear the same 3-*O*-sulfo-galactose head group, the binding of rHIgM22 to these two lipids was compared. The binding to lysosulfatide was assessed using both TLC immunostaining and SPR experiments and, in both experimental settings, the antibody resulted able to bind to both lipids. In fact, rHIgM22, in TLC immunostaining assay, was able to recognize lysosulfatide even if the binding resulted 3-4 times weaker than that to sulfatide for equimolar amounts of the two lipids (Figure 13, panels A-B). The surface plasmon resonance experiments confirmed that the binding of rHIgM22 to the lyso lipid was specific, and also showed that the binding affinity for lysosulfatide is actually comparable with that to sulfatide (Figure 13, panel C).

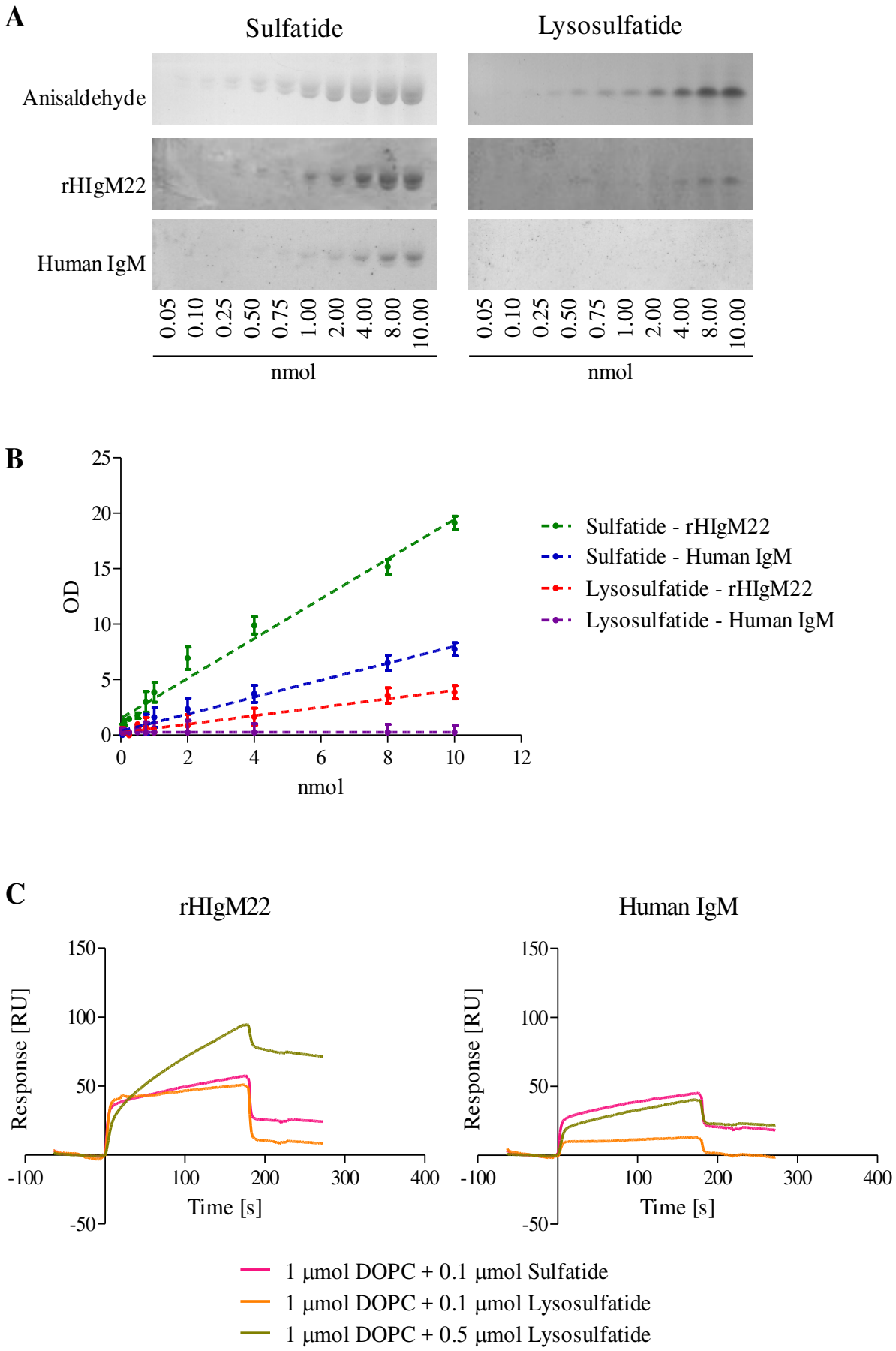
A
Sulfatide
Lysosulfatide
Anisaldehyde
rHIgM22
Human IgM
0.05
0.10
0.25
0.50
0.75
1.00
2.00
4.00
8.00
10.00
nmol
B
OD
nmol
Sulfatide - rHIgM22
Sulfatide - Human IgM
Lysosulfatide - rHIgM22
Lysosulfatide - Human IgM
C
rHIgM22
Human IgM
Response [RU]
Time [s]
1 µmol DOPC + 0.1 µmol Sulfatide
1 µmol DOPC + 0.1 µmol Lysosulfatide
1 µmol DOPC + 0.5 µmol Lysosulfatide

Figure 13. rHIgM22 binding to purified sulfatide and lysosulfatide. rHIgM22 binding to different amounts of sulfatide and lysosulfatide (from 0.05 to 10 nmol) was assessed using TLC immunostaining as shown in *Panel A*. Briefly, after chromatographic separation (solvent system: $CHCl_3$:CH_3OH:H_2O 110:40:6), TLC plates were fixed with a polyisobuthylmethacrylate solution, air dried and incubated with 3% BSA in PBS for 1 hour. The plates were then incubated with either rHIgM22 or Human IgM at 5 µg/mL in 1% BSA in PBS for 2 hours at room temperature (RT). The plates were then incubated with a HRP-conjugated anti-Human IgM µ-chain antibody for 1 hour at RT, and immunoreactive bands were revealed using *o*-phenylenediamine (OPD)/H_2O_2 in 0.05 M citrate-phosphate buffer pH 5.0. Optical density of each band was calculated by densitometry and the results are shown in *Panel B*. Data in *Panel B* is expressed as mean ± SD of three independent experiments.
The binding of rHIgM22 to sulfatide and lysosulfatide was also assessed using SPR (*Panel C*). DOPC (1 µmol) was mixed with either sulfatide (0.1 µmol) or lysosulfatide (0.1 or 0.5 µmol) and dried. The lipid mixture was resuspended in HBS-N buffer, mixed vigorously and sonicated. The liposome solutions were immobilized on an HPA sensor chip. The surface was washed briefly with 50mM NaOH and blocked with 100 µg/mL BSA. For analysis, 5 µg/mL rHIgM22 or Human IgM was injected.

Binding to glycerophospholipids

From a quantitative point of view, the most significant lipids present in the myelin membrane, comprising 65% of the total lipid dry weight, are cholesterol, GalCer and phosphatidylethanolamine (PE), the latter consisting in large part of plasmalogens [318]. Considering the abundance of PE, and also of phosphatidylcholine (PC), in myelin, the binding of rHIgM22 to several glycerophospholipids was assessed through TLC immunostaining. As shown in Figure 14, while neither rHIgM22 nor the control IgM showed a significant binding to PC, the most abundant phospholipid in any biological membrane, they both weakly bound to PE, phosphatidylserine (PS) and phosphatidylinositol (PI), under experimental conditions similar to those used to assess binding to sulfatide, but there was no significant difference between the binding of the two antibodies. rHIgM22, on the other hand, showed a significant binding to phosphatidic acid (PA), which is not only a constituent of all cell membranes and an intermediate in the biosynthesis of triacylglycerols and other phospholipids, but is also suggested to act as an intracellular lipid second messenger [15]. In the case of PA, the control IgM gave no significant binding (Figure 14, panel A), suggesting that binding of rHIgM22 to this lipid might be specific.

A recent paper by Nair S. et al [319], highlighted that immunoglobulins present in the sera of patients with monoclonal gammopathies are reactive against lyso PC. Considering this, binding to lyso PC was also assessed, although nor rHIgM22 nor control IgM showed a significant binding to this lysolipid.

The binding of rHIgM22 to different amounts of phosphatidyl-β-D-glucoside (PtdGlc), a lipid characterized by a unique fatty acid composition and expressed at membrane level in several mammalian cell types but particularly enriched in the brain where it is localized to radial glia and nascent astrocytes [320], was also analyzed. The binding to other four uncharacterized lipids obtained from Dr. Hirabayashi (RIKEN, Wako, Japan), all structurally related to PtdGlc, was also analyzed however, neither rHIgM22 nor isotype IgM gave a significant binding for any of these lipids (Figure 15).

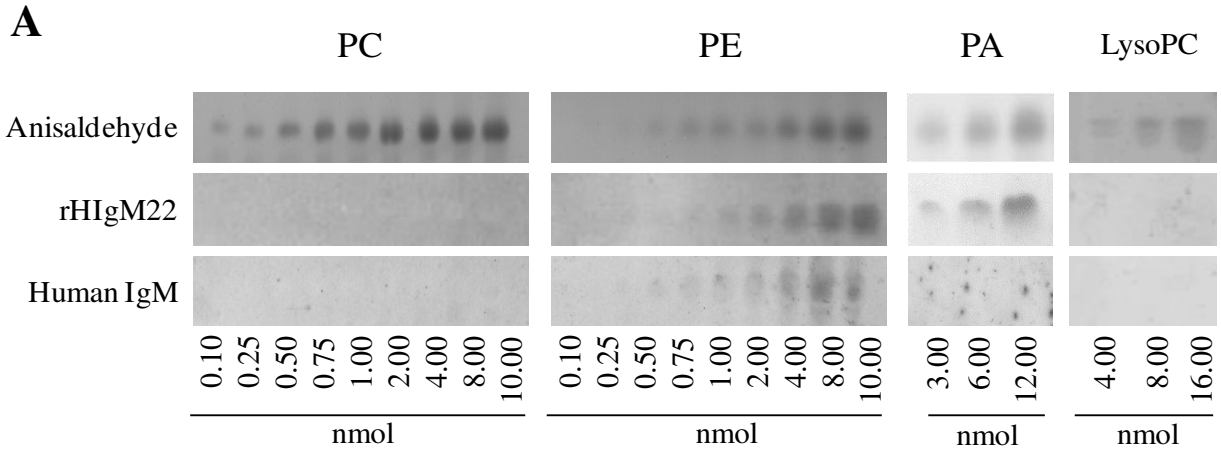
A
PC
PE
PA
LysoPC
Anisaldehyde
rHIgM22
Human IgM
0.10
0.25
0.50
0.75
1.00
2.00
4.00
8.00
10.00
3.00
6.00
12.00
16.00
nmol

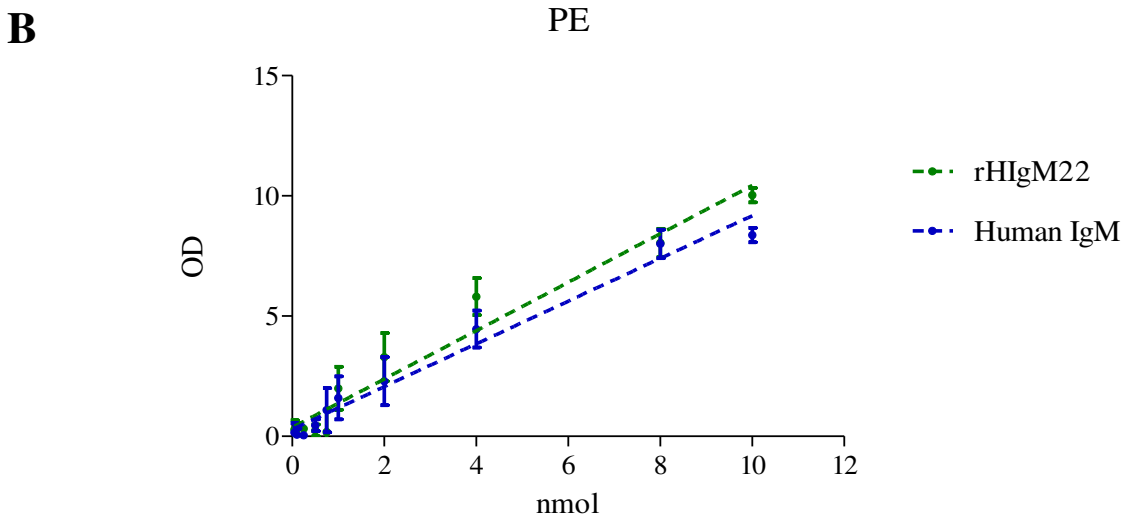
B
PE
OD
nmol
rHIgM22
Human IgM

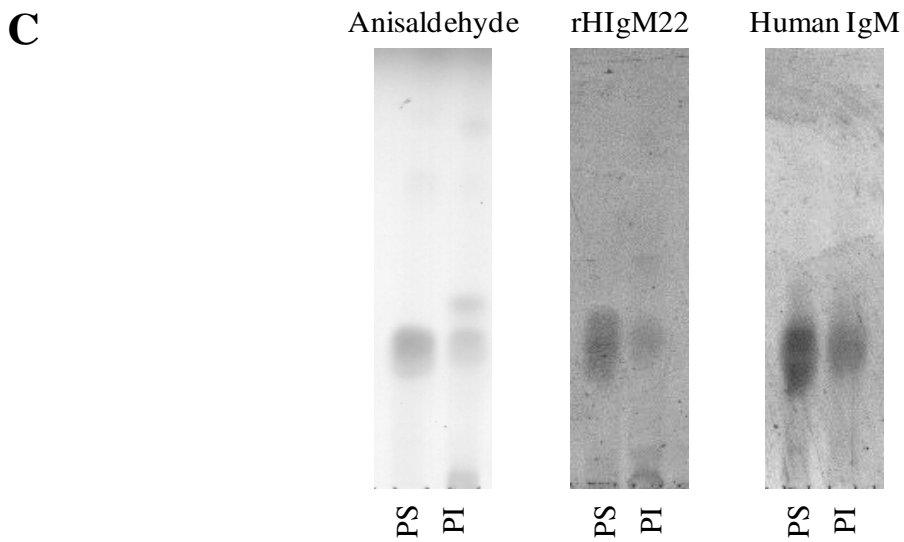
C
Anisaldehyde
rHIgM22
Human IgM
PS
PI

Figure 14. rHIgM22 binding to glycerophospholipids. rHIgM22 binding to different glycerophospholipids was assessed using TLC immunostaining as shown in *Panel A and C*. Briefly, after chromatographic separation (solvent system: $CHCl_3$:CH_3OH:CH_3COOH:H_2O 30:20:2:1), TLC plates were fixed with a polyisobuthylmethacrylate solution, air dried and incubated with 3% BSA in PBS for 1h. The plates were then incubated with either rHIgM22 or Human IgM (negative control) at 5 μg/mL in 1% BSA in PBS for 2 hours at room temperature (RT). The plates were then incubated with a HRP-conjugated anti-Human IgM μ-chain antibody for 1 hour, RT, and developed using *o*-phenylenediamine (OPD)/H_2O_2 in 0.05 M citrate-phosphate buffer pH 5.0. For PE, optical density of each band was calculated by densitometry and the results are shown in *Panel B*. Data in *Panel B* is expressed as mean ± SD of three independent experiments.

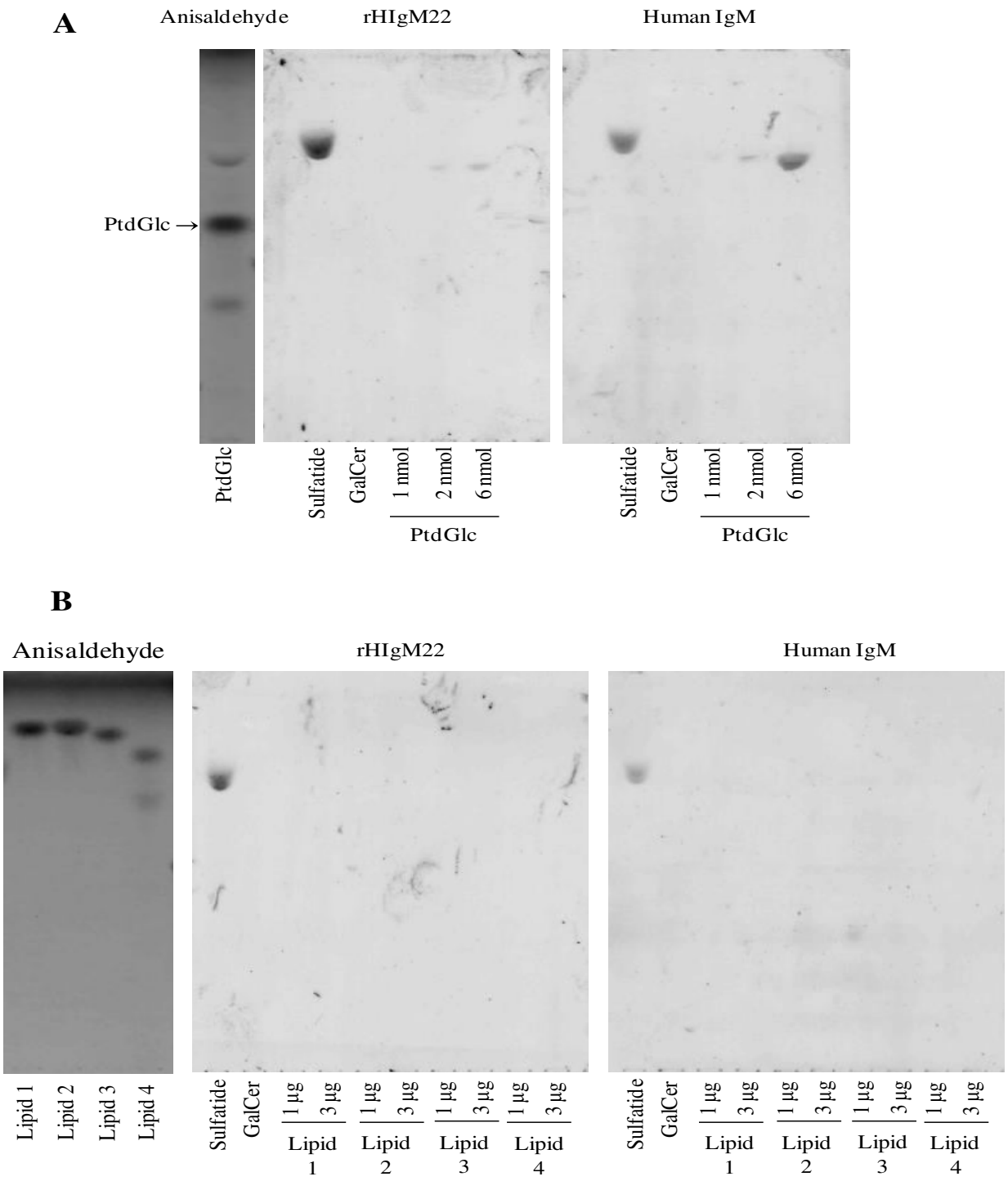

Figure 15. rHIgM22 binding to PtdGlc and structurally related lipids. rHIgM22 binding to PtdGlc (*panel A*) and to four uncharacterized lipids structurally related to PtdGlc (*panel B*) was assessed using TLC immunostaining. Briefly, after chromatographic separation (solvent system: $CHCl_3$:CH_3OH:$CaCl_2$ 50:42:11), TLC plates were fixed with a polyisobuthylmethacrylate solution, air dried and incubated with 3% BSA in PBS for 1h. The plates were then incubated with either rHIgM22 or Human IgM (negative control) at 5 µg/mL in 1% BSA in PBS overnight at 4°C. The plates were then incubated with a HRP-conjugated anti-Human IgM µ-chain antibody for 1 hour, RT, and developed using *o*-phenylenediamine (OPD)/H_2O_2 in 0.05 M citrate-phosphate buffer pH 5.0.

Binding to glycolipids

As stated in previous sections, the myelin membrane has a high lipid content and is enriched in glycolipids [107, 314], the most abundant being galactosylceramide. Another major component of the myelin membrane is sphingomyelin (~5% of total lipids). Gangliosides, on the other hand, are minor components of the myelin membrane (<1% of total lipids) [105].

Binding of rHIgM22 to different glycolipids was assessed using TLC immunostaining. rHIgM22 was not able to bind significantly to galactosylceramide, lactosylceramide (LacCer), sphingomyelin (SM), nor to any of the gangliosides analyzed (Figure 16, panel A-B). A recent paper by Nair S. et al [319], reported that immunoglobulins present in the sera of patients with monoclonal gammopathies are reactive not only against lyso-PC, but also against glucosylsphingosine (GlcSph, lyso-GlcCer), so binding to glucosylsphingosine was assessed. Due to its role as a precursor for the synthesis of GlcSph, the binding to glucosylceramide (GlcCer) was also analyzed. Nor rHIgM22, nor control IgM, however, showed a significant binding to any of the aforementioned lipids (Figure 16, panel C).

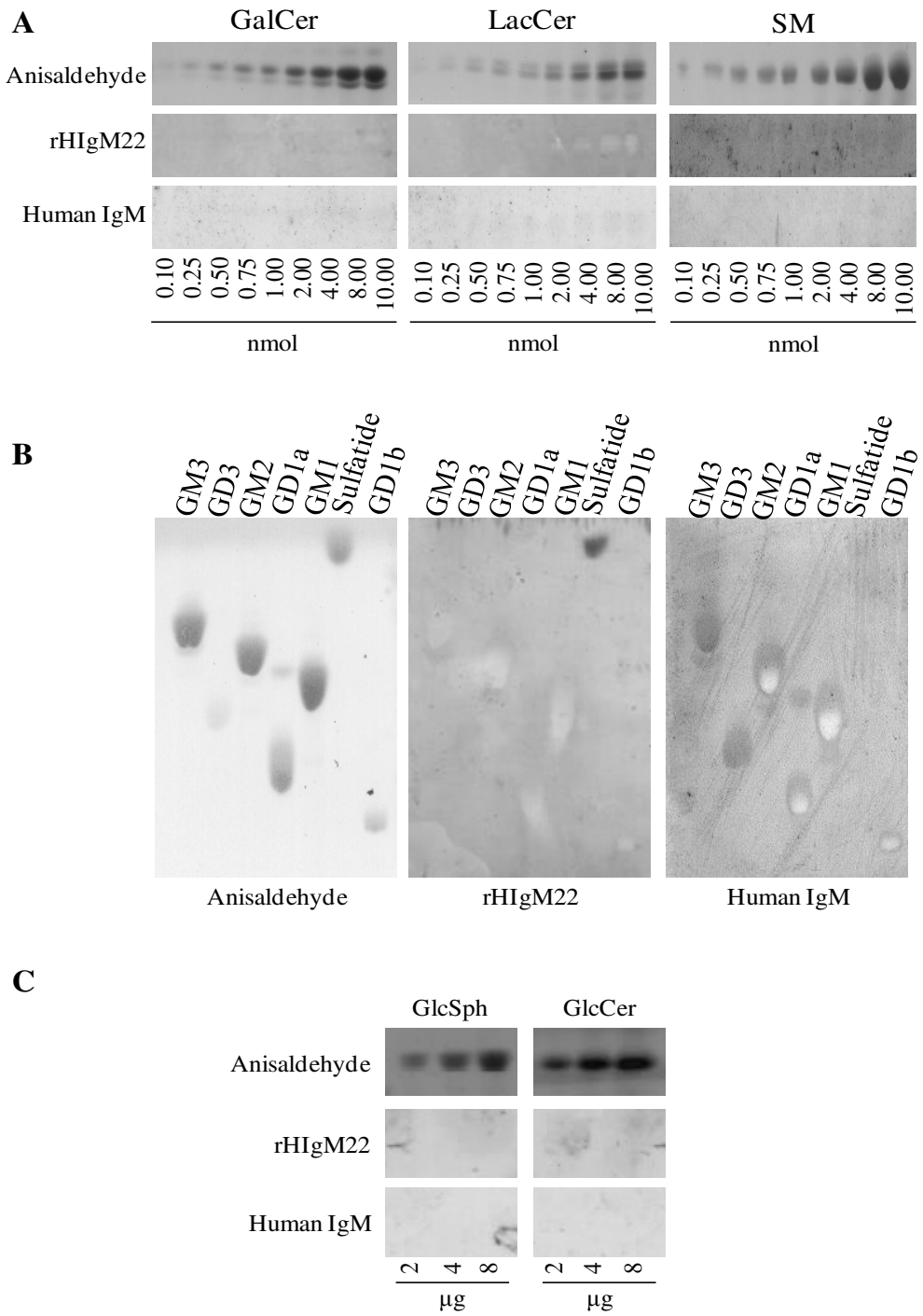

Figure 16. rHIgM22 binding to glycolipids in TLC immunostaining. rHIgM22 binding to different glycolipids was assessed using TLC immunostaining. Briefly, after chromatographic separation (solvent system: $CHCl_3$:CH_3OH:H_2O 110:40:6, panel A; $CHCl_3$:CH_3OH:$CaCl_2$ 50:42:11, panel B), TLC plates were fixed with a polyisobuthylmethacrylate solution, air dried and incubated with 3% BSA in PBS for 1 hour. The plates were then incubated with either rHIgM22 or Human IgM (negative control) at 5 µg/mL in 1% BSA in PBS for 2 hours at room temperature (RT). Gangliosides were deposited at 3 µg each. The plates were then incubated with a HRP-conjugated anti-Human IgM µ-chain antibody for 1 hour at RT, and immunoreactive bands were revealed using *o*-phenylenediamine (OPD)/H_2O_2 in 0.05 M citrate-phosphate buffer pH 5.0.

TLC immuno-dot blot

The data obtained allowed to establish that rHIgM22 is able to bind to sulfatide and to lysosulfatide, in both TLC immunostaining assays and in surface plasmon resonance experiments. rHIgM22 however does not bind to other sphingolipids *in vitro*. On the other hand, this antibody shows a weak binding to some glycerophospholipids, especially PE. To quantitatively compare the binding of rHIgM22 and control IgM to sulfatide and PE in a different experimental setting, TLC-dot blot was set up. In these experiments, equimolar amounts of GalCer were used as background signals, since the previous experiments showed very weak or no binding for both rHIgM22 and control IgM to these lipids. As shown in Figure 17, for all the amounts of sulfatide and PE tested, the ratios of the binding signals between sulfatide and GalCer for rHIgM22 were always higher than those for control IgM, while the ratios of the binding signals between sulfatide and PE for rHIgM22 were always lower than those for control IgM, suggesting that rHIgM22 binding to sulfatide is specific, while rHIgM22 binding to PE is not. This hypothesis was further confirmed by TLC immunostaining experiments performed using stringent blocking conditions for non-specific binding, in particular by adding 1% heat-inactivated goat serum to the primary antibody (rHIgM22 or control IgM) solutions during incubation. In the presence of goat serum, binding of rHIgM22 to sulfatide was lower than in the absence of goat serum, however still detectable, while binding of rHIgM22 to PE, as well as binding control IgM to sulfatide or to PE was completely abolished (Figure 18).

Using the TLC-dot blot approach, binding of rHIgM22 to sulfatide under different conditions of incubation of the primary antibody, was also assessed. In particular, the binding was analyzed modifying either time (2 hours *vs* overnight), temperature (room temperature *vs* 4°C) or stringency (presence or absence of 1% heat-inactivated goat serum in the antibody diluting solution). The data obtained suggests that a longer incubation time and a lower temperature might be enough to overcome the stability problems associated with the primary antibody (Figure 19). Regarding the addition of goat serum, these results, and the ones shown in Figure 18, suggest that it might be more useful in the analysis of lipid extracts than in the analysis of pure lipids.

A

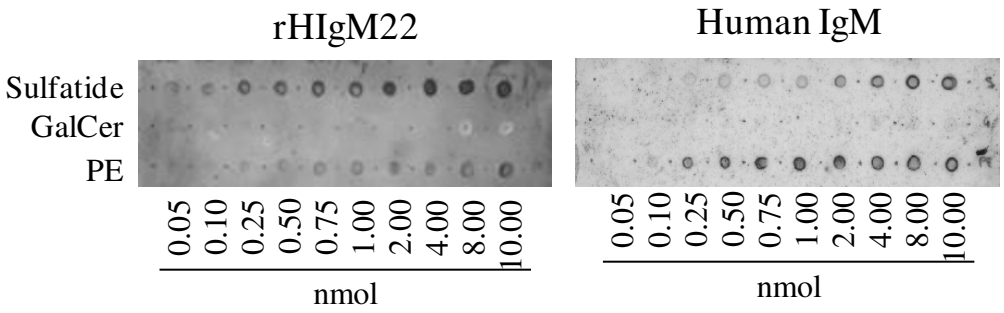
rHIgM22
Human IgM
Sulfatide
GalCer
PE
0.05
0.10
0.25
0.50
0.75
1.00
2.00
4.00
8.00
10.00
nmol

B

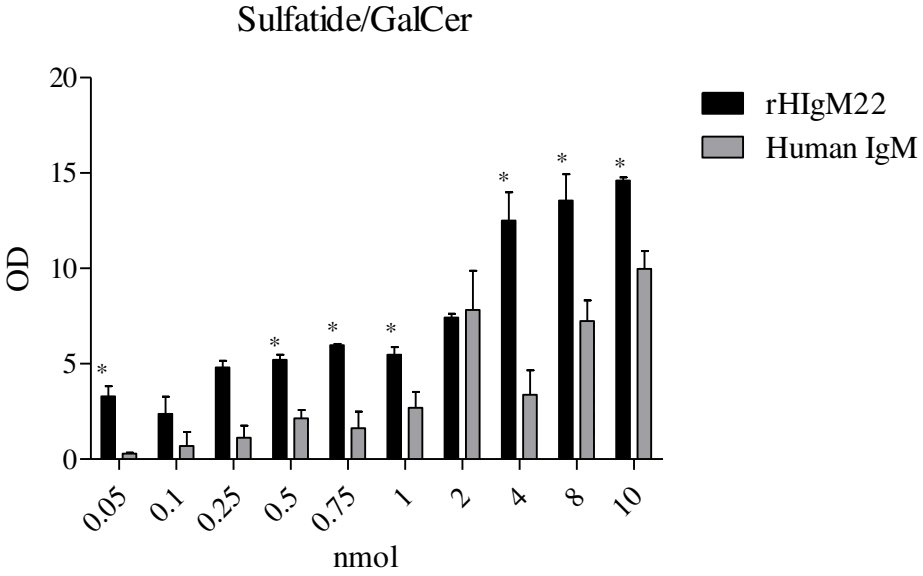
Sulfatide/GalCer
OD
20
15
10
5
0
rHIgM22
Human IgM
0.05
0.1
0.25
0.5
0.75
1
2
4
8
10
nmol

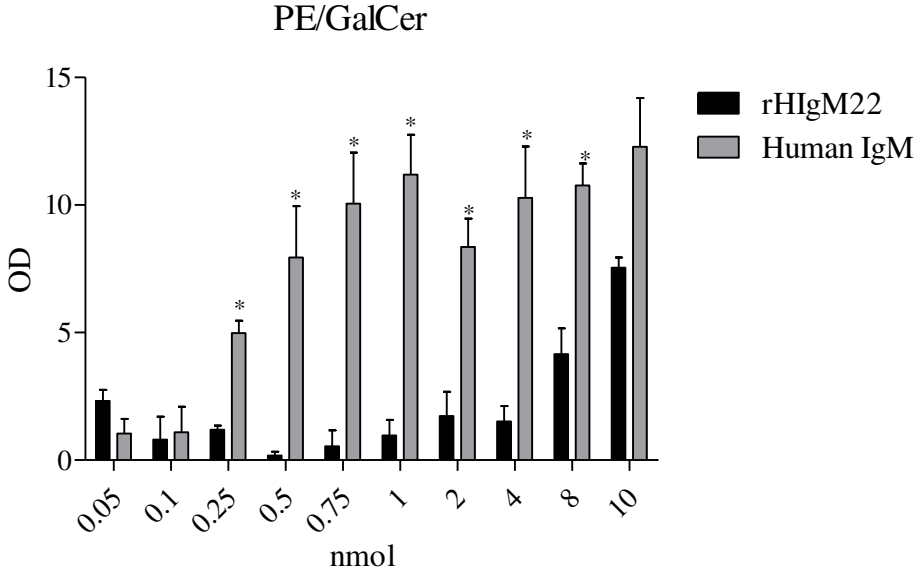
PE/GalCer
OD
15
10
5
0
rHIgM22
Human IgM
0.05
0.1
0.25
0.5
0.75
1
2
4
8
10
nmol

Figure 17. rHIgM22 binding to purified PE, GalCer and sulfatide in TLC immuno-dot blot. rHIgM22 binding to different amounts of various purified lipids was assessed using TLC immuno-dot blot.
Briefly, known amounts of pure lipids were deposited as spot on the TLC plates, without any chromatographic run. TLC plates were fixed with a polyisobuthylmethacrylate solution, air dried and incubated with 3% BSA in PBS for 1 hour. The plates were then incubated with either rHIgM22 or Human IgM (negative control) at 5 μg/mL in 1% BSA in PBS for 2 hours at room temperature (RT). The plates were then incubated with a HRP-conjugated anti-Human IgM μ-chain antibody for 1 hour, RT, and developed using *o*-phenylenediamine (OPD)/H_2O_2 in 0.05 M citrate-phosphate buffer pH 5.0. Optical density of each spot was calculated by densitometry. The obtained density was divided by that of GalCer and the results are reported in *panel C*. Data are expressed as mean ± SD of three different experiments. *, $p<0.05$ versus control.

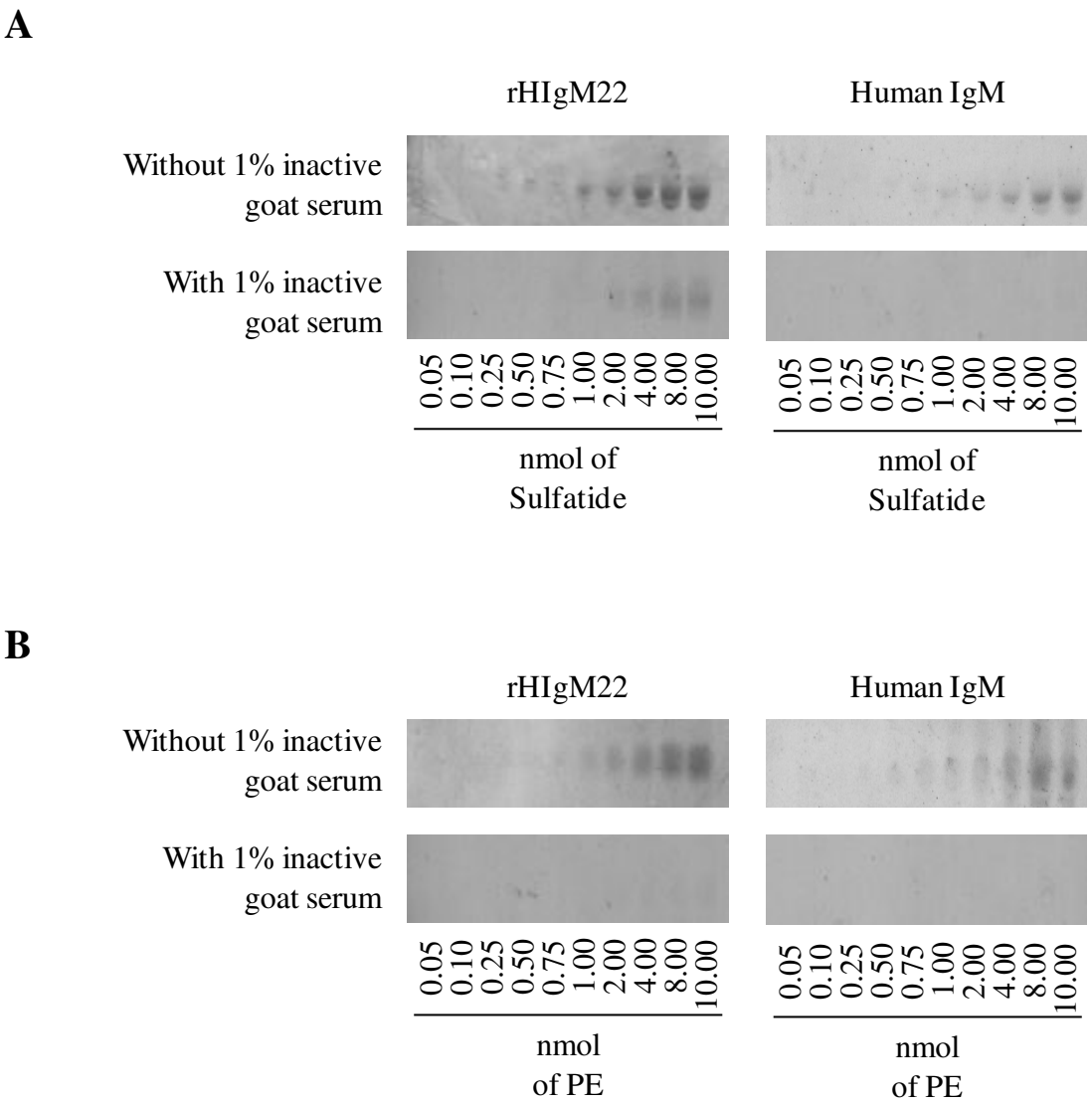

Figure 18. rHIgM22 binding to purified PE and sulfatide in presence of 1% heat-inactived goat serum in TLC immunostaining. rHIgM22 binding to different amounts of purified PE and sulfatide in presence or absence of 1% inactive goat serum was assessed using TLC immunostaining. Briefly, after chromatographic separation (solvent system: $CHCl_3$:CH_3OH:H_2O 110:40:6), TLC plates were fixed with a polyisobuthylmethacrylate solution, air dried and incubated with 3% BSA in PBS for 1 hour. The plates were then incubated with either rHIgM22 or Human IgM (negative control) at 5 µg/mL in 1% BSA in PBS or 5 µg/mL in 1% BSA, 1% heat inactivated goat serum in PBS for 2 hours at room temperature (RT). The plates were then incubated with a HRP-conjugated anti-Human IgM µ-chain antibody for 1 hour, RT, and developed using *o*-phenylenediamine (OPD)/H_2O_2 in 0.05 M citrate-phosphate buffer pH 5.0.

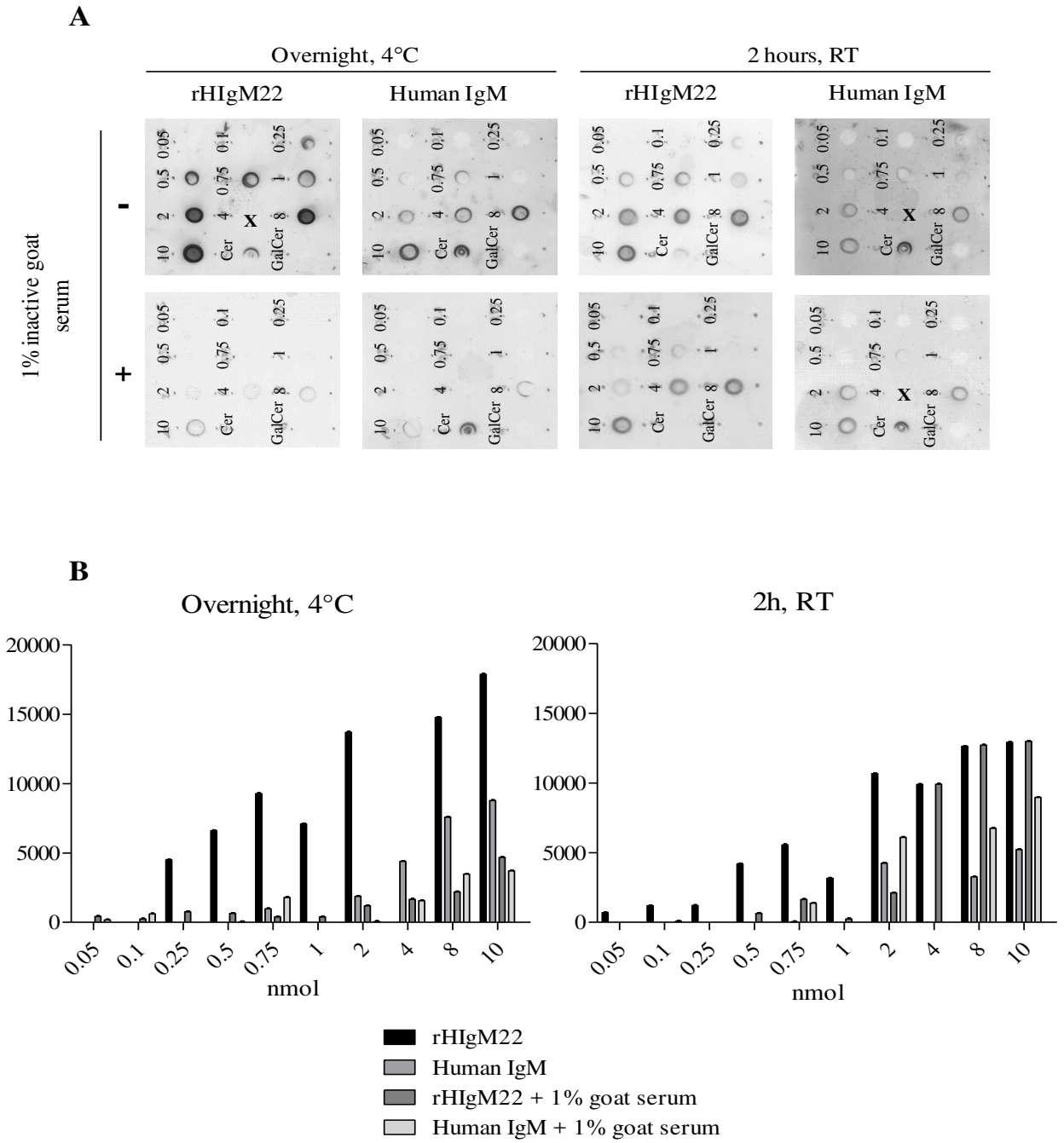

Figure 19. rHIgM22 binding to purified sulfatide in TLC immuno-dot blot. rHIgM22 binding to purified sulfatide was assessed using TLC immuno-dot blot. Briefly, known amounts of pure lipids were deposited as spot on the TLC plates, without any chromatographic run. TLC plates were fixed with a polyisobuthylmethacrylate solution, air dried and incubated with 3% BSA in PBS for 1 hour. The plates were then incubated with either rHIgM22 or Human IgM (negative control) at 5 µg/mL in 1% BSA in PBS ± 1% inactive goat serum either for 2 hours at room temperature (RT) or overnight at 4°C. The plates were then incubated with a HRP-conjugated anti-Human IgM µ-chain antibody for 1 hour, RT, and developed using *o*-phenylenediamine (OPD)/H_2O_2 in 0.05 M citrate-phosphate buffer pH 5.0. Optical density of each spot was calculated by densitometry. The results are reported in the *panel B*. Data in *panel B* is expressed as mean ± SD of three independent experiments.

Effect of different lipids on the binding of rHIgM22 to sulfatide containing monolayers

Previous studies, performed using model membranes, have shown that antibody recognition of sulfatide is affected by the membrane lipid microenvironment. In fact, it has been seen that in a polyclonal anti-sulfatide serum fewer antibodies were able to recognize their own target in a sphingomyelin/cholesterol environment than in a phosphatidylcholine/cholesterol environment. Moreover, length and hydroxylation of fatty acid chain of PC or of SM seemed to restrict the recognition to higher affinity antibodies [321, 322]. Therefore, to verify whether the binding of rHIgM22 could be affected by lipid microenvironment, antibody binding to sulfatide containing monolayers was assessed through surface plasmon resonance experiments. In these experiments, monolayers were prepared by mixing a fixed amount of DOPC and of sulfatide, respectively 1 µmol and 0.01 µmol, with a third lipid using either molar ratios corresponding to those found in the myelin membrane or a 10 fold higher amount of the third lipid (Figure 20-21), reflecting the molar ratio expected for a lipid raft-like microenvironment.

Binding analysis revealed that the binding response of rHIgM22 to sulfatide containing monolayers is reduced in the presence of either GalCer (0.66 or 0.066 µmol) or cholesterol (0.1 µmol), while the addition of SM (0.12 µmol) or of lysosulfatide (0.005 – 0.01 – 0.1 – 0.5 µmol) to the monolayers determined a reduction of the binding. These finding suggest that the presence of different lipids, at a certain density might be required to allow an optimal recognition of the antigen by rHIgM22.

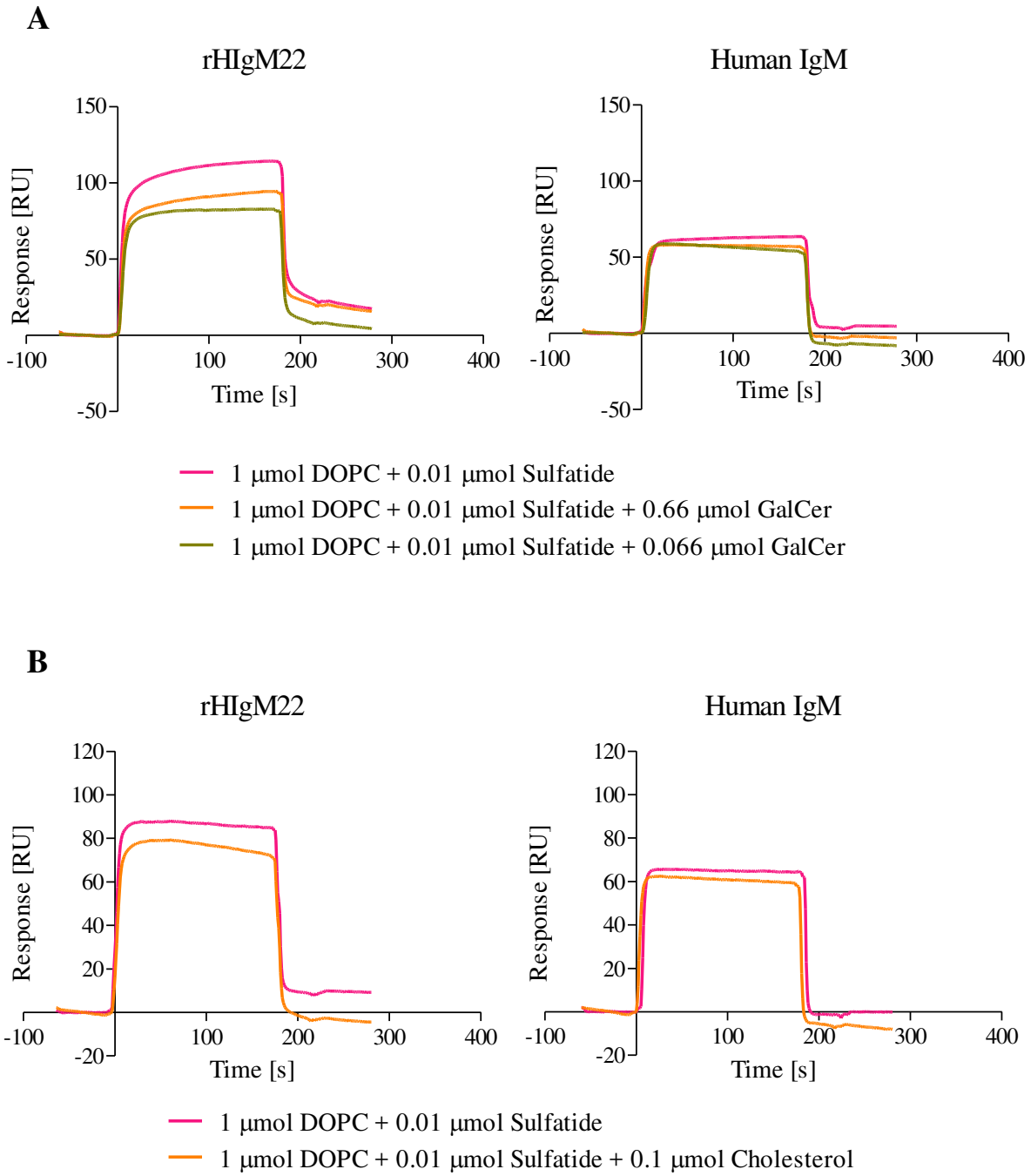

Figure 20. Effect of GalCer and Cholesterol on rHIgM22 binding to sulfatide. DOPC (1 µmol) and Sulfatide (0.01 µmol) were mixed with GalCer (0.66 µmol or 0.066 µmol) (*Panel A*) or with Cholesterol (0.1 µmol) (*Panel B*) and dried. The lipid mixture was resuspended in HBS-N buffer, mixed vigorously and sonicated. The liposome solutions were immobilized on an HPA sensor chip. The surface was washed briefly with 50mM NaOH and blocked with 100 µg/mL BSA. For analysis, 5 µg/mL rHIgM22 or Human IgM was injected.

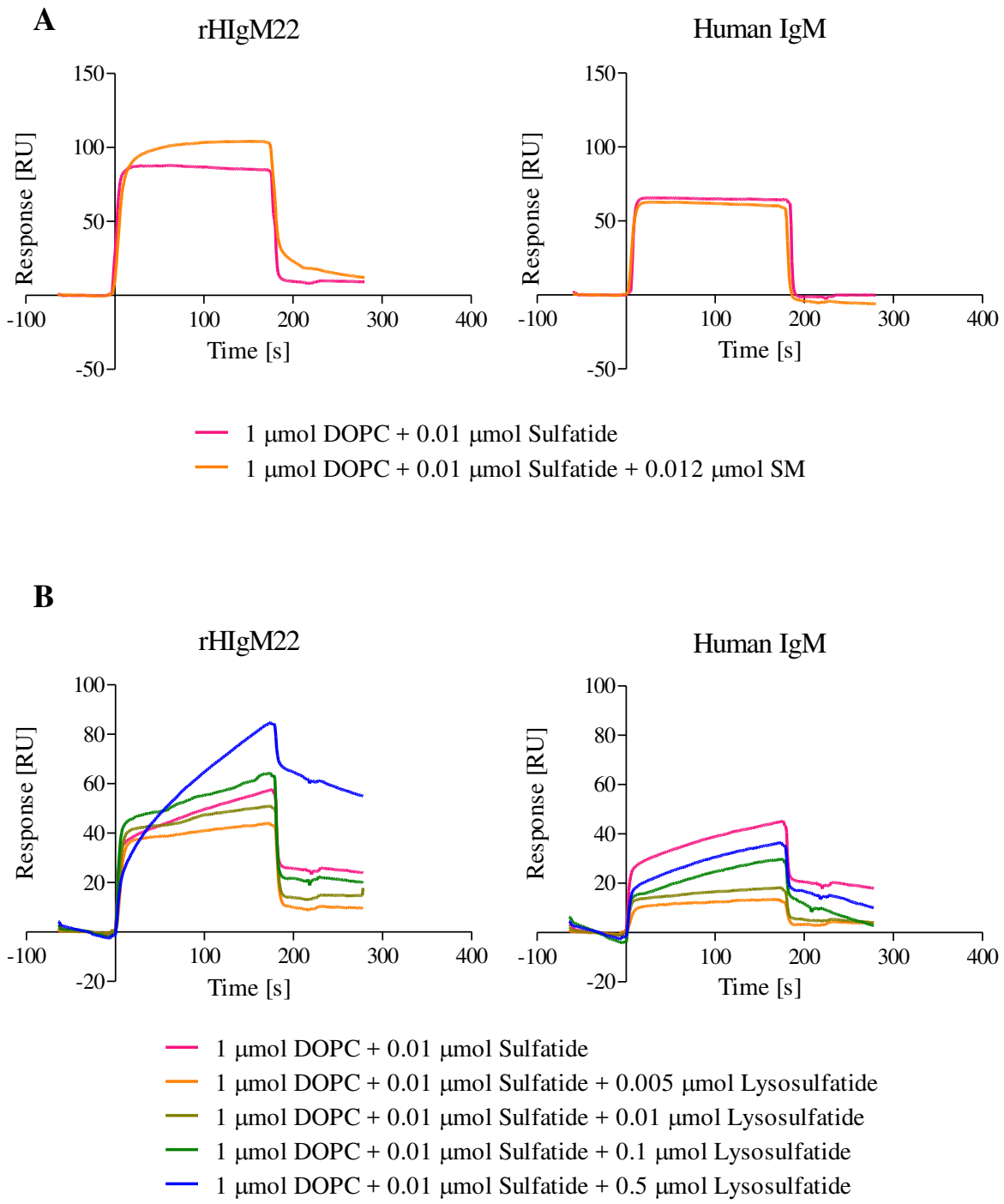

Figure 21. Effect of SM and Lysosulfatide on rHIgM22 binding to sulfatide. DOPC (1 µmol) and Sulfatide (0.01 µmol) were mixed with SM (0.012 µmol) (*Panel A*) or with lysosulfatide (0.005 or 0.01 or 0.1 or 0.5 µmol) (*Panel B*) and dried. The lipid mixture was resuspended in HBS-N buffer, mixed vigorously and sonicated. The liposome solutions were immobilized on an HPA sensor chip. The surface was washed briefly with 50mM NaOH and blocked with 100 µg/mL BSA. For analysis, 5 µg/mL rHIgM22 or Human IgM was injected.

Binding of rHIgM22 to lipid extracts

The experiments described in the previous sections allowed to set up the experimental conditions for the analysis of rHIgM22 binding to lipids after HPTLC separation using the TLC immunostaining procedure. The results obtained from the experiments on pure lipids suggest that rHIgM22 binds to pure sulfatide and, even if weaker, to lysosulfatide and to phosphatidic acid, whereas it does not show any significant binding to any other sphingolipid. On the other hand, a weak binding to glycerophospholipids was observed for both rHIgM22 and control IgM. The experiments that will be described in the following sections were aimed to analyze the binding of rHIgM22 to lipid mixtures obtained from a variety of relevant biological samples. Using standard lipid extraction and purification procedures, we have prepared a total lipid extract that has been further fractionated as described in Materials and Methods. The decision to prepare partially purified lipid mixtures from biological samples was taken considering that glycerophospholipids, that are present in higher amounts than sulfatide and sphingolipids in general in total lipid extracts, represent a significant source of interference in the TLC immunostaining procedure. Total lipid extracts (TLE), prepared in the experimental conditions used, contain all cellular lipids, including hydrophobic (cholesterol and triglycerides) and amphipathic lipids: glycerophospholipids and sphingolipids, neutral glycosphingolipids (GlcCer, LacCer, and in myelin and myelin producing cells, GalCer), and acidic sphingolipids (gangliosides, enriched in neurons, and sulfatide, enriched in myelin). Total lipid extracts were subjected to a two-phase Folch's partitioning (with minor modifications) and further purified using procedures aimed at obtaining lipid mixtures devoid of potentially interfering glycerophospholipids and enriched in sulfatide and other sphingolipids. Figures 22-27 show representative patterns obtained after chromatographic separation and chemical detection of the different lipid samples that we have prepared to be tested for the binding to rHIgM22 by immuno-TLC. The patterns are consistent with the known lipid composition of the biological samples.

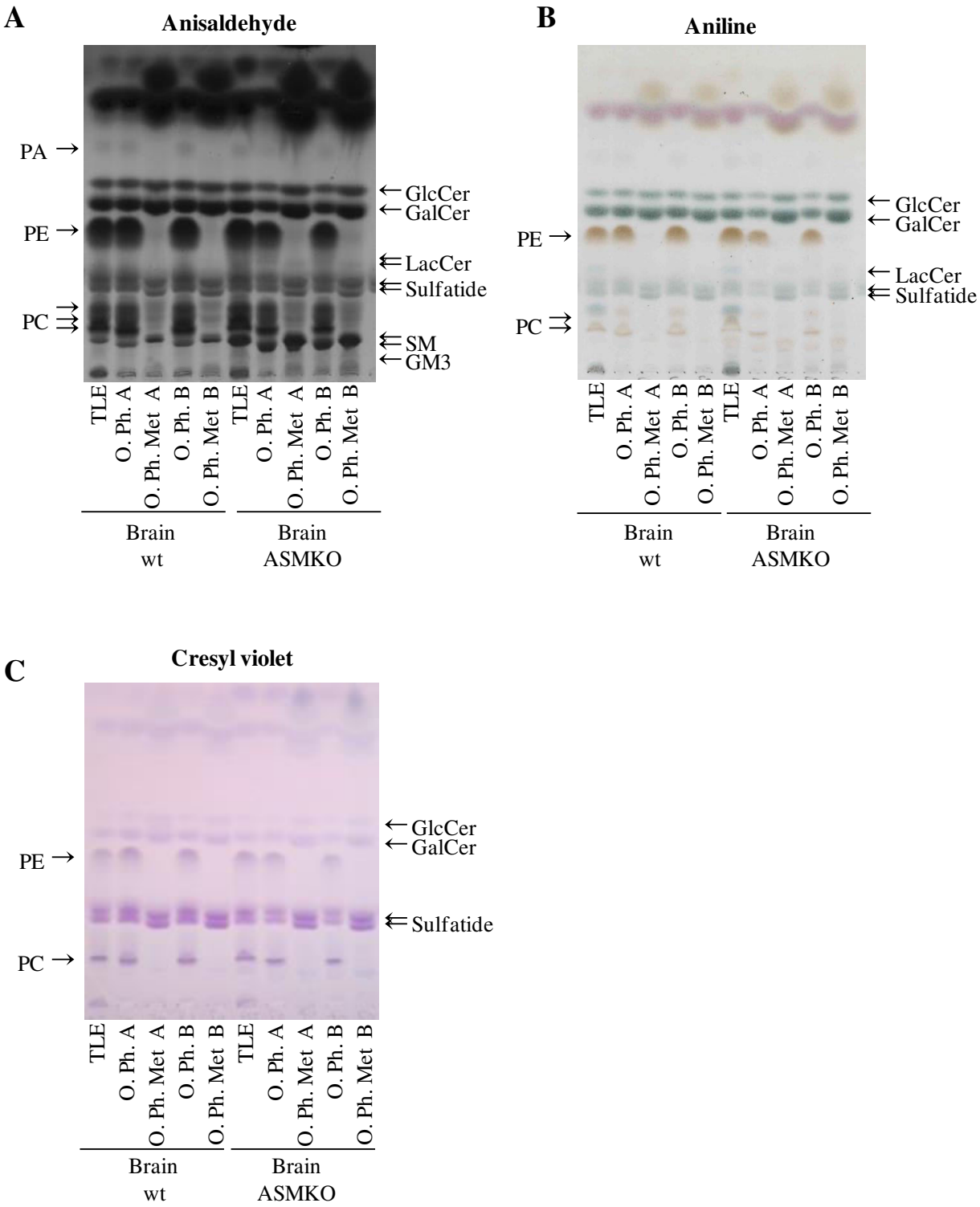
A
Anisaldehyde
PA
PE
PC
GlcCer
GalCer
LacCer
Sulfatide
SM
GM3
TLE
O. Ph. A
O. Ph. Met A
O. Ph. B
O. Ph. Met B
Brain wt
Brain ASMKO
B
Aniline
PE
PC
GlcCer
GalCer
LacCer
Sulfatide
C
Cresyl violet
PE
PC
GlcCer
GalCer
Sulfatide

Figure 22. TLC analysis of total lipid extracts and organic phases from mouse brain. Frozen brains from C57BL/6N mice (either wild type or ASMKO) ranging from 7 to 10 months of age were resuspended in ice-cold water and briefly subjected to sonication before being lyophilized. The samples were then subjected to lipid extraction with $CHCl_3$:CH_3OH:H_2O 20:10:1 (v/v/v). Two aliquots of TLE were further subjected to a two-phase partitioning resulting in the separation of an aqueous phase containing gangliosides and in an organic phase containing all other lipids. One aliquot was partitioned adding 20% (volume) of water, the other adding 20% of 0.88% aqueous KCl. Aliquots of the organic phases were then subjected to alkaline treatment to remove glycerophospholipids. For the analysis, we loaded 400 µg protein for each TLE, 350 µg for O. Ph. and Met. O. Ph. Wt, and 250 µg for O. Ph. and Met. O. Ph. ASMKO. The lipids were analyzed by HPTLC, using either $CHCl_3$:CH_3OH:H_2O 110:40:6 (*Panel A and B*) or $CHCl_3$:CH_3OH:H_2O 70:25:4 (*Panel C*). The lipids were then revealed using colorimetric detection (*Panel A*: anisaldehyde; *panel B*: aniline; *panel C*: cresyl violet).

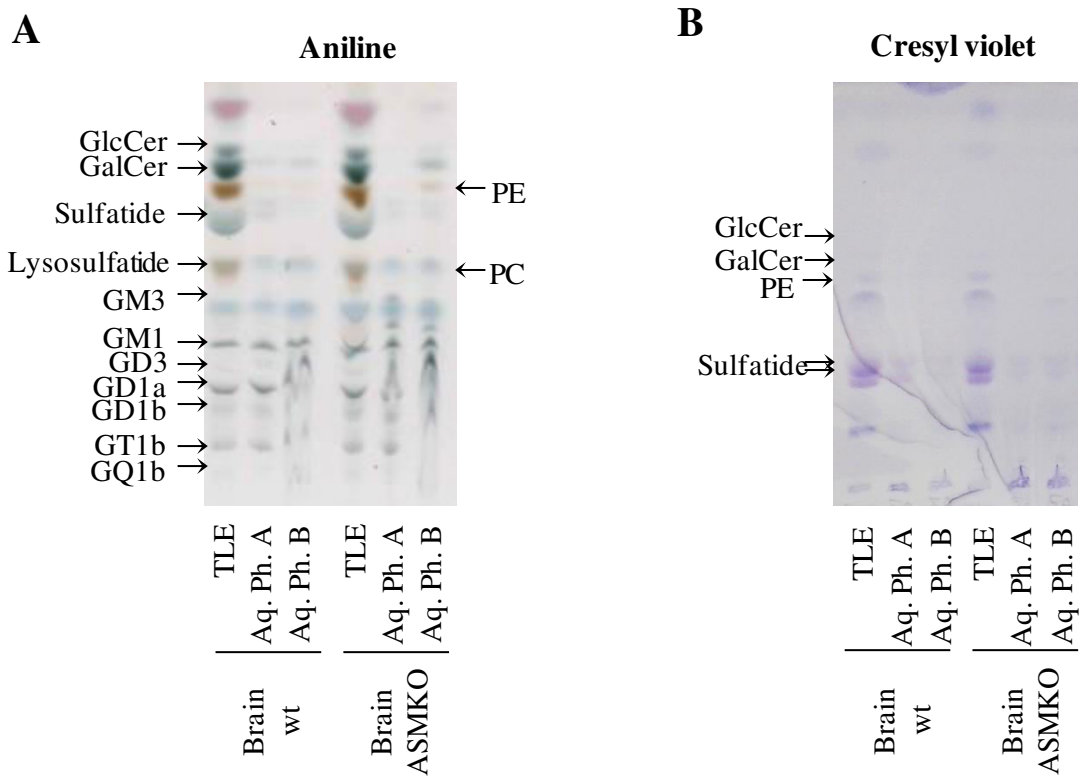

Figure 23. TLC analysis of total lipid extracts and aqueous phases from mouse brain. Frozen brains from C57BL/6N mice (either wild type or ASMKO) ranging from 7 to 10 months of age were resuspended in ice-cold water and briefly subjected to sonication before being lyophilized. The samples were then subjected to lipid extraction with $CHCl_3$:CH_3OH:H_2O 20:10:1 (v/v/v). Two aliquots of TLE were further subjected to a two-phase partitioning resulting in the separation of an aqueous phase containing gangliosides and in an organic phase containing all other lipids. For the analysis, we loaded 400 µg protein for each brain sample. The lipids were analyzed by HPTLC, using either $CHCl_3$:CH_3OH:$CaCl_2$ 0.2% 50:42:11 (*Panel A*) or $CHCl_3$:CH_3OH:H_2O 70:25:4 (*Panel B*). The lipids were then revealed using colorimetric detection (*Panel A*: anisaldehyde; *panel B*: cresyl violet).

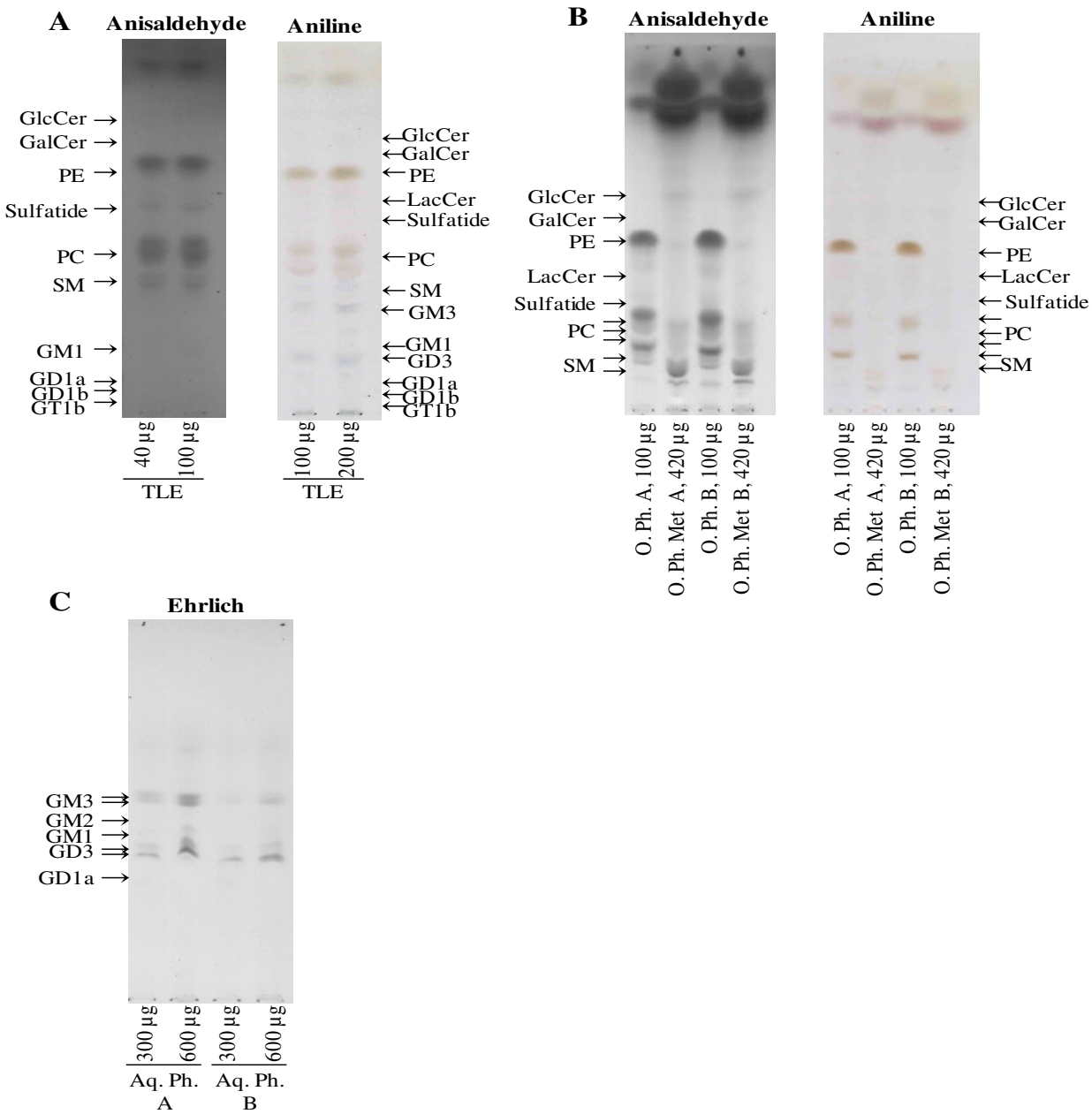

Figure 24. TLC analysis of total lipid extracts, organic phases, and aqueous phases from mixed glial cells. Mixed glial cells at the 14th day of culture were collected in PBS and frozen. The frozen cells were then resuspended in water and lyophilized.Lyophilized samples were then subjected to lipid extraction with $CHCl_3$:CH_3OH:H_2O 20:10:1 (v/v/v). Two aliquots of TLE were further subjected to a two-phase partitioning resulting in the separation of an aqueous phase containing gangliosides and in an organic phase containing all other lipids. One aliquot was partitioned adding 20% (volume) of water, the other adding 20% of 0.88% aqueous KCl. Aliquots of the organic phases were then subjected to alkaline treatment to remove glycerophospholipids. The lipids were analyzed by HPTLC, using either $CHCl_3$:CH_3OH:$CaCl_2$ 0.2% 60:35:8 (*Panel A*), $CHCl_3$:CH_3OH:H_2O 110:40:6 (*Panel B*) or $CHCl_3$:CH_3OH:H_2O 70:25:4 (*Panel C*). The lipids were then revealed using colorimetric detection (*Panel A and B*: anisaldehyde and aniline; *panel C*: Ehrlich).

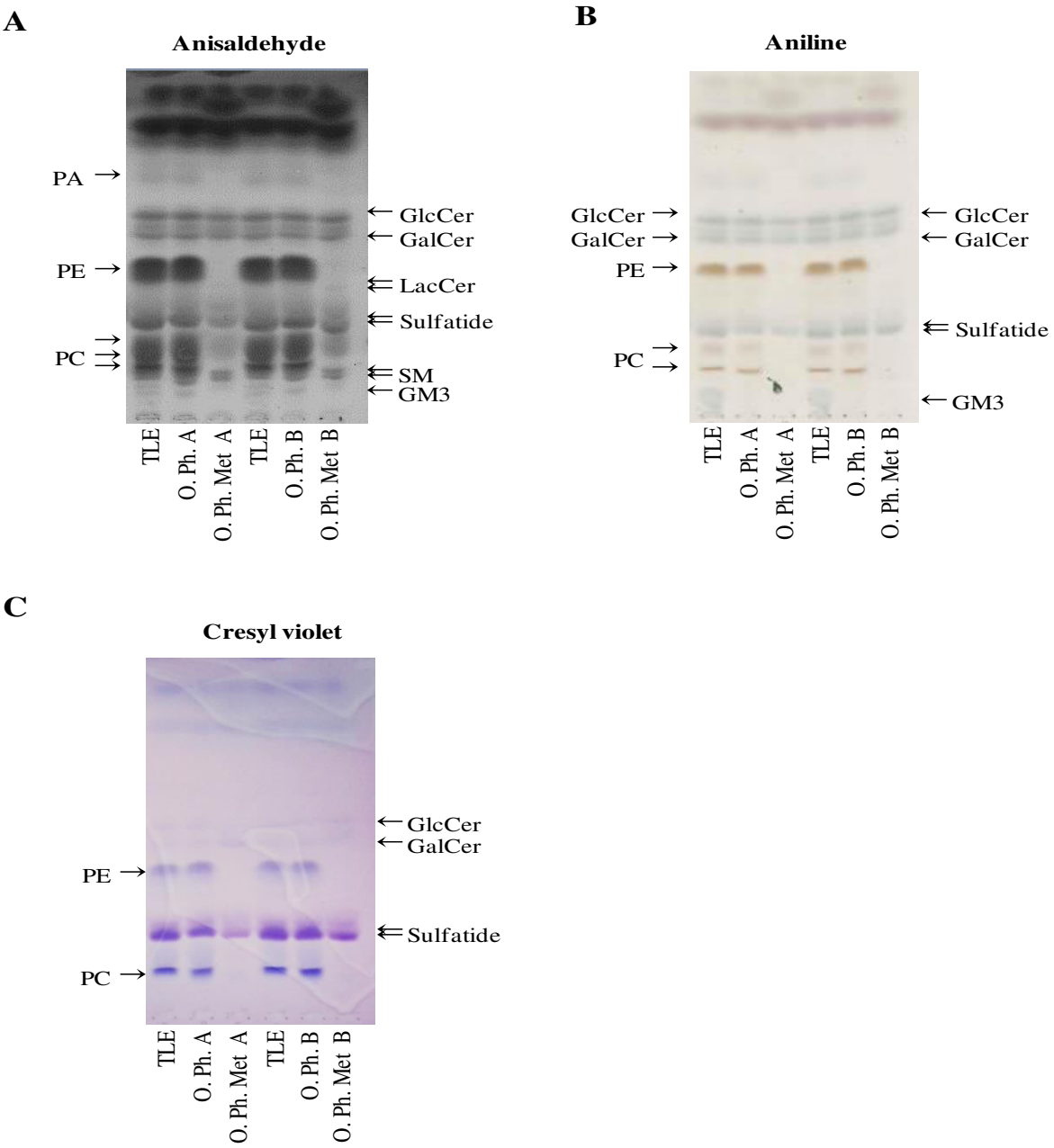

Figure 25. TLC analysis of total lipid extracts, organic phases from rHIgM22 positive oligodendrocytes. The frozen OPC were resuspended in water and lyophilized. Lyophilized samples were then subjected to lipid extraction with $CHCl_3$:CH_3OH:H_2O 20:10:1 (v/v/v). Two aliquots of TLE were further subjected to a two-phase partitioning resulting in the separation of an aqueous phase containing gangliosides and in an organic phase containing all other lipids. One aliquot was partitioned adding 20% (volume) of water, the other adding 20% of 0.88% aqueous KCl. Aliquots of the organic phase were then subjected to alkaline treatment to remove glycerophospholipids from the phase. For the analysis, we loaded 200 µg protein for each sample. The lipids were analyzed by HPTLC, using either $CHCl_3$:CH_3OH:H_2O 110:40:6 (*Panel A and B*) or $CHCl_3$:CH_3OH:H_2O 70:25:4 (*Panel C*). The lipids were then revealed using colorimetric detection (*Panel A*: anisaldehyde; *panel B*: aniline; *panel C*: cresyl violet).

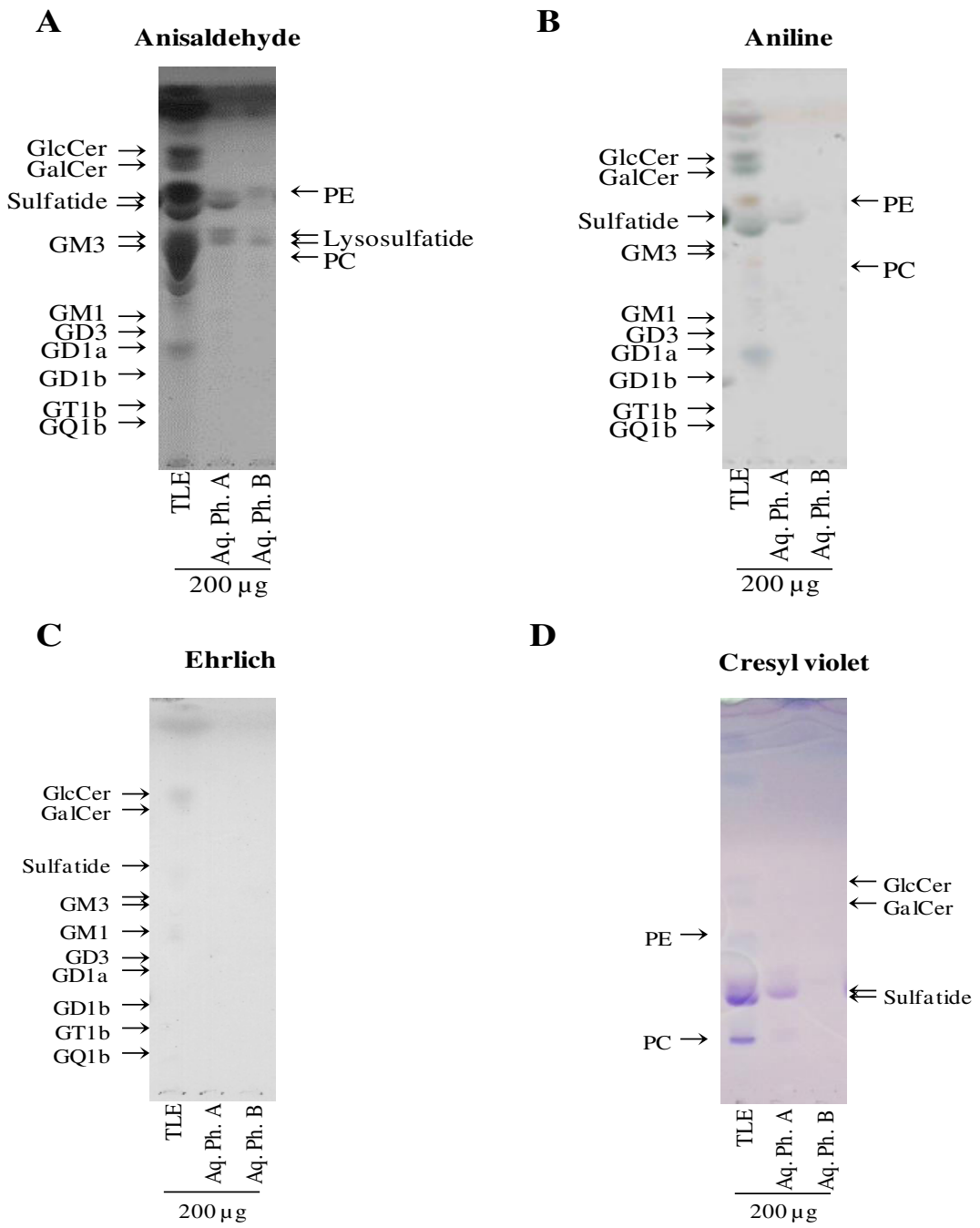

Figure 26. TLC analysis of total lipid extracts and aqueous phases from rHIgM22 positive oligodendrocytes. The frozen OPC cells were resuspended in water and lyophilized. Lyophilized samples were then subjected to lipid extraction with $CHCl_3$:CH_3OH:H_2O 20:10:1 (v/v/v). Two aliquots of TLE were further subjected to a two-phase partitioning resulting in the separation of an aqueous phase containing gangliosides and in an organic phase containing all other lipids. One aliquot was partitioned adding 20% (volume) of water, the other adding 20% of 0.88% aqueous KCl. For the analysis, we loaded 200 µg protein for each sample. The lipids were analyzed by HPTLC, using either $CHCl_3$:CH_3OH:$CaCl_2$ 0.2% 50:42:11 (*Panel A, B, and C*) or $CHCl_3$:CH_3OH:H_2O 70:25:4 (*Panel D*). The lipids were then revealed using colorimetric detection (*Panel A*: anisaldehyde; *panel B*: aniline; *panel C*: Ehrlic's reagent; *panel D*: cresyl violet).

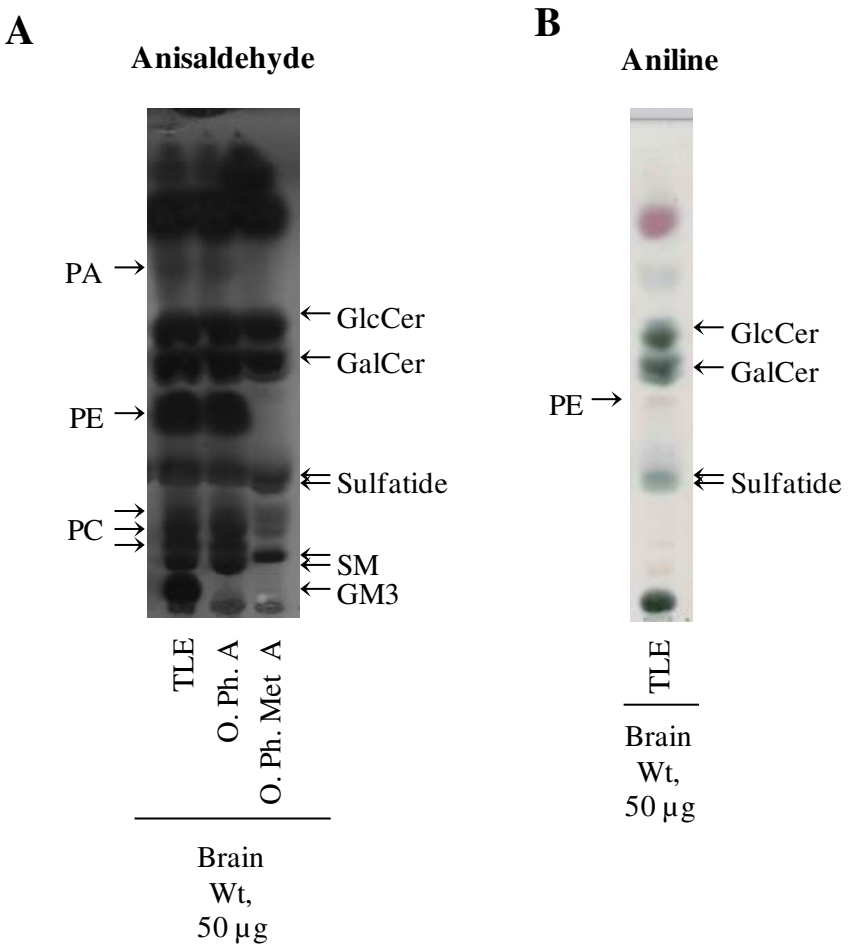

Figure 27. TLC analysis of total lipid extracts, organic phases from mouse myelin. Frozen myelin samples were resuspended in water and lyophilized. Lyophilized samples were then subjected to lipid extraction with $CHCl_3$:CH_3OH:H_2O 20:10:1 (v/v/v). Two aliquots of TLE were further subjected to a two-phase partitioning resulting in the separation of an aqueous phase containing gangliosides and in an organic phase containing all other lipids. One aliquot was partitioned adding 20% (volume) of water, the other adding 20% of 0.88% aqueous KCl. Aliquots of the organic phases were then subjected to alkaline treatment to remove glycerophospholipids. For the analysis, we loaded 50 µg protein for each sample. The lipids were analyzed by HPTLC, using either $CHCl_3$:CH_3OH:H_2O 110:40:6 (*Panel A and B*). The lipids were then revealed using colorimetric detection (*Panel A*: anisaldehyde; *panel B*: aniline).

Binding to total lipid extracts and organic phases

Binding of rHIgM22 to various lipid samples was assessed using TLC immunostaining. Total lipid extracts and organic phases from different CNS cells and tissues (mixed glial cells, mice brain, oligodendrocytes, and myelin) were analyzed and, as shown in Figure 28, the presence of glycerophospholipids in these samples strongly affected the binding of both rHIgM22 and control IgM. Both the antibodies, in fact, showed a binding to multiple bands with an intensity that was not proportional to the amount of the lipid samples. Therefore, even if the amount of sulfatide theoretically present in the samples was comparable to the amount detectable using pure sulfatide, the identification of signals corresponding to sulfatide was impossible. The removal of glycerophospholipids through alkali treatment of the organic phases proved to be a useful tool for the analysis of the binding of rHIgM22. When the binding of rHIgM22 to the methanolyzed organic phases, devoid of glycerophospholipids, was assessed through TLC immunostaining, a double band co-migrating with the sulfatide standard was detectable in all the samples analyzed (Figure 29). The control IgM also shows a weak reactivity for the same antigen however the binding of control IgM is significantly lower than that of rHIgM22 in all the analyzed samples.

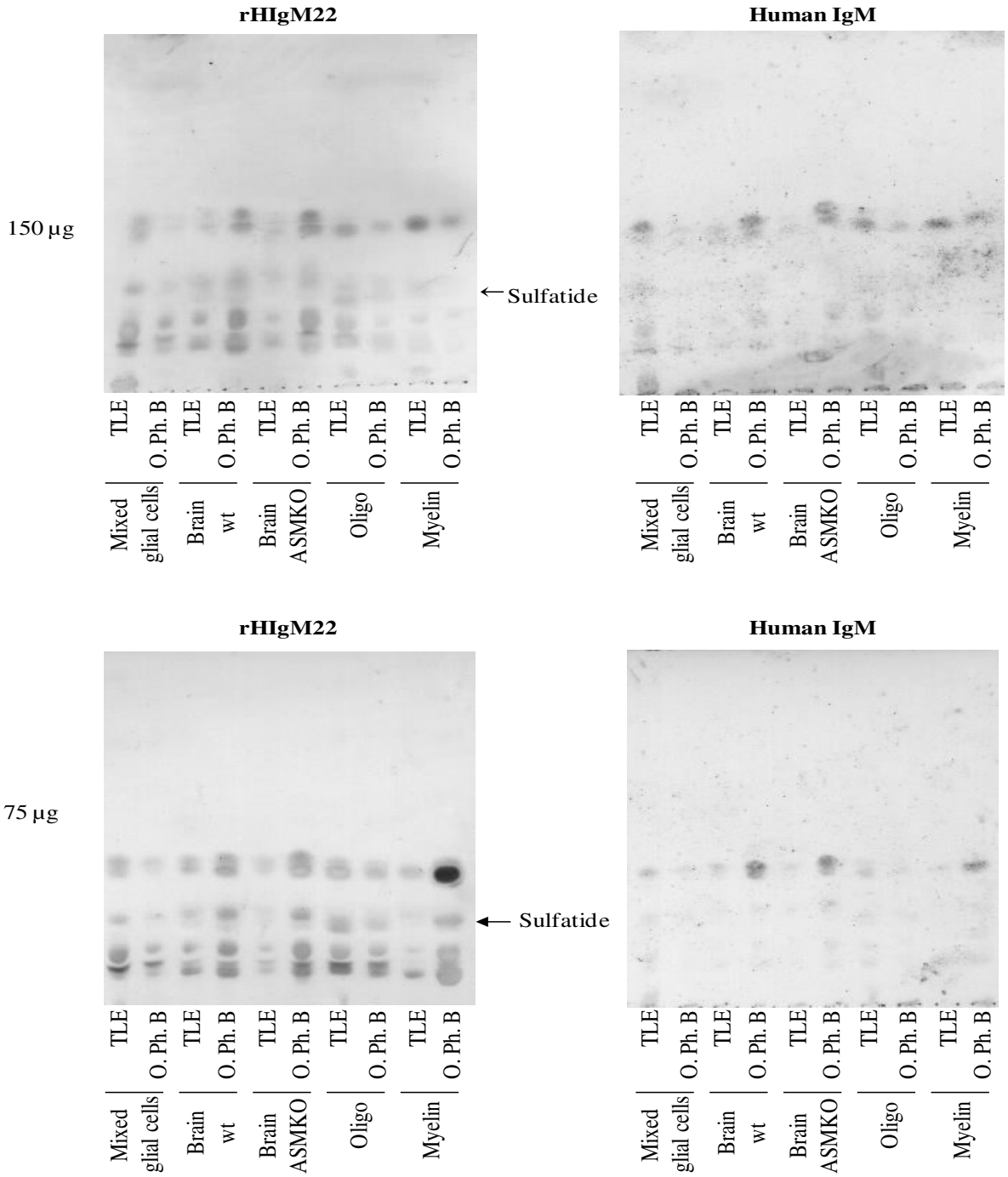
rHIgM22
Human IgM
150 µg
75 µg
Sulfatide
Sulfatide
Mixed glial cells
Brain wt
Brain ASMKO
Oligo
Myelin
TLE
O. Ph. B

Figure 28. rHIgM22 binding to total lipid extracts and organic phases. Using TLC immunostaining we assessed rHIgM22 binding to different total lipid extracts (TLE) and organic phases (O.Ph.) obtained from different cells and tissues such as mixed glial cells, wild type mouse brain, ASMKO mouse brain, rHIgM22 positive OPC, and mouse myelin. For each extract and organic phase, either 150 µg protein (*Panel A*) or 75 µg protein (*Panel B*) were loaded on the TLC plates. The organic phases used for the analysis were obtained through partition in presence of 0.88% aqueous KCl. After chromatographic separation (solvent system: $CHCl_3$:CH_3OH:H_2O 110:40:6), TLC plates were fixed with a polyisobuthylmethacrylate solution, air dried and incubated with 3% BSA in PBS for 1h. The plates were then incubated with either rHIgM22 or Human IgM (negative control) at 5 µg/mL in 1% BSA in PBS or 5 µg/mL in 1% BSA, 1% heath inactivated goat serum in PBS for 2 hours at room temperature (RT). The plates were then incubated with a HRP-conjugated anti-Human IgM µ-chain antibody for 1 hour, RT, and developed using *o*-phenylenediamine (OPD)/H_2O_2 in 0.05 M citrate-phosphate buffer pH 5.0.

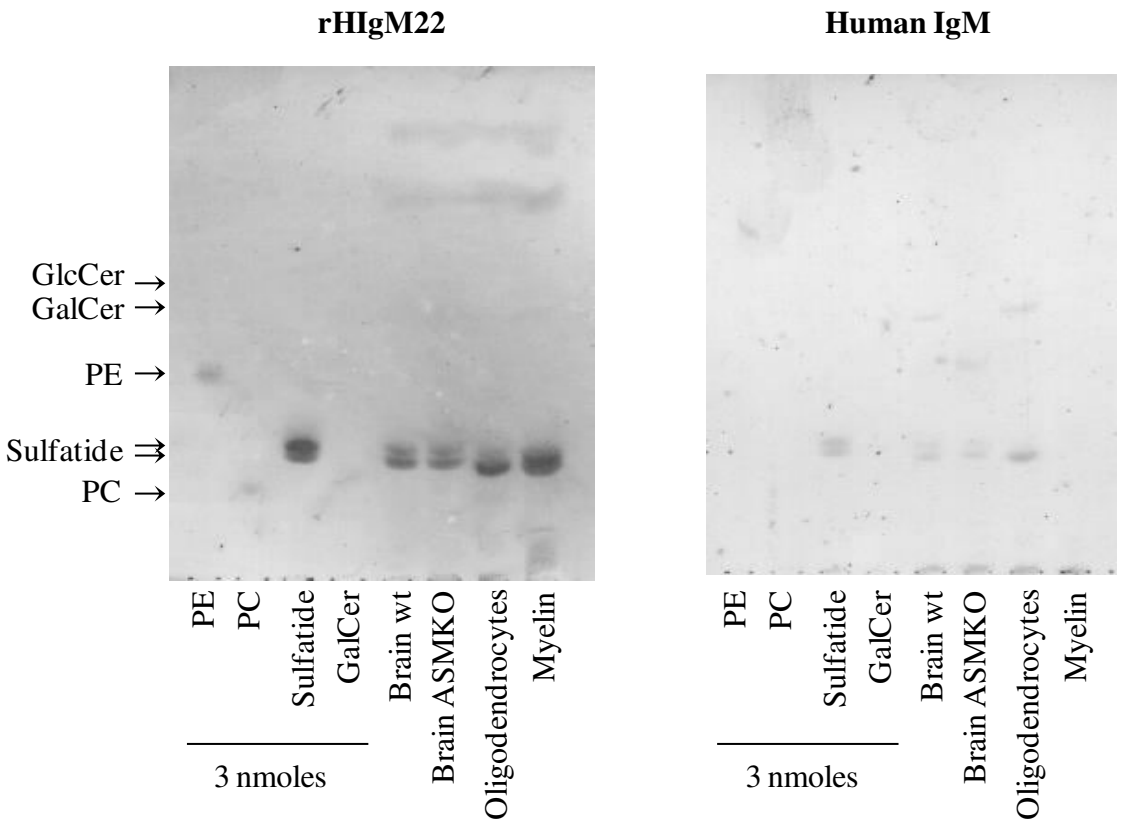

Figure 29. rHIgM22 binding to methanolyzed organic phases in TLC immunostaining. Using TLC immunostaining we assessed rHIgM22 binding to methanolyzed organic phases (O.Ph.Met) obtained from different tissues such as wild type mouse brain, ASMKO mouse brain, rHIgM22 positive OPC, and mouse myelin. For each methanolyzed organic phase amounts equivalent to 150 µg protein were loaded on the plate, while for each pure lipid standard 3 nmol were loaded. The methanolyzed organic phases used for the analysis were obtained from organic phases partitioned in presence of 0.88% aqueous KCl. After chromatographic separation (solvent system: $CHCl_3$:CH_3OH:H_2O 110:40:6), TLC plates were fixed with a polyisobuthylmethacrylate solution, air dried and incubated with 3% BSA in PBS for 1h. The plates were then incubated with either rHIgM22 or Human IgM (negative control) at 5 µg/mL in 1% BSA, 1% heath inactivated goat serum in PBS for 2 hours at room temperature (RT).
The plates were then incubated with a HRP-conjugated anti-Human IgM µ-chain antibody for 1 hour, RT, and developed using o-phenylenediamine (OPD)/H_2O_2 in 0.05 M citrate-phosphate buffer pH 5.0.

Binding to aqueous phases

Aqueous phases obtained partitioning in presence of water, which contained a significant amount of sulfatide, were also analyzed using TLC immunostaining (Figure 30). rHIgM22-immunoreactive bands co-migrating with the sulfatide standard were observed in samples from mice brain, rHIgM22 positive oligodendrocytes, and myelin. Interestingly, in all the samples the presence of a second rHIgM22 immunoreactive antigen, migrating below sulfatide, was observed. The position of these bands corresponds to that of the pure lysosulfatide standard, however literature suggests that lysosulfatide levels are quite low in non-pathological nervous tissue. Moreover, the experiments performed on pure lysosulfatide indicated that the binding of rHIgM22, at least in these experimental settings, should be weaker than the one to sulfatide. Nevertheless, the signal corresponding to these bands resulted quite strong, suggesting that rHIgM22 might recognize this antigen with a stronger affinity than that to sulfatide. Remarkably, this unidentified rHIgM22 positive antigen is also present in the aqueous phases obtained from samples that do not contain any sulfatide. In fact, it is present in aqueous phases from hemibrains harvested from mice that are knock-out for the cerebroside sulfotransferase (CST) enzyme, responsible for the synthesis of sulfatide. Moreover, the antigen can be detected in samples from mixed glial cell cultures, which do not contain sulfatide, consistently with their lack of O4 positive oligodendrocytes, and in samples from rat microglia and mice astrocytes (Figure 31). The presence of these bands in samples devoid of mature oligodendrocytes suggests a possible role of other glial cells in the biological response mediated by rHIgM22.

The presence of the second immunoreactive band also seems to be affected by the protocol of partitioning chosen. In fact, in samples partitioned by adding 0.88% KCl instead of water, following immunostaining with rHIgM22, the intensity of the unknown band is reduced as shown in Figure 32.

rHIgM22

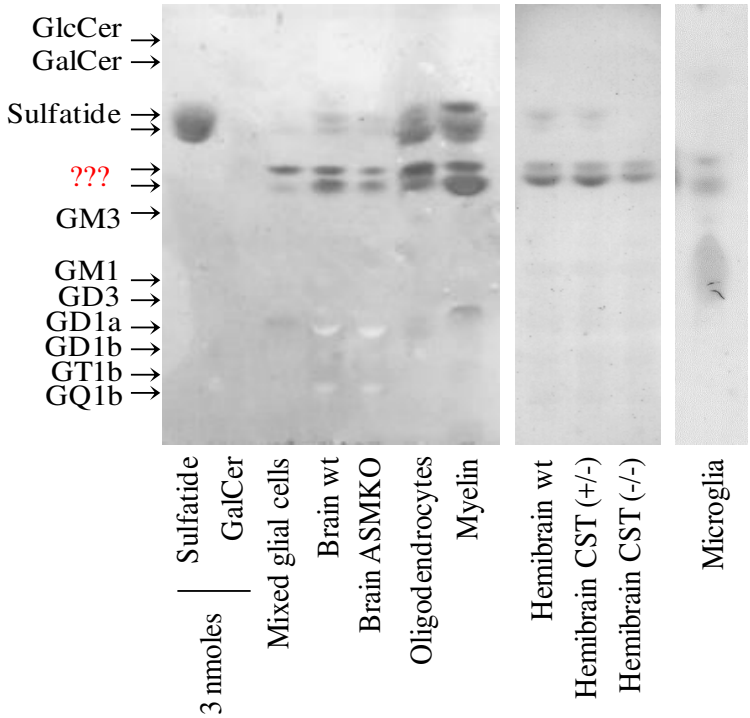

Human IgM

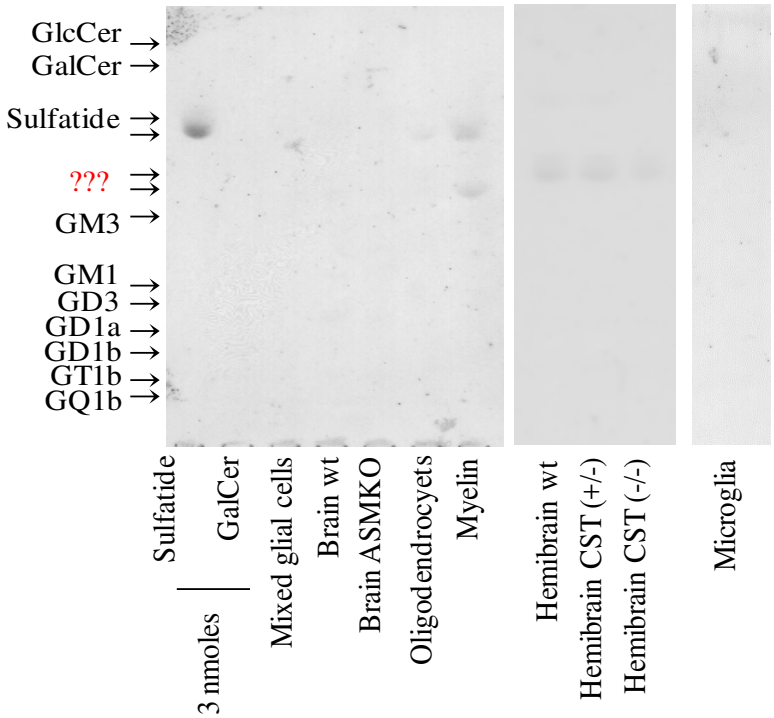

Figure 30. rHIgM22 binding to aqueous phases in TLC immunostaining. Using TLC immunostaining we assessed rHIgM22 binding to aqueous phases (A.Ph.A, obtained by partitioning the TLE with water) obtained from different cells and tissues such as mixed glial cells, wild type mouse brain and hemibrain, ASMKO mouse brain, rHIgM22 positive OPC, mouse myelin, CST (+/-) and (-/-) hemibrain, and rat microglia. For each A.Ph. amounts equivalent to 150 µg protein were loaded on the plate, while for each pure lipid 3 nmol were loaded. After chromatographic separation (solvent system: $CHCl_3$:CH_3OH:$CaCl_2$ 50:42:11), TLC plates were fixed with a polyisobuthylmethacrylate solution, air dried and incubated with 3% BSA in PBS for 1h. The plates were then incubated with either rHIgM22 or Human IgM (negative control) at 5 µg/mL in 1% BSA, 1% heath inactivated goat serum in PBS for 2 hours at room temperature (RT). The plates were then incubated with a HRP-conjugated anti-Human IgM µ-chain antibody for 1 hour, RT, and developed using *o*-phenylenediamine (OPD)/H_2O_2 in 0.05 M citrate-phosphate buffer pH 5.0.

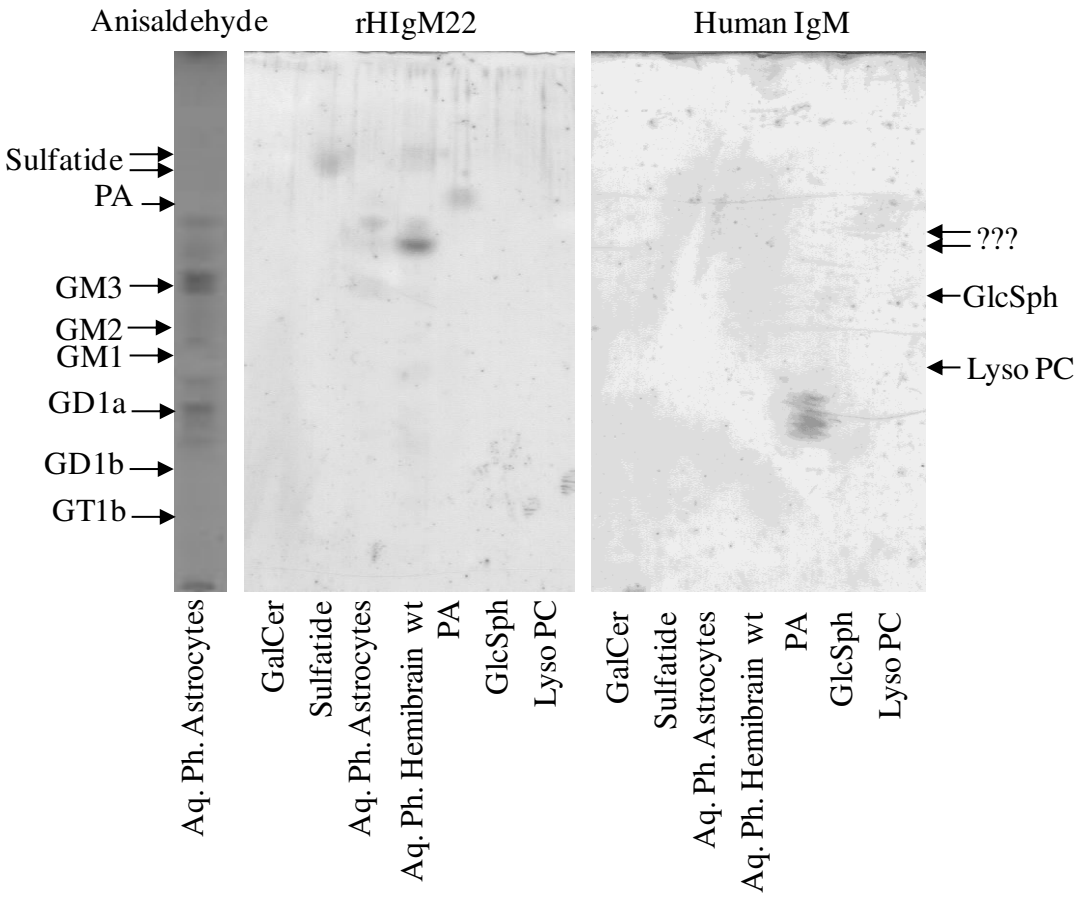

Figure 31. rHIgM22 binding to aqueous phases from astrocytes. Using TLC immunostaining we assessed rHIgM22 binding to aqueous phases (A.Ph.A, obtained by partitioning the TLE with water) obtained from wild type mouse hemibrain, and astrocytes. For each A.Ph. amounts equivalent to 150 µg protein were loaded on the plate, while for each pure lipid 3 nmol were loaded. After chromatographic separation (solvent system: $CHCl_3$:CH_3OH:$CaCl_2$ 50:42:11), TLC plates were fixed with a polyisobuthylmethacrylate solution, air dried and incubated with 3% BSA in PBS for 1 hour. The plates were then incubated with either rHIgM22 or Human IgM (negative control) at 5 µg/mL in 1% BSA in PBS overnight at 4°C. The plates were then incubated with a HRP-conjugated anti-Human IgM µ-chain antibody for 1 hour, RT, and developed using *o*-phenylenediamine (OPD)/H_2O_2 in 0.05 M citrate-phosphate buffer pH 5.0.

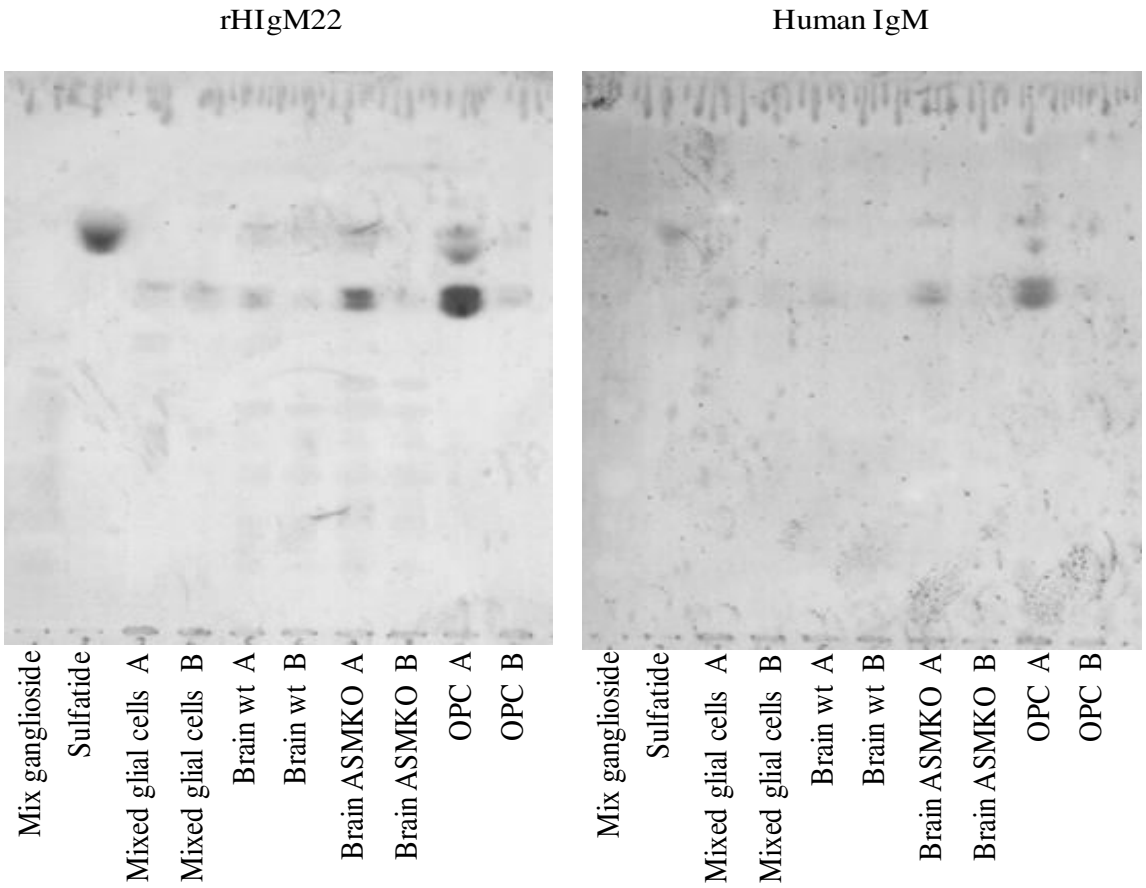

Figure 32. rHIgM22 binding to aqueous phases in TLC immunostaining. Using TLC immunostaining we assessed rHIgM22 binding to aqueous phases (A.Ph.A, obtained by partitioning the TLE with water; A. Ph. B, obtained by partitioning TLE with 0.88% aqueous KCl) obtained from wild type mouse hemibrain, CST (+/-) and (-/-) hemibrain. For each A.Ph. amounts equivalent to 150 µg protein were loaded on the plate, while for each pure lipid 3 nmol were loaded. After chromatographic separation (solvent system: $CHCl_3$:CH_3OH:$CaCl_2$ 50:42:11), TLC plates were fixed with a polyisobuthylmethacrylate solution, air dried and incubated with 3% BSA in PBS for 1 hour. The plates were then incubated with either rHIgM22 or Human IgM (negative control) at 5 µg/mL in 1% BSA in PBS for 2 hours at room temperature (RT). The plates were then incubated with a HRP-conjugated anti-Human IgM µ-chain antibody for 1 hour, RT, and developed using *o*-phenylenediamine (OPD)/H_2O_2 in 0.05 M citrate-phosphate buffer pH 5.0.

Characterization of rHIgM22 immunoreactive unknown antigen

Colorimetric assays

To identify the second rHIgM22 immunoreactive antigen, aqueous phases obtained from wild type mice hemibrains, as well as ones obtained from CST (+/-) and CST (-/-) mice hemibrains have been analyzed with different colorimetric reagents after chromatographic run. As shown in Figure 33, the unknown bands were positive for anisaldehyde, a reagent for the non-selective detection of lipids, and they were also positive for ninidrine and for the phosphorous spray [323], reagents selective, respectively, for free NH_2 groups-containing lipids and for phosphate-containing lipids. In the case of aniline, a reagent for the selective detection of glycolipids, there was a reactivity but the presence of multiple bands with non characteristic color in that area did not allow to conclusively say whether or not the unknown antigen could be a glycolipid.

Aqueous phases obtained from wild type mice hemibrains were also analyzed through two-dimensional TLC. To verify if the unknown antigen is an alkali-sensitive lipid, which are relatively common in brain lipid extracts, the plates, in some experiments, were exposed to ammonia vapors between the first and the second chromatographic separations (Figure 34). The binding of rHIgM22 to the antigen after two-dimensional separation, with or without alkali treatment, was assessed through TLC immunostaining (Figure 35-36). As shown in Figure 36, rHIgM22 is able to recognize the second immunoreactive band, which is modified by the alkali treatment (as indicated by its altered migration in the second run after exposure to ammonia vapors), even after a 3 hour treatment with ammonia vapors, suggesting that while the antigen is modified by the treatment, this is not altering the motif recognized by the antibody.

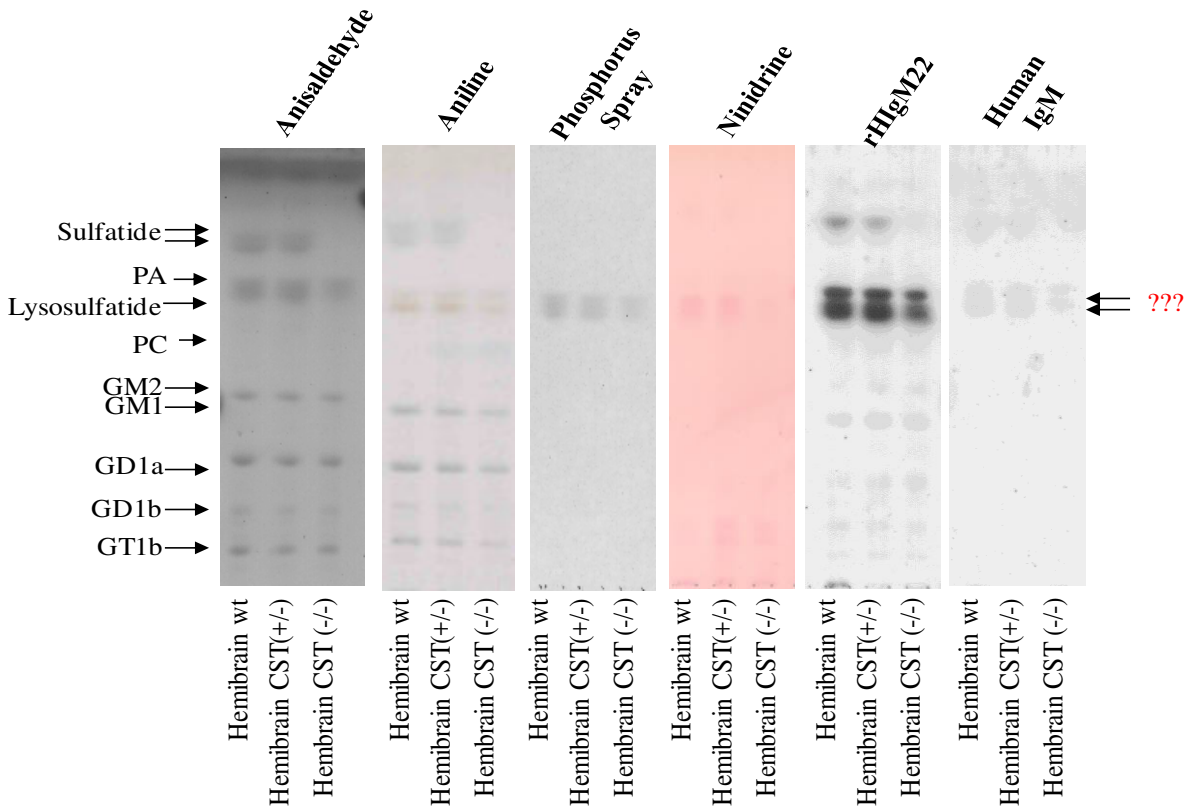

Figure 33. Characterization of unknown rHIgM22 positive antigen in aqueous phases from mouse hemibrain. Aqueous phases from hemibrains from wild type, CST (+/-) and CST (-/-) mice have been analyzed. For each extract, amounts equivalent to 150 µg protein were loaded. Briefly, after separation with $CHCl_3$:CH_3OH: 0.2%$CaCl_2$ in H_2O 50:42:11, the plates were sprayed with appropriate chemical reagents. Binding of rHIgM22 to the unknown antigen was assessed using TLC immunostaining. Briefly, after chromatographic running, TLC plates were fixed with a polyisobuthylmethacrylate solution, air dried and incubated with 3% BSA in PBS. The plates were then incubated with either rHIgM22 or Human IgM (negative control) at 5 µg/mL in 1% BSA in PBS for 2 hours at room temperature (RT). The plates were then incubated with a HRP-conjugated anti Human IgM µ-chain antibody for 1 hour, RT, and developed using o-phenylenediamine (OPD)/H_2O_2 in 0.05 M citrate-phosphate buffer pH 5.0.

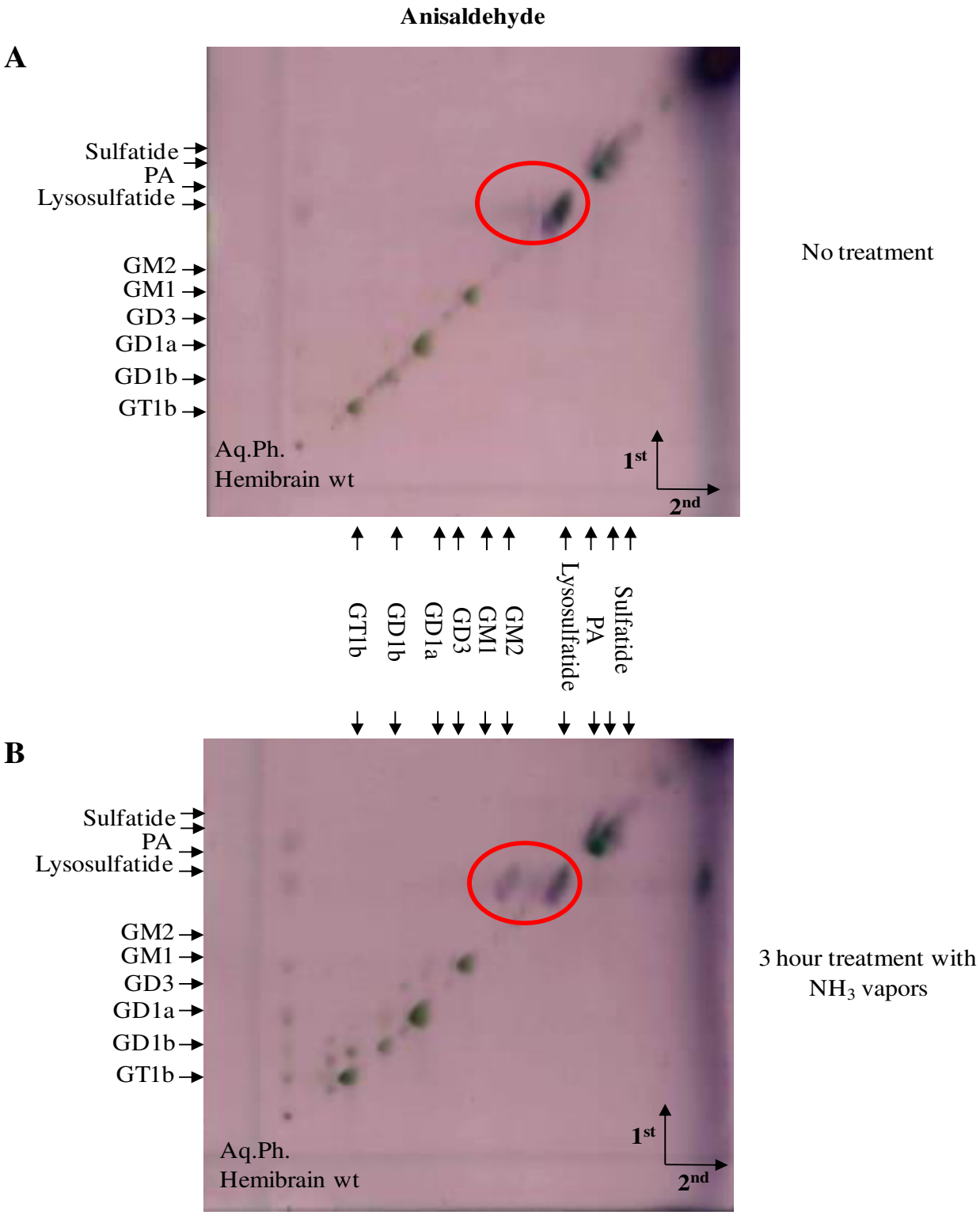

Figure 34.Two-dimensional separation of wild type mouse hemibrain aqueous phases. Aqueous phases from hemibrains from wild type mice have been analyzed. For each extract, amounts equivalent to 750 µg protein were loaded. The samples were subjected to two dimensional separation with $CHCl_3$:CH_3OH: 0.2%$CaCl_2$ in H_2O 50:42:11 as a solvent system for both run. To verify if the antigen sensitivity to alkali treatment the plates were treated for 3 hours with ammonia vapors between the first and the second chromatographic run (*Panel B*).

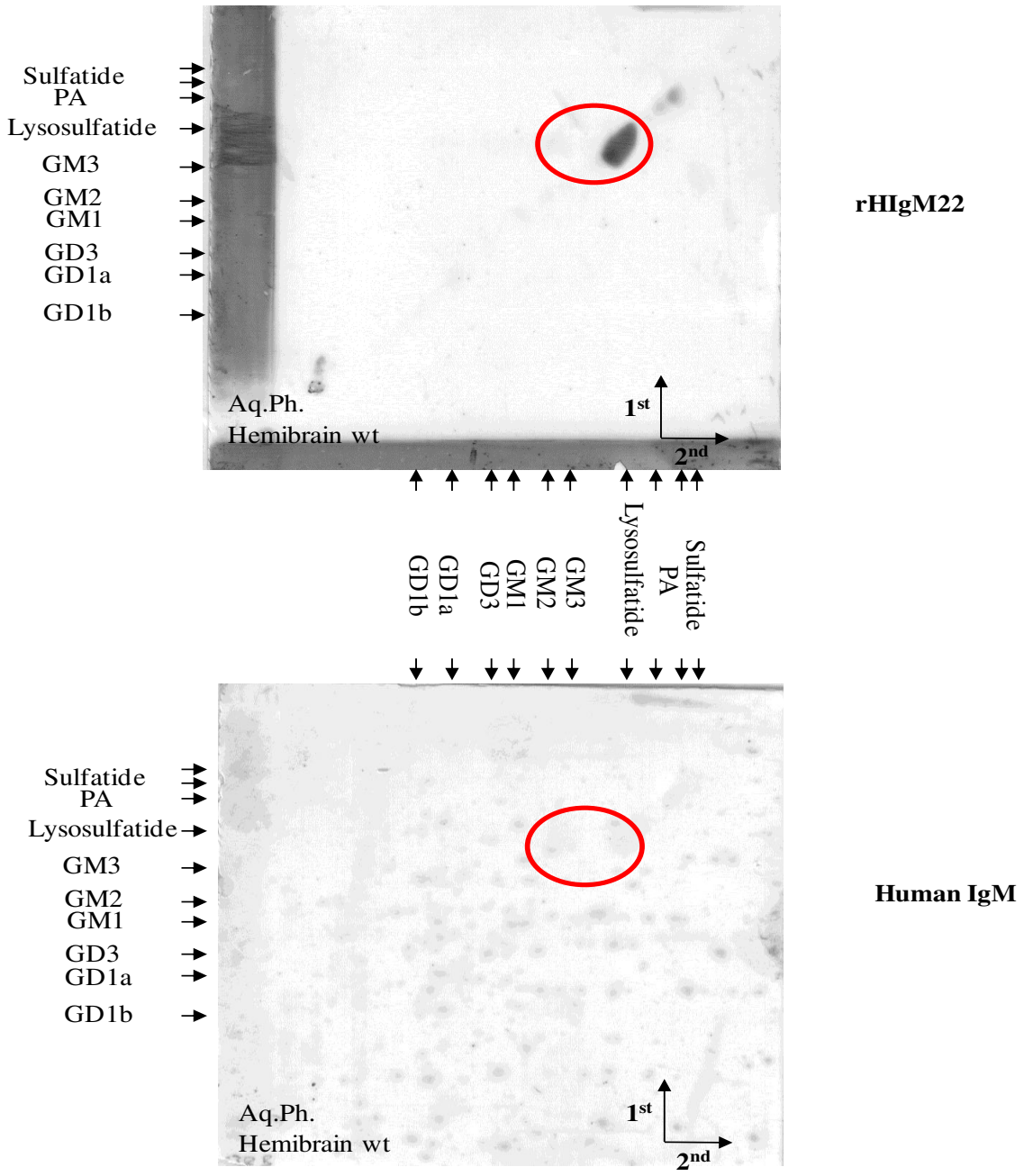

Figure 35. rHIgM22 binding to aqueous phases from wild type mice hemibrain after two-dimensional separation. Aqueous phases from hemibrains from wild type mice have been analyzed. For each extract, amounts equivalent to 750 µg protein were loaded. Briefly, the samples were subjected to two dimensional separation with $CHCl_3$:CH_3OH: 0.2% $CaCl_2$ in H_2O 50:42:11 as a solvent system for both run. Binding of rHIgM22 to the unknown antigen was assessed using TLC immunostaining. Briefly, after chromatographic running, TLC plates were fixed with a polyisobuthylmethacrylate solution, air dried and incubated with 3% BSA in PBS. The plates were then incubated with either rHIgM22 or Human IgM (negative control) at 5 µg/mL in 1% BSA in PBS overnight at 4°C. The plates were then incubated with a HRP-conjugated anti Human IgM µ-chain antibody for 1 hour, RT, and developed using *o*-phenylenediamine (OPD)/H_2O_2 in 0.05 M citrate-phosphate buffer pH 5.0.

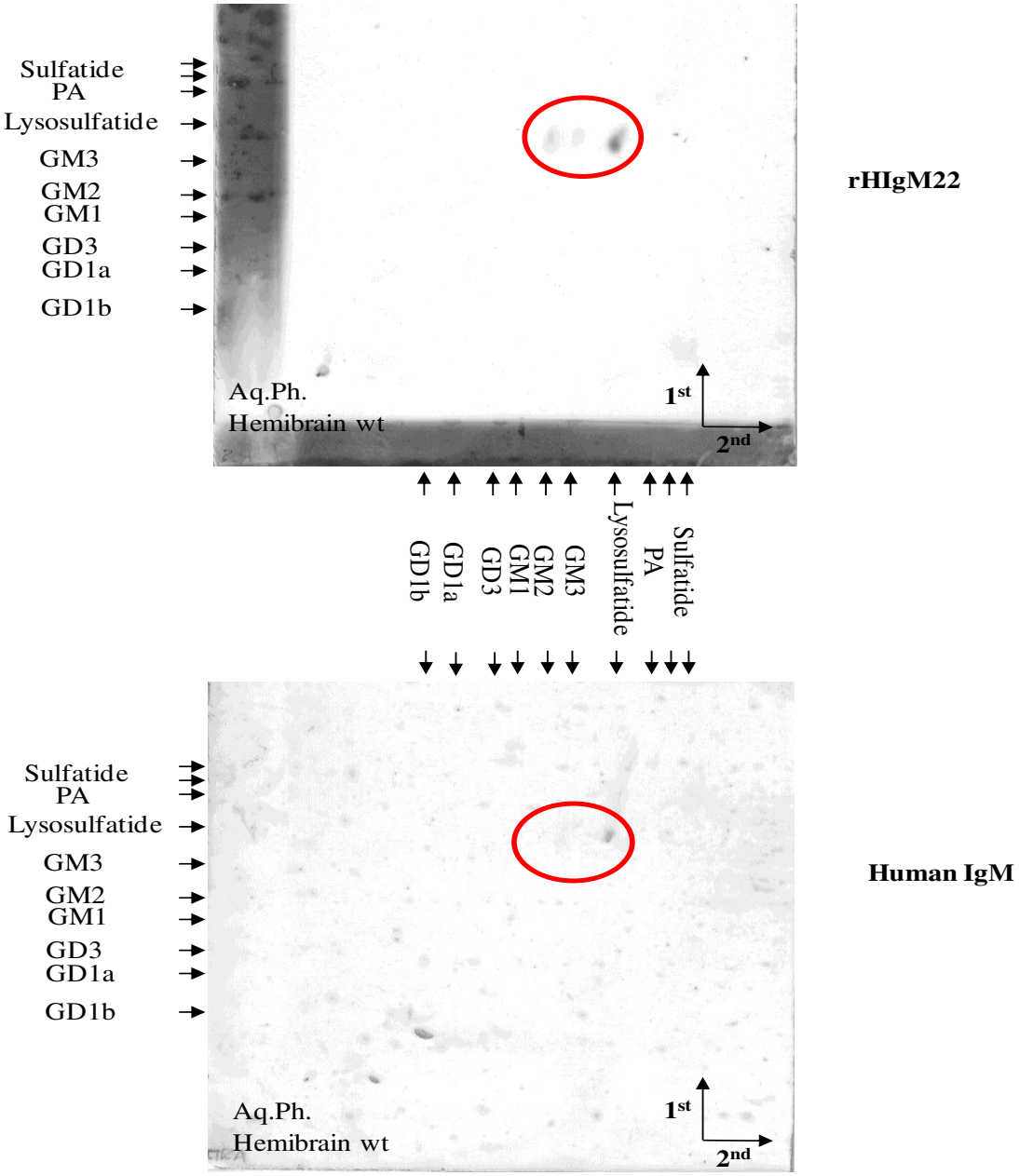

Figure 36. rHIgM22 binding to aqueous phases from wild type mice hemibrain after alkali treatment. Aqueous phases from hemibrains from wild type mice have been analyzed. For each extract, amounts equivalent to 750 µg protein were loaded. Briefly, the samples were subjected to two dimensional separation with $CHCl_3$:CH_3OH: 0.2% $CaCl_2$ in H_2O 50:42:11 as a solvent system for both run. To verify if the antigen sensitivity to alkali treatment the plates were treated for 3 hours with ammonia vapors between the first and the second chromatographic run. Binding of rHIgM22 to the unknown antigen was assessed using TLC immunostaining. Briefly, after chromatographic running, TLC plates were fixed with a polyisobuthylmethacrylate solution, air dried and incubated with 3% BSA in PBS. The plates were then incubated with either rHIgM22 or Human IgM (negative control) at 5 µg/mL in 1% BSA in PBS overnight at 4°C. The plates were then incubated with a HRP-conjugated anti Human IgM µ-chain antibody for 1 hour, RT, and developed using *o*-phenylenediamine (OPD)/H_2O_2 in 0.05 M citrate-phosphate buffer pH 5.0.

Mass spectrometry

To attempt the identification of the antigen, purified myelin was prepared from mouse brain. This was followed by lipid extraction, partitioning, and chromatographic separation of the aqueous phases. Following the chromatographic separation of the aqueous phases, the area corresponding to the unidentified band was scraped. The scraped gel was subjected to lipid extraction, dialyzed and lyophilized. The lyophilized samples were then resuspended in chloroform and analyzed by ESI mass spectrometry in negative mode (the specific conditions are reported in the section Materials and Methods). The full MS spectrum revealed the presence of two ions with an m/z of 662 and 762, respectively (Figure 38). These fragments were not detected in the spectrum of the negative control sample, *i.e.* the eluate obtained from a TLC area not containing any compound (Figure 39). The MS/MS spectra obtained by the fragmentation of the 762 and 662 ions show ions with an m/z of 718 and 618, respectively, indicating the loss of a fragment with m/z=44 consistent with an ethanolamine fragment (Figure 39).

The results obtained (Figure 38-39) led to hypothesize that one of the molecules, present in the scraped area, could be a PE with fatty acid containing 26 C atoms, two double bonds and 2 OH groups (MW 662) or containing 32 C atoms, two double bonds and 3 OH groups (MW 762). The hypothetical PE structure would be consistent with the chemical characterization, indicating the presence in the molecule of a free amino group and of phosphate. The hypothesized presence of multiple hydroxylations in the fatty acid residues is in principle consistent with the partitioning of the molecule with a preferential association with the aqueous phase. Further analysis in different MS conditions (ionization conditions, temperature, etc.) need to be performed in order to confirm the identity of this molecule and of the other molecules that could be present.

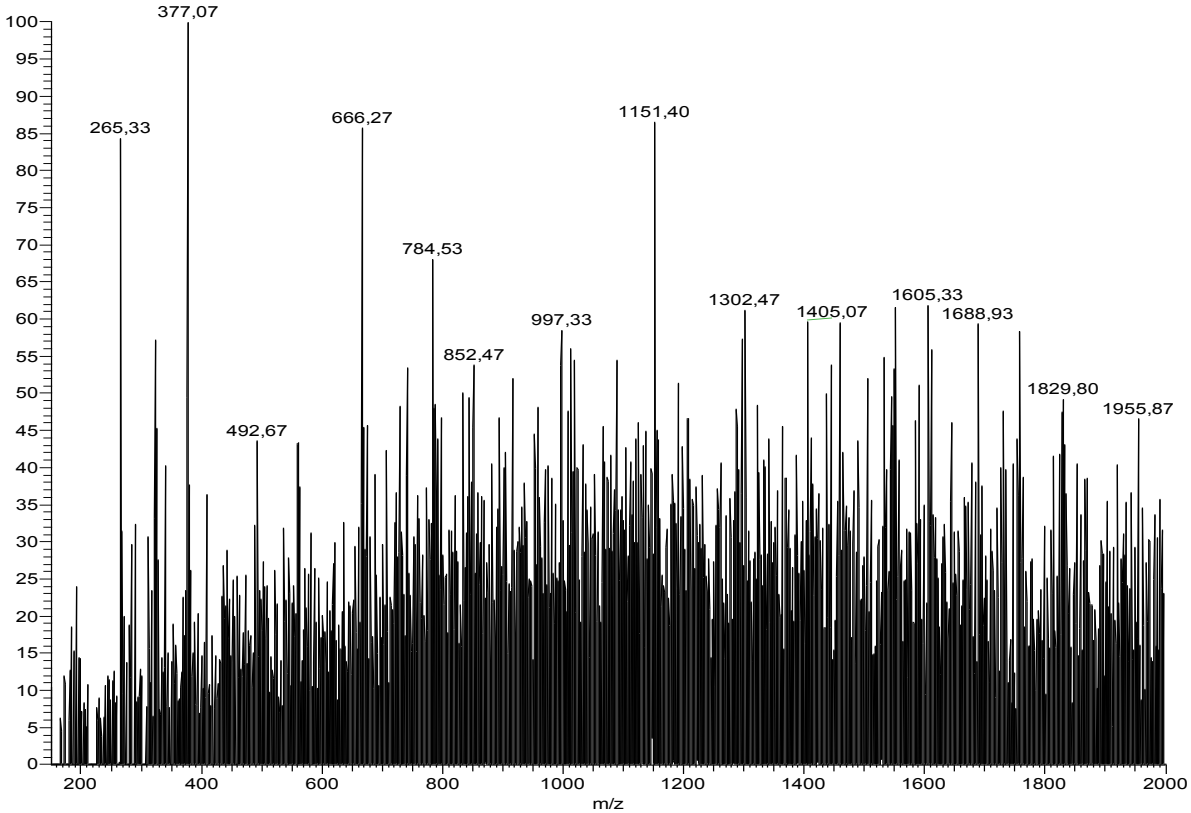

Figure 37. ESI-MS analysis of negative control sample. After chromatographic run in CHCl3:CH3OH: 0.2%CaCl2 in H2O 50:42:11, the silica gel (that did not contain any lipid) was scraped and subjected to lipid extraction. The lipid extract was subjected to ESI-MS analysis. The full negative mass spectra of the m/z range 100-2,000 is reported in the figure.

A

MW 762 R1+R2=$C_{32}H_{62}O_3$

MW 662 R1+R2=$C_{26}H_{50}O_2$

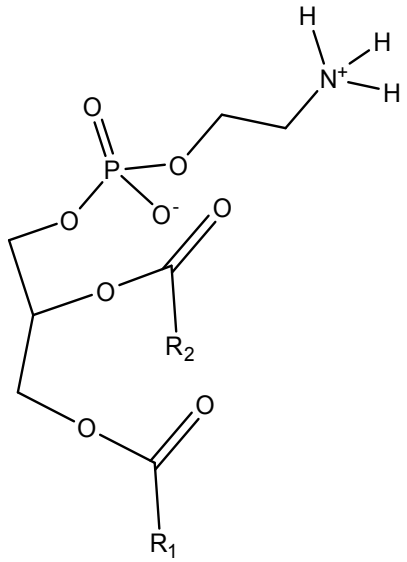

B

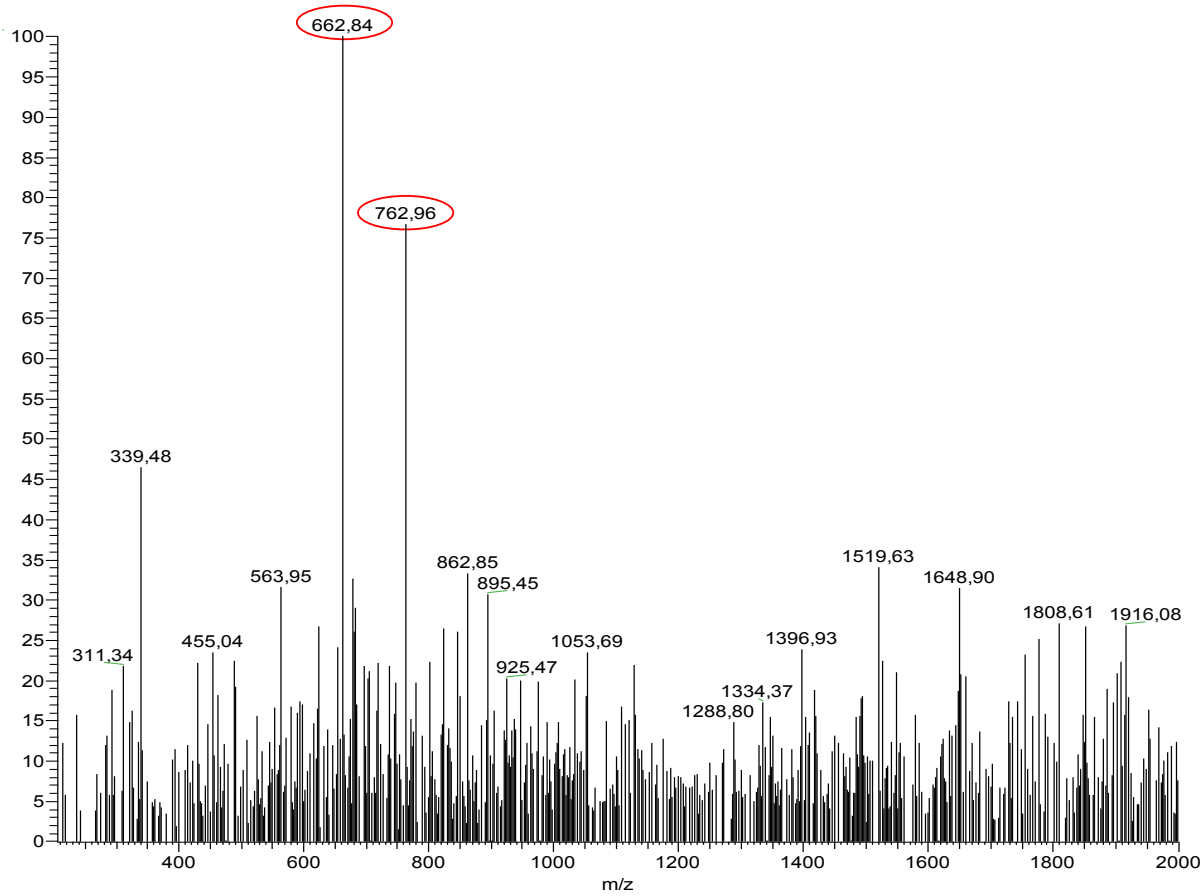

Figure 38. ESI-MS analysis of unknown antigen immunoreactive to rHIgM22. After chromatographic separation of aqueous phases from myelin, the area corresponding to the unidentified band was scraped and subjected to lipid extraction. The lipids extracted were then subjected to ESI-MS analysis. The full negative mass spectra of the m/z range 200-2,000 is reported in *panel B*. The hypothetical structure of the molecule analyzed is reported in *panel A*.

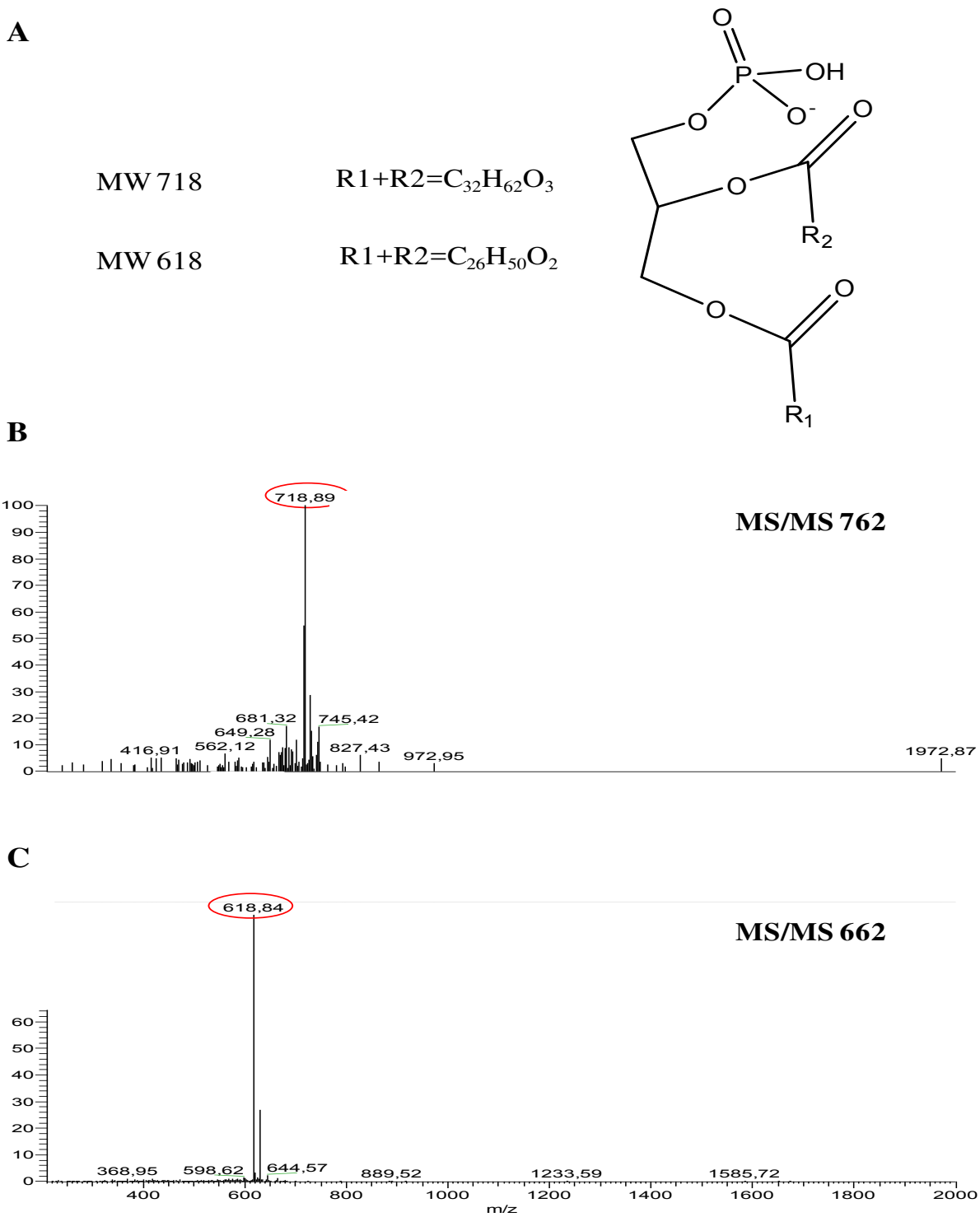

Figure 39. ESI MS/MS analysis of unknown antigen immunoreactive to rHIgM22. After chromatographic separation of aqueous phases from myelin, the area corresponding to the unidentified band was scraped and subjected to lipid extraction. The lipids extracted were then subjected to ESI MS analysis (Figure 12) and subsequently to ESI MS/MS. The ESI MS/MS of the ions at m/z 762 and 662 are reported, respectively, in *panel B and C*. The hypothetical structure of the molecule after fragmentation is reported in panel *A*.

Binding to protein antigens

It is reported in the literature that all remyelination-promoting antibodies, at least those with a known antigen, are polyreactive. For example, A2B5, a glycolipid-binding antibody, is able to recognize several sialylated glycosphingolipids that have in common a similar carbohydrate epitope [294, 324]; O4 instead is able to bind not only to sulfatide, but also to seminolipid, to the proligodendroblast antigen (POA), and also to cholesterol [297, 325-327]. Taking all this into account, western blotting analysis were performed using different samples, with the aim to verify if there was any rHIgM22 reactivity associated with proteins. Cell lysates, total lipid extracts (that could contain highly hydrophobic proteins or peptides), and delipidized protein pellets from mixed glial cells (Figure 40) and also from mice brains (wild type and ASMKO) (Figure 41-42) were subjected to SDS PAGE followed by immunoblotting. In the mixed glial cell samples rHIgM22 was able to recognize some bands with an apparent molecular weight around 50 kDa in the cell lysates, and another immunoreactive band with an apparent molecular weight around 15 kDa, in the delipidized samples. However the reactivity of rHIgM22 for these bands was comparable to that of control IgM. Neither antibody was able to recognize any antigen in the lipid extracts and in the delipidized samples from mice brain. Nevertheless, two rHIgM22 immunoreactive bands migrating between 37 and 50 kDa were present in the homogenates from mice brain and these bands were not reactive to the control IgM. Since the myelin-associated glycoprotein MAG bears a sulfated glycosylated epitope, a western blot using an anti-MAG antibody was run on the same samples (Figure 42). MAG immunoreactive bands were found in all the samples, however their apparent molecular weight did not correspond to that of the rHIgM22 positive band.

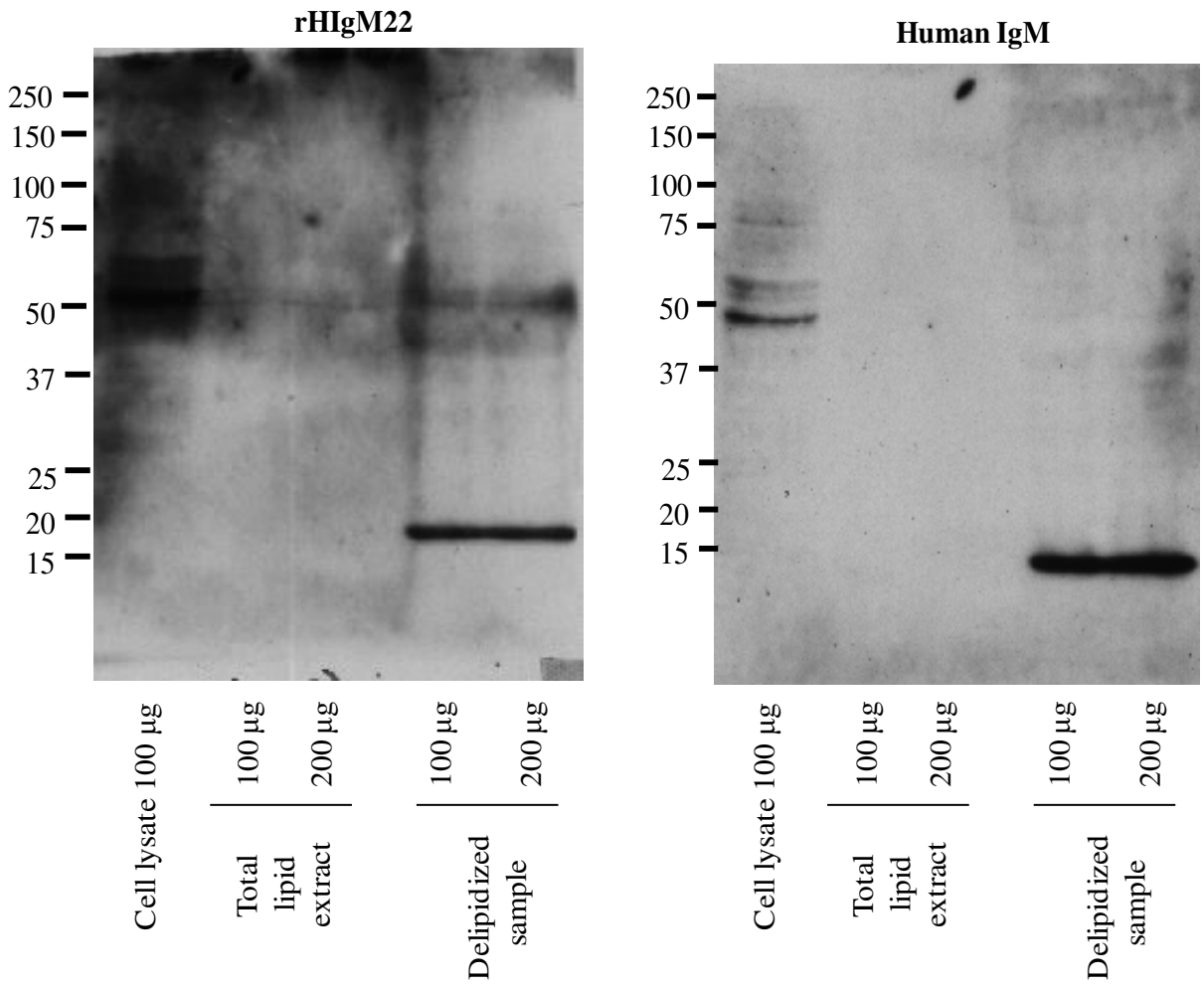

Figure 40. rHIgM22 binding to cell lysate, TLE, and delipidized samples from mixed glial cells. Mixed glial cells at the 14th day of culture were collected. Part was lysed in a solution containing Triton X-100, part was lyophilized and subjected to lipid extraction with $CHCl_3$:CH_3OH:H_2O 20:10:1 (v/v/v). All the samples were resuspended in modified Laemmli buffer and boiled for 5 minutes at 100°C before being analyzed. Proteins were separated by SDS-PAGE and transferred on a PVDF membrane. For the detection of possible rHIgM22 antigens 100 µg of cell lysate and either 100 µg or 200 µg of TLE and delipidized sample were loaded. The membranes were incubated in 5% milk in TBS-T 0.05% overnight before incubation with 5 µg/mL rHIgM22 or Human IgM (negative control) diluted in 1% BSA in TBS-T 0.05% for 1 hour at RT. After washing a few times with TBS-T 0.05%, the membranes were incubated with a HRP-conjugated anti human IgM µ-chain in 1% BSA in TBS-T 0.05% for 45 minutes at RT. Peroxidase activity was assessed through incubation with a non-radioactive light emitting substrate for the detection of immobilized specific antigens conjugated with horseradish peroxidase-linked antibodies for 2 minutes. The luminescent compound generated following the reaction was detected through exposition to a photographic film.

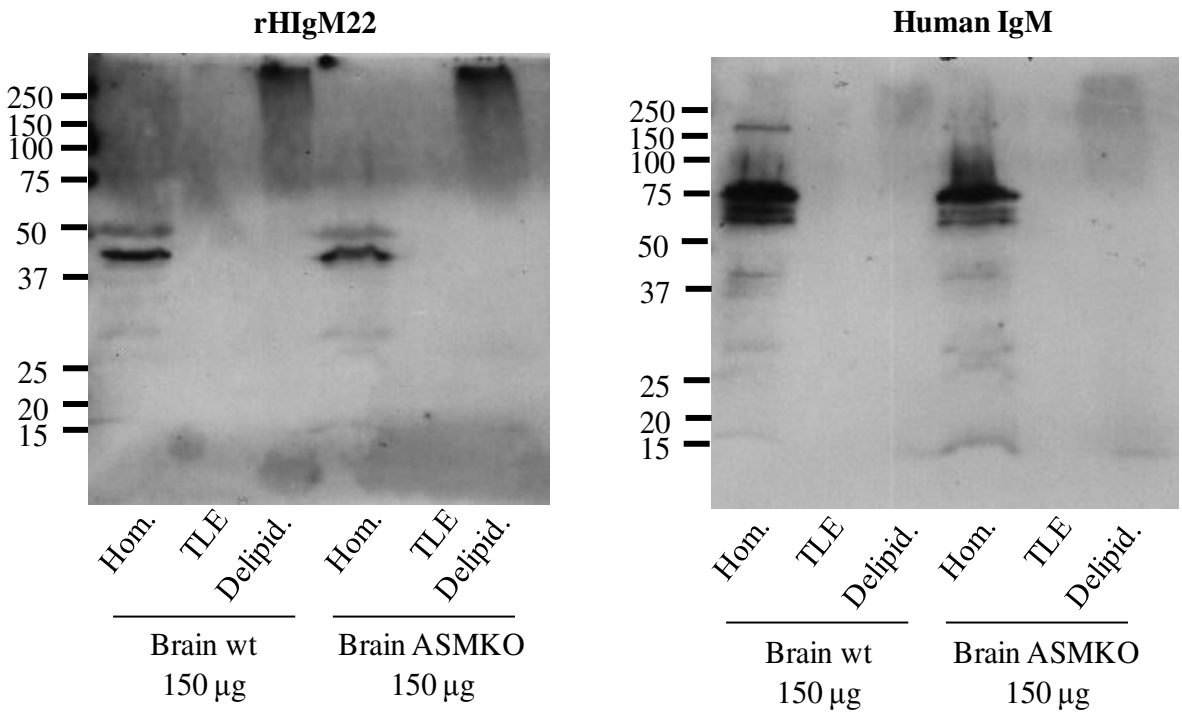

Figure 41. rHIgM22 binding to mouse brain homogenate, TLE, and delipidized samples. Brains from C57BL/6N mice (wild type or ASMKO) ranging from 7 to 10 months of age were lysed in a solution containing Triton X-100 and homogenized using a dounce homogenizer (10 times, tight). The homogenate was centrifuged for 5 minutes at 1300 rcf at 4°C and the surnatant was used for the analysis. To obtain TLE and delipidized sample, frozen brains from C57BL/6N mice ranging from 7 to 10 months of age were resusupended in water and briefly subjected to sonication before being lyophilized. The samples were then subjected to lipid extraction with $CHCl_3$:CH_3OH:H_2O 20:10:1 (v/v/v). All the samples were resuspended in modified Laemmli buffer and boiled for 5 minutes at 100°C before being analyzed. Proteins were separated by SDS-PAGE and transferred on a PVDF membrane. For the detection of possible rHIgM22 antigens 150 µg of each sample were loaded. The membranes were incubated in 5% milk in TBS-T 0.05% overnight before incubation with 5 µg/mL rHIgM22 or Human IgM (negative control) diluted in 1% BSA in TBS-T 0.05% for 1 hour at RT. After washing a few times with TBS-T 0.05%, the membranes were incubated with a HRP-conjugated anti human IgM µ-chain in 1% BSA in TBS-T 0.05% for 45 minutes at RT. Peroxidase activity was assessed through incubation with a non-radioactive light emitting substrate for the detection of immobilized specific antigens conjugated with horseradish peroxidase-linked antibodies for 2 minutes. The luminescent compound generated following the reaction was detected through exposition to a photographic film.

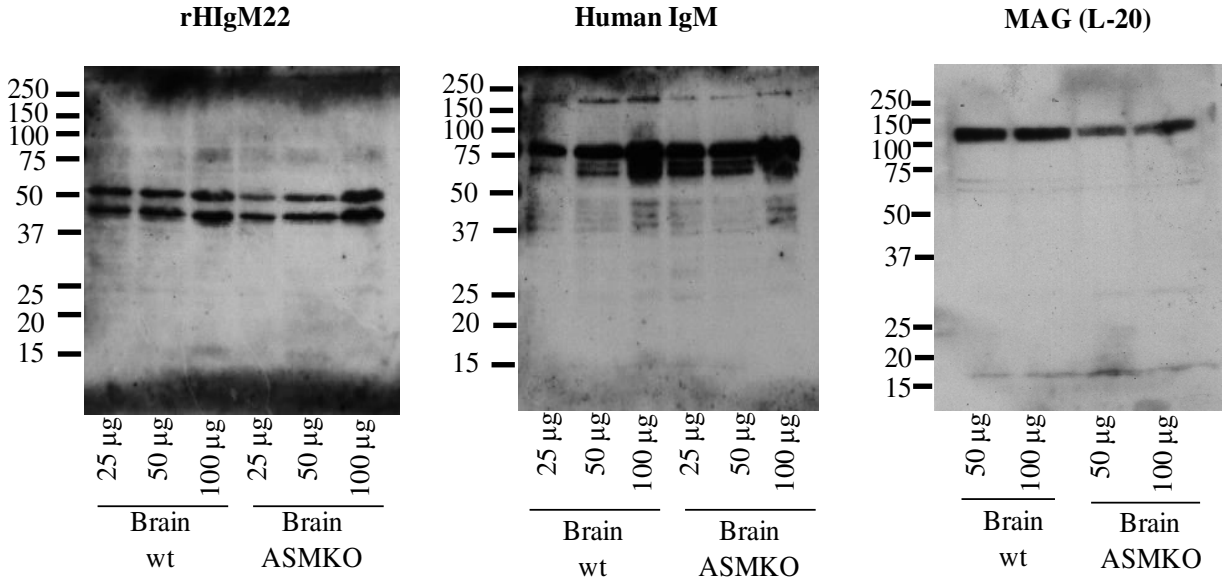

Figure 42. rHIgM22 binding to mouse brain homogenate. Brains from C57BL/6N mice (wild type or ASMKO) ranging from 7 to 10 months of age were lysed in a solution containing Triton X-100 and homogenized using a dounce homogenizer (10 times, tight). The homogenate was centrifuged for 5 minutes at 1300 rcf at 4°C and the surnatant was used for the analysis. All the samples were resuspended in modified Laemmli buffer and boiled for 5 minutes at 100°C before being analyzed. Proteins were separated by SDS-PAGE and transferred on a PVDF membrane. For the detection of possible rHIgM22 antigens different amounts of samples (from 25 to 100 µg protein) were loaded. The membranes were incubated in 5% milk in TBS-T 0.05% overnight before incubation with 5 µg/mL rHIgM22 or Human IgM (negative control) diluted in 1% BSA in TBS-T 0.05% for 1 hour at RT. After washing a few times with TBS-T 0,05%, the membranes were incubated with a HRP-conjugated anti human IgM µ-chain in 1% BSA in TBS-T 0.05% for 45 minutes at RT. Peroxidase activity was assessed through incubation with a non-radioactive light emitting substrate for the detection of immobilized specific antigens conjugated with horseradish peroxidase-linked antibodies for 2 minutes. The luminescent compound generated following the reaction was detected through exposition to a photographic film.

DISCUSSION

More than 100 years have passed since Charcot, Carswell, Cruveilhier and others first described the pathological characteristics of multiple sclerosis (MS) [328]. MS is a chronic inflammatory disease of the central nervous system whose hallmark is the development of focal plaques of demyelination, which in turn leads to diffuse neurodegeneration throughout the grey and white matter of the brain and spinal cord [329]. MS is the most common cause of non traumatic disability in young people, and approximately 2.5 million people worldwide are affected by this disease [237]. Despite its high prevalence, multiple sclerosis remains a challenging ailment to study. The aetiology is unknown, the pathophysiologic mechanisms are various, and the chronic and unpredictable course of the pathology represent a drawback when it comes to defining whether the positive effects of short-term treatment will be sustained [328]. In MS the development of focal areas of demyelination is characterized by myelin loss that occurs on a background of inflammation and, while as of now there is no actual cure for MS, the current FDA approved therapies mainly target the inflammatory component, in order to contain myelin damage. Some of these strategies however, for example the use of Fingolimod, are also able to increase the efficiency of the remyelination process [282-285]. In most mouse models remyelination is a spontaneous process, occurring in response to demyelination, and leads to functional recovery. In MS in humans, however, this process is poorly efficient and its failure ultimately results in axonal dysfunction, degeneration, and loss of sensory and motor function [203]. For this reason, therapies that increase the chances of the regenerative outcome of demyelination have been getting more and more attention recently.

The strategies that are currently being developed to increase efficiency of remyelination can be grouped as follows: 1) cell transplant, involving the transplantation of myelination-competent cells directly into lesion sites [286, 287]; 2) promotion of repair by the resident CNS stem- and precursor-cell populations, through the administration of growth, trophic, and neuroprotective factors [289]; 3) use of CNS reactive antibodies to induce remyelination [6]. Two of these remyelination promoting antibodies, BIIB033 and rHIgM22, are currently in clinical trial for MS treatment. The first is an anti-LINGO-1 IgG acting on LINGO-1, a protein known to inhibit remyelination via RhoA activation, and is currently being tested in a Phase II study in RRMS (ClinicalTrial.gov: NCT01864148). The second antibody, instead, is an IgM sharing several features with naturally occurring antibodies and is currently undergoing a phase I clinical trial aimed to evaluate safety and tolerability in relapsing MS patients (ClinicalTrial.gov:

NCT02398461), after the first phase I clinical trial in MS patients was completed successfully (ClinicalTrial.gov: NCT01803867). This antibody, rHIgM22, first identified from a patient with Waldenström macroglobulinemia, has been shown to bind selectively to myelin and to the surface of oligodendrocytes *in vitro* [8, 278]. Moreover, there is evidence showing that this antibody is able to enter the central nervous system, accumulate in the demyelinated lesions, and promote remyelination in mouse models of chronical demyelination [7, 8]. Both the antigen recognized by rHIgM22 and the signaling mechanisms through which this antibody exerts its function are still unclear, even though, recent evidence suggests the involvement of a pathway involving Lyn and ERK cascade, which leads to inhibition of the apoptotic pathway and also to inhibition of OPCs differentiation and promotion of OPCs proliferation [305, 306]. Moreover, evidence suggests that Lyn activation could be subsequent to an rHIgM22 mediated reorganization of a signaling complex which includes Lyn, integrin αvβ3 and PDGFαR [10, 304]. Nevertheless, the actual binding target of rHIgM22 has yet to be identified.

Evidence suggests that the antigen recognized by rHIgM22 could be associated with plasma membrane lipid rafts and that this target could be represented either by a sulfated glycolipid or by a multimolecular complex including a sulfated antigen. rHIgM22, in fact, binds the CNS tissues with a pattern similar to that of O4, an anti-sulfatide antibody. Moreover, binding of rHIgM22 is abolished in CNS tissues from CST (-/-) mice, suggesting that the antigen recognized by rHIgM22 could be one or more CST-sulfated antigens present in myelin and on the surface of oligodendrocyte [9, 10]. These mice are completely devoid of sulfatide, whereas other glycolipids in the brain, galactosylceramide included, are not significantly altered [136].

The analysis of the binding of rHIgM22 to different amounts of sulfatide, tested in different conditions (incubation time, temperature, stringency, etc.) and with different techniques (TLC immunostaining and surface plasmon resonance assays), revealed that rHIgM22 is indeed able to recognize sulfatide *in vitro*. Moreover, SPR experiments, where antigen presentation is closer to the one happening in a biological membrane respect to TLC immunostaining, showed that the binding of this remyelination promoting antibody to sulfatide is specific, suggesting that sulfatide could actually be one of the molecular targets of rHIgM22. Interestingly, rHIgM22 is also able to recognize lysosulfatide, the deacylated form of sulfatide, usually present in the normal CNS as a minor component, but whose levels can be increased in some pathological conditions, such as methachromatic leukodystrophy, a demyelinating disease [315-317].

Moreover, the binding of rHIgM22 to lysosulfatide not only is specific, but has an affinity is comparable to that exhibited for sulfatide, at least in SPR assays. In both cases, however, the affinity resulted quite low if compared to that of other known anti-glycolipid antibodies, such as the anti-lactosylceramide T5A7, for their own target [312]. Evidence reported in the literature, on the other hand, shows that, in model membranes, antibody recognition of sulfatide is affected by the membrane lipid microenvironment. This evidence suggests that the lipid environment might play a role in the determination of the surface topology of sulfatide. Distinct populations of anti-sulfatide antibodies show a different reactivity to sulfatide in a dipalmitoyl-PC/cholesterol environment or in a sphingomyelin/cholesterol environment. Moreover, length and hydroxylation of fatty acid chain of PC or of SM seem to restrict the recognition to higher affinity antibodies [321, 322]. Interestingly, our data obtained using SPR assays suggests that the binding of rHIgM22 to sulfatide might be affected by the composition of the lipid microenvironment. In particular, the presence of either GalCer or cholesterol lead to a reduction of the binding of rHIgM22 to sulfatide-containing monolayers, whereas SM and lysosulfatide have the opposite effect, suggesting that that the presence of different lipids, at a certain density might be required to allow an optimal recognition of the antigen by rHIgM22. Sulfatide topology, distribution and dynamics in phospholipid bilayers, however, is also affected by the presence of proteins that are supposed to be physiologically relevant partners of sulfatide, such as myelin basic protein (MBP) [330, 331]. Moreover, several studies highlighted a role of external factors, like the presence of soluble sulfatide binding proteins [332], pH [333, 334], and the presence of cations [335, 336] in the dynamics and distribution of sulfatide in phospholipid bilayers. This suggests that the binding of rHIgM22 to sulfatide in oligodendrocytes and in myelin could be affected by a plethora of factors, and could actually be different than the one observed in the *in vitro* experiments.

The analysis regarding the binding of rHIgM22 was not limited to sulfatide and its deacylated form. Considering that glycerophospholipids in myelin represent approximately 43% of the total dry weight [105], the binding of rHIgM22 to several glycerophospholipids was assessed through TLC immunostaining. This set of experiments revealed no significant binding of rHIgM22 to PC, the most abundant phospholipid in any biological membrane, or to its deacylated form, lyso-PC, whereas a non specific weak binding to PE, PS and PI was observed under experimental

conditions similar to those used to assess binding to sulfatide. rHIgM22 also showed no significant binding to phosphatidyl-β-D-glucoside (PtdGlc), a lipid characterized by a unique fatty acid composition particularly enriched in the brain where it is highly expressed in the two neurogenic regions of the adult brain [161], or to other four uncharacterized lipids structurally related to PtdGlc.

On the other hand, rHIgM22 showed a significant binding to phosphatidic acid (PA), which is not only a constituent of all cell membranes and a precursor of all neural membrane glycerophospholipids, but also acts as an intracellular second messenger regulating different signaling proteins [15, 16]. Moreover, the binding of rHIgM22 seems to be specific, even though further analysis, with different techniques, might be required to confirm this.

The binding of rHIgM22 to other myelin glycolipids, including GalCer, GlcCer, LacCer, SM, and several gangliosides, was also assessed, however the antibody did not show a significant binding to any of the aforementioned lipids.

The binding of rHIgM22 was also observed in lipid mixtures obtained from a variety of relevant biological samples, including wild type, ASM (-/-), CST (+/-) and CST (-/-) mice brains, mouse mixed glial cells (MGC), mouse astrocytes, rat rHIgM22^{+} oligodendrocytes (OL), rat microglia, and mouse myelin. The analysis of these samples not only showed the presence of a double band co-migrating with the sulfatide standard, thus confirming the data obtained using pure sulfatide from a commercial source, but also revealed the presence of a second antigen in the aqueous phases of all the sample analyzed, including the CST (-/-) brains which lack sulfatide. The position of this antigen roughly corresponds to that of the lysosulfatide standard, however literature suggests that lysosulfatide levels are quite low in non-pathological nervous tissue. Moreover, the experiments performed on pure lysosulfatide indicated that the binding of rHIgM22, at least in a TLC immunostaining experimental setting, should be weaker than the one to sulfatide. Nevertheless, the signal corresponding to these bands resulted quite strong, suggesting that rHIgM22 might recognize this antigen with a stronger affinity than that to sulfatide. Interestingly, the unknown antigen is also present in samples devoid of oligodendrocytes, such as MGC, astrocytes and microglia, suggesting a possible involvement of other glial cells in the biological response mediated by rHIgM22. This is consistent with the observation that in isolated OPCs, PDGF is required for rHIgM22-mediated inhibition of apoptotic signaling and differentiation. PDGF is produced by neurons and astrocytes, and stimulates OPC proliferation and

promotes OPC survival both *in vivo* and *in vitro*. Indeed, IgM-mediated OPC proliferation is detectable only in cultures containing substantial amounts of astrocytes, microglia and OPCs (mixed glial cultures) but not in highly enriched OPC population [305]. Moreover, both astrocytes and microglia play a role in the rapid activation of OPCs that kick-start the remyelination process and in the removal of myelin debris, whose presence impairs remyelination [202].

Several experiments aimed to identified the unknown rHIgM22-positive antigen found in aqueous phases of various samples, revealed that this lipid is positive for colorimetric reagents selective for free NH_2 groups-containing lipids and for phosphate containing lipids. An analysis using a reagent for the selective detection of glycolipid was also performed however, while there is a reactivity, the presence of multiple bands with non characteristic color in that area did not allow to conclusively say whether or not the unknown antigen could be a glycolipid. Moreover, analysis of the aqueous phases through two-dimensional TLC coupled with alkali treatment revealed not only that the antigen is sensitive to this treatment, but also that rHIgM22 is able to recognize the unknown antigen even after alkali treatment, suggesting that while the antigen is modified by the treatment, this is not altering the motif recognized by the antibody.

To attempt the identification of the antigen, after chromatographic separation of aqueous phases from mouse CNS myelin the area corresponding to the unidentified band was scraped and the antigen eluted from the silica gel. This purified sample was then analyzed through mass spectrometry. The results led to hypothesize that one of the molecules migrating in the area corresponding to the unknown antigen could be a PE with fatty acid containing 26 C atoms, two double bonds and 2 OH groups (MW 662) or containing 32 C atoms, two double bonds and 3 OH groups (MW 762). The hypothetical PE structure would be consistent with the chemical characterization, indicating the presence in the molecule of a free amino group and of phosphate. Moreover, the hypothesized presence of multiple hydroxylation in the fatty acid residues is consistent with the partitioning of the molecule with a preferential association with the aqueous phase. However, further analysis in different MS conditions (ionization conditions, temperature, etc.) need to be performed in order to confirm the identity of this molecule and of the other molecules that could be present.

Considering that all remyelination promoting antibodies with identified antigens are polyreactive and that several of these antibodies recognize not only protein antigens but also multiple sphingolipids [202, 294, 295, 297-299, 325], it is not possible to exclude

that rHIgM22 might be able to recognize a protein antigen. Taking this into account, western blotting analysis were performed using different samples, with the aim to verify if there was any rHIgM22 reactivity associated with proteins. While in MGC lysates and delipidized samples, the bands recognized by rHIgM22 were also recognized by the control IgM with comparable reactivity, in mice brain homogenates rHIgM22 was able to recognize two antigens, migrating between 37 and 50 kDa, not reactive to the control IgM. Taking these results together, it cannot be excluded that rHIgM22 might be able to recognize a protein antigen however further analysis need to be performed to confirm it.
Summarizing, the data so far collected demonstrate that rHIgM22 binds to sulfatide and, to a lesser extent, to lysosulfatide *in vitro*, which is in agreement with the observation that rHIgM22 is able to bind to myelin and to olidendrocytes, and that its binding is abolished in CNS tissue from CST(-/-) mice. Moreover, the binding affinity for both sulfatide and its deacylated derivate is low, even if the binding is specific. However, our data shows that the binding affinity of rHIgM22 for sulfatide can be modulated by the presence of other lipids suggesting a possible role of the membrane microenvironment in the recognition of the antigen by rHIgM22. In addition, rHIgM22 also reacts with phosphatidic acid, and with an unknown molecule present in lipid extracts from various sources, including CST knock-out mice brains, MGC, and isolated astrocytes and microglia. This suggests that not only sulfatide, but also other membrane lipids might play a role in the binding of rHIgM22 to oligodendrocytes and other cell types. Moreover, binding of rHIgM22 to intact cells might require a complex molecular arrangement, and, in particular, sulfatide might be part of the functional rHIgM22 antigen localized at the cell surface. Understanding whether rHIgM22 effect on remyelination involves a lipid-organized membrane complex, and the exact identity of the antigen involved and their organization in this complex is of great importance. The identification of the binding targets of this antibody, able to promote remyelination in validated mouse models of MS, and the characterization of their membrane microenvironment could significantly contribute to the reveal the signaling mechanisms underlying the biological activity of rHIgM22. This, in turn, would allow to obtain a better comprehension of the process of (re)myelination, and of the molecular mechanism involved in the pathophysiology of multiple sclerosis, thus allowing to define new potential therapeutic targets.

REFERENCES

1. Sherman, D.L. and P.J. Brophy, (2005), *Nature reviews. Neuroscience*. **6**(9), 683-90.
2. Aggarwal, S., L. Yurlova, and M. Simons, (2011), *Trends Cell Biol.* **21**(10), 585-93.
3. Susuki, K. and M.N. Rasband, (2008), *Curr. Opin. Cell Biol.* **20**(6), 616-23.
4. Trapp, B.D., J. Peterson, R.M. Ransohoff, R. Rudick, S. Mork, and L. Bo, (1998), *N. Engl. J. Med.* **338**(5), 278-85.
5. Chard, D.T., C.M. Griffin, G.J. Parker, R. Kapoor, A.J. Thompson, and D.H. Miller, (2002), *Brain*. **125**(Pt 2), 327-37.
6. Warrington, A.E., A.J. Bieber, B. Ciric, V. Van Keulen, L.R. Pease, Y. Mitsunaga, M.M. Paz Soldan, and M. Rodriguez, (2001), *J. Allergy Clin. Immunol.* **108**(4 Suppl), S121-5.
7. Pirko, I., B. Ciric, J. Gamez, A.J. Bieber, A.E. Warrington, A.J. Johnson, D.P. Hanson, L.R. Pease, S.I. Macura, and M. Rodriguez, (2004), *FASEB J.* **18**(13), 1577-9.
8. Warrington, A.E., K. Asakura, A.J. Bieber, B. Ciric, V. Van Keulen, S.V. Kaveri, R.A. Kyle, L.R. Pease, and M. Rodriguez, (2000), *Proc. Natl. Acad. Sci. U. S. A.* **97**(12), 6820-5.
9. Howe, C.L., A.J. Bieber, A.E. Warrington, L.R. Pease, and M. Rodriguez, (2004), *Neurobiol. Dis.* **15**(1), 120-31.
10. Wright, B.R., A.E. Warrington, D.D. Edberg, and M. Rodriguez, (2009), *Arch. Neurol.* **66**(12), 1456-9.
11. Lahiri, S. and A.H. Futerman, (2007), *Cell. Mol. Life Sci.* **64**(17), 2270-84.
12. Sonnino, S., S. Grassi, S. Prioni, M.G. Ciampa, E. Chiricozzi, and A. Prinetti, *Lipid Rafts and Neurological Diseases*, in *eLS*2001, John Wiley & Sons, Ltd.
13. Farooqui, A.A. and L.A. Horrocks, (1985), *Mol. Cell. Biochem.* **66**(1), 87-95.
14. Farooqui, A.A., L.A. Horrocks, and T. Farooqui, (2000), *Chem. Phys. Lipids*. **106**(1), 1-29.
15. Andresen, B.T., M.A. Rizzo, K. Shome, and G. Romero, (2002), *FEBS Lett.* **531**(1), 65-8.
16. Fang, Y., M. Vilella-Bach, R. Bachmann, A. Flanigan, and J. Chen, (2001), *Science*. **294**(5548), 1942-5.
17. Carrasco, S. and I. Merida, (2007), *Trends Biochem. Sci.* **32**(1), 27-36.
18. Antal, C.E. and A.C. Newton, (2013), *Molecular & cellular proteomics : MCP*. **12**(12), 3498-508.
19. Michailidis, I.E., Y. Zhang, and J. Yang, (2007), *Pflugers Arch.* **455**(1), 147-55.
20. Thudichum, J.L.W., *A Treatise on the Chemical Constitution of the Brain*1962: Archon Books.
21. Wennekes, T., R.J. van den Berg, R.G. Boot, G.A. van der Marel, H.S. Overkleeft, and J.M. Aerts, (2009), *Angew. Chem. Int. Ed. Engl.* **48**(47), 8848-69.
22. Feizi, T., (1985), *Nature*. **314**(6006), 53-7.
23. Merrill, A.H., Jr., M.D. Wang, M. Park, and M.C. Sullards, (2007), *Trends Biochem. Sci.* **32**(10), 457-68.

24. Kolesnick, R.N., (1991), *Prog. Lipid Res.* **30**(1), 1-38.
25. Menaldino, D.S., A. Bushnev, A. Sun, D.C. Liotta, H. Symolon, K. Desai, D.L. Dillehay, Q. Peng, E. Wang, J. Allegood, S. Trotman-Pruett, M.C. Sullards, and A.H. Merrill, Jr., (2003), *Pharmacol. Res.* **47**(5), 373-81.
26. Yu, R.K., Y.T. Tsai, T. Ariga, and M. Yanagisawa, (2011), *Journal of oleo science*. **60**(10), 537-44.
27. Ohmi, Y., Y. Ohkawa, Y. Yamauchi, O. Tajima, and K. Furukawa, (2012), *Neurochem. Res.* **37**(6), 1185-91.
28. Bosio, A., E. Binczek, and W. Stoffel, (1996), *Proc. Natl. Acad. Sci. U. S. A.* **93**(23), 13280-5.
29. Coetzee, T., N. Fujita, J. Dupree, R. Shi, A. Blight, K. Suzuki, and B. Popko, (1996), *Cell*. **86**(2), 209-19.
30. Eckhardt, M., (2008), *Mol. Neurobiol.* **37**(2-3), 93-103.
31. Gielen, E., W. Baron, M. Vandeven, P. Steels, D. Hoekstra, and M. Ameloot, (2006), *Glia*. **54**(6), 499-512.
32. Futerman, A.H. and H. Riezman, (2005), *Trends Cell Biol.* **15**(6), 312-8.
33. Futerman, A.H., (2006), *Biochim. Biophys. Acta*. **1758**(12), 1885-92.
34. Bosio, A., E. Binczek, and W. Stoffel, (1996), *Genomics*. **35**(1), 223-6.
35. Sprong, H., B. Kruithof, R. Leijendekker, J.W. Slot, G. van Meer, and P. van der Sluijs, (1998), *J. Biol. Chem.* **273**(40), 25880-8.
36. Grassi, S., S. Prioni, L. Cabitta, M. Aureli, S. Sonnino, and A. Prinetti, (2016), *Neurochem. Res.* **41**(1-2), 130-43.
37. Hayakawa, Y., D.I. Godfrey, and M.J. Smyth, (2004), *Curr. Med. Chem.* **11**(2), 241-52.
38. Hanada, K., K. Kumagai, S. Yasuda, Y. Miura, M. Kawano, M. Fukasawa, and M. Nishijima, (2003), *Nature*. **426**(6968), 803-9.
39. Futerman, A.H., B. Stieger, A.L. Hubbard, and R.E. Pagano, (1990), *J. Biol. Chem.* **265**(15), 8650-7.
40. Jeckel, D., A. Karrenbauer, R. Birk, R.R. Schmidt, and F. Wieland, (1990), *FEBS Lett.* **261**(1), 155-7.
41. Hanada, K., (2006), *Mol. Cell. Biochem.* **286**(1-2), 23-31.
42. Hanada, K., K. Kumagai, N. Tomishige, and T. Yamaji, (2009), *Biochim. Biophys. Acta*. **1791**(7), 684-91.
43. Jeckel, D., A. Karrenbauer, K.N. Burger, G. van Meer, and F. Wieland, (1992), *J. Cell Biol.* **117**(2), 259-67.
44. Buton, X., P. Herve, J. Kubelt, A. Tannert, K.N. Burger, P. Fellmann, P. Muller, A. Herrmann, M. Seigneuret, and P.F. Devaux, (2002), *Biochemistry (Mosc).* **41**(43), 13106-15.
45. Halter, D., S. Neumann, S.M. van Dijk, J. Wolthoorn, A.M. de Maziere, O.V. Vieira, P. Mattjus, J. Klumperman, G. van Meer, and H. Sprong, (2007), *J. Cell Biol.* **179**(1), 101-15.
46. Gault, C.R., L.M. Obeid, and Y.A. Hannun, (2010), *Adv. Exp. Med. Biol.* **688**, 1-23.

47. Kolter, T., R.L. Proia, and K. Sandhoff, (2002), *J. Biol. Chem.* **277**(29), 25859-62.
48. Hirabayashi, Y., (2012), *Proceedings of the Japan Academy. Series B, Physical and biological sciences*. **88**(4), 129-43.
49. Mullen, T.D., Y.A. Hannun, and L.M. Obeid, (2012), *Biochem. J.* **441**(3), 789-802.
50. Poduslo, S.E. and K. Miller, (1985), *Neurochem. Res.* **10**(9), 1285-97.
51. Hardy, R. and R. Reynolds, (1991), *Development*. **111**(4), 1061-80.
52. Yu, R.K., Y.T. Tsai, and T. Ariga, (2012), *Neurochem. Res.* **37**(6), 1230-44.
53. Yu, R.K., Y. Nakatani, and M. Yanagisawa, (2009), *J. Lipid Res.* **50 Suppl**, S440-5.
54. Stern, C.A., T.R. Braverman, and M. Tiemeyer, (2000), *Glycobiology*. **10**(4), 365-74.
55. Ramakrishnan, B. and P.K. Qasba, (2010), *Curr. Opin. Struct. Biol.* **20**(5), 536-42.
56. Li, Y. and X. Chen, (2012), *Appl. Microbiol. Biotechnol.* **94**(4), 887-905.
57. Merrill, A.H., Jr., (2011), *Chem. Rev.* **111**(10), 6387-422.
58. Roseman, S., (1970), *Chem. Phys. Lipids*. **5**(1), 270-97.
59. Singh, R.D., V. Puri, J.T. Valiyaveettil, D.L. Marks, R. Bittman, and R.E. Pagano, (2003), *Mol. Biol. Cell*. **14**(8), 3254-65.
60. Kolter, T. and K. Sandhoff, (2005), *Annu. Rev. Cell Dev. Biol.* **21**, 81-103.
61. Yamashita, T., R. Wada, T. Sasaki, C. Deng, U. Bierfreund, K. Sandhoff, and R.L. Proia, (1999), *Proc. Natl. Acad. Sci. U. S. A.* **96**(16), 9142-7.
62. Kumagai, T., T. Sato, S. Natsuka, Y. Kobayashi, D. Zhou, T. Shinkai, S. Hayakawa, and K. Furukawa, (2010), *Glycoconj. J.* **27**(7-9), 685-95.
63. Yamashita, T., Y.P. Wu, R. Sandhoff, N. Werth, H. Mizukami, J.M. Ellis, J.L. Dupree, R. Geyer, K. Sandhoff, and R.L. Proia, (2005), *Proc. Natl. Acad. Sci. U. S. A.* **102**(8), 2725-30.
64. Sonnino, S., L. Mauri, V. Chigorno, and A. Prinetti, (2007), *Glycobiology*. **17**(1), 1R-13R.
65. Cantu, L., E. Del Favero, S. Sonnino, and A. Prinetti, (2011), *Chem. Phys. Lipids*. **164**(8), 796-810.
66. Hakomori, S., (2003), *Curr. Opin. Hematol.* **10**(1), 16-24.
67. Hakomori, S. and K. Handa, (2003), *Methods Enzymol.* **363**, 191-207.
68. Lencer, W.I., T.R. Hirst, and R.K. Holmes, (1999), *Biochim. Biophys. Acta*. **1450**(3), 177-90.
69. Basu, I. and C. Mukhopadhyay, (2014), *Langmuir : the ACS journal of surfaces and colloids*. **30**(50), 15244-52.
70. Sandvig, K., J. Bergan, S. Kavaliauskiene, and T. Skotland, (2014), *Prog. Lipid Res.* **54**, 1-13.
71. Lingwood, C.A., (2011), *Cold Spring Harbor perspectives in biology*. **3**(7).
72. Varki, N.M. and A. Varki, (2007), *Lab. Invest.* **87**(9), 851-7.
73. Bhat, S., S.L. Spitalnik, F. Gonzalez-Scarano, and D.H. Silberberg, (1991), *Proc. Natl. Acad. Sci. U. S. A.* **88**(16), 7131-4.

74. Bhat, S., R.V. Mettus, E.P. Reddy, K.E. Ugen, V. Srikanthan, W.V. Williams, and D.B. Weiner, (1993), *AIDS Res. Hum. Retroviruses*. **9**(2), 175-81.
75. Lingwood, C.A. and D.R. Branch, (2011), *Discovery medicine*. **11**(59), 303-13.
76. Hammache, D., N. Yahi, M. Maresca, G. Pieroni, and J. Fantini, (1999), *J. Virol.* **73**(6), 5244-8.
77. Nakayama, H., F. Yoshizaki, A. Prinetti, S. Sonnino, L. Mauri, K. Takamori, H. Ogawa, and K. Iwabuchi, (2008), *J. Leukoc. Biol.* **83**(3), 728-41.
78. Iwabuchi, K., A. Prinetti, S. Sonnino, L. Mauri, T. Kobayashi, K. Ishii, N. Kaga, K. Murayama, H. Kurihara, H. Nakayama, F. Yoshizaki, K. Takamori, H. Ogawa, and I. Nagaoka, (2008), *Glycoconj. J.* **25**(4), 357-74.
79. Sonnino, S., A. Prinetti, H. Nakayama, M. Yangida, H. Ogawa, and K. Iwabuchi, (2009), *Glycoconj. J.* **26**(6), 615-21.
80. Bergelson, L.D., E.V. Dyatlovitskaya, T.E. Klyuchareva, E.V. Kryukova, A.F. Lemenovskaya, V.A. Matveeva, and E.V. Sinitsyna, (1989), *Eur. J. Immunol.* **19**(11), 1979-83.
81. Kabayama, K., T. Sato, F. Kitamura, S. Uemura, B.W. Kang, Y. Igarashi, and J. Inokuchi, (2005), *Glycobiology*. **15**(1), 21-9.
82. Kabayama, K., T. Sato, K. Saito, N. Loberto, A. Prinetti, S. Sonnino, M. Kinjo, Y. Igarashi, and J. Inokuchi, (2007), *Proc. Natl. Acad. Sci. U. S. A.* **104**(34), 13678-83.
83. Bremer, E.G., J. Schlessinger, and S. Hakomori, (1986), *J. Biol. Chem.* **261**(5), 2434-40.
84. Fernandes, H., S. Cohen, and S. Bishayee, (2001), *J. Biol. Chem.* **276**(7), 5375-83.
85. Miljan, E.A., E.J. Meuillet, B. Mania-Farnell, D. George, H. Yamamoto, H.G. Simon, and E.G. Bremer, (2002), *J. Biol. Chem.* **277**(12), 10108-13.
86. Wang, X.Q., P. Sun, and A.S. Paller, (2003), *J. Biol. Chem.* **278**(49), 48770-8.
87. Wang, X.Q., Q. Yan, P. Sun, J.W. Liu, L. Go, S.M. McDaniel, and A.S. Paller, (2007), *Cancer Res.* **67**(20), 9986-95.
88. Hakomori, S., (2002), *Proc. Natl. Acad. Sci. U. S. A.* **99**(16), 10231-3.
89. Ogretmen, B. and Y.A. Hannun, (2004), *Nature reviews. Cancer*. **4**(8), 604-16.
90. Vinson, M., P.J. Strijbos, A. Rowles, L. Facci, S.E. Moore, D.L. Simmons, and F.S. Walsh, (2001), *J. Biol. Chem.* **276**(23), 20280-5.
91. Vyas, A.A., H.V. Patel, S.E. Fromholt, M. Heffer-Lauc, K.A. Vyas, J. Dang, M. Schachner, and R.L. Schnaar, (2002), *Proc. Natl. Acad. Sci. U. S. A.* **99**(12), 8412-7.
92. Allen, N.J. and B.A. Barres, (2009), *Nature*. **457**(7230), 675-7.
93. Doetsch, F., (2003), *Nat. Neurosci.* **6**(11), 1127-34.
94. Barres, B.A., (2008), *Neuron*. **60**(3), 430-40.
95. Fields, R.D., D.H. Woo, and P.J. Basser, (2015), *Neuron*. **86**(2), 374-86.
96. Burda, J.E. and M.V. Sofroniew, (2014), *Neuron*. **81**(2), 229-48.
97. Nave, K.A., (2010), *Nature*. **468**(7321), 244-52.
98. Gallo, V. and B. Deneen, (2014), *Neuron*. **83**(2), 283-308.
99. Ffrench-Constant, C. and M.C. Raff, (1986), *Nature*. **323**(6086), 335-8.

100. Raff, M.C., R.H. Miller, and M. Noble, (1983), *Nature*. **303**(5916), 390-6.
101. Barateiro, A. and A. Fernandes, (2014), *Biochim. Biophys. Acta*. **1843**(9), 1917-29.
102. Pfeiffer, S.E., A.E. Warrington, and R. Bansal, (1993), *Trends Cell Biol.* **3**(6), 191-7.
103. Norton, W.T., (1981), *Adv. Neurol.* **31**, 93-121.
104. Chrast, R., G. Saher, K.A. Nave, and M.H. Verheijen, (2011), *J. Lipid Res.* **52**(3), 419-34.
105. O'Brien, J.S. and E.L. Sampson, (1965), *J. Lipid Res.* **6**(4), 537-44.
106. O'Brien, J.S., (1965), *Science*. **147**(3662), 1099-107.
107. Jackman, N., A. Ishii, and R. Bansal, (2009), *Physiology (Bethesda)*. **24**, 290-7.
108. Saher, G., S. Quintes, and K.A. Nave, (2011), *Neuroscientist*. **17**(1), 79-93.
109. Koper, J.W., M. Lopes-Cardozo, and L.M. Van Golde, (1981), *Biochim. Biophys. Acta*. **666**(3), 411-7.
110. Saher, G., B. Brugger, C. Lappe-Siefke, W. Mobius, R. Tozawa, M.C. Wehr, F. Wieland, S. Ishibashi, and K.A. Nave, (2005), *Nat. Neurosci.* **8**(4), 468-75.
111. Schmitt, S., L.C. Castelvetri, and M. Simons, (2015), *Biochim. Biophys. Acta*. **1851**(8), 999-1005.
112. Braverman, N.E. and A.B. Moser, (2012), *Biochim. Biophys. Acta*. **1822**(9), 1442-52.
113. Han, X.L. and R.W. Gross, (1990), *Biochemistry (Mosc)*. **29**(20), 4992-6.
114. Paltauf, F., (1994), *Chem. Phys. Lipids*. **74**(2), 101-39.
115. Broniec, A., R. Klosinski, A. Pawlak, M. Wrona-Krol, D. Thompson, and T. Sarna, (2011), *Free Radic. Biol. Med.* **50**(7), 892-8.
116. Wallner, S. and G. Schmitz, (2011), *Chem. Phys. Lipids*. **164**(6), 573-89.
117. Miljan, E.A. and E.G. Bremer, (2002), *Science's STKE : signal transduction knowledge environment*. **2002**(160), re15.
118. Van Brocklyn, J., E.G. Bremer, and A.J. Yates, (1993), *J. Neurochem.* **61**(1), 371-4.
119. Rusnati, M., E. Tanghetti, C. Urbinati, G. Tulipano, S. Marchesini, M. Ziche, and M. Presta, (1999), *Mol. Biol. Cell*. **10**(2), 313-27.
120. Bansal, R., (2002), *Dev. Neurosci.* **24**(1), 35-46.
121. Yim, S.H., R.G. Farrer, J.A. Hammer, E. Yavin, and R.H. Quarles, (1994), *J. Neurosci. Res.* **38**(3), 268-81.
122. Schnaar, R.L. and P.H. Lopez, (2009), *J. Neurosci. Res.* **87**(15), 3267-76.
123. Kawai, H., M.L. Allende, R. Wada, M. Kono, K. Sango, C. Deng, T. Miyakawa, J.N. Crawley, N. Werth, U. Bierfreund, K. Sandhoff, and R.L. Proia, (2001), *J. Biol. Chem.* **276**(10), 6885-8.
124. Takamiya, K., A. Yamamoto, K. Furukawa, S. Yamashiro, M. Shin, M. Okada, S. Fukumoto, M. Haraguchi, N. Takeda, K. Fujimura, M. Sakae, M. Kishikawa, H. Shiku, and S. Aizawa, (1996), *Proc. Natl. Acad. Sci. U. S. A.* **93**(20), 10662-7.
125. Stoffel, W. and A. Bosio, (1997), *Curr. Opin. Neurobiol.* **7**(5), 654-61.

126. Benjamins, J.A., T. Hadden, and R.P. Skoff, (1982), *J. Neurochem.* **38**(1), 233-41.
127. Schulte, S. and W. Stoffel, (1993), *Proc. Natl. Acad. Sci. U. S. A.* **90**(21), 10265-9.
128. Stahl, N., H. Jurevics, P. Morell, K. Suzuki, and B. Popko, (1994), *J. Neurosci. Res.* **38**(2), 234-42.
129. Meixner, M., J. Jungnickel, C. Grothe, V. Gieselmann, and M. Eckhardt, (2011), *BMC Neurosci.* **12**, 22.
130. Dupree, J.L., T. Coetzee, K. Suzuki, and B. Popko, (1998), *J. Neurocytol.* **27**(9), 649-59.
131. Bosio, A., E. Binczek, W.F. Haupt, and W. Stoffel, (1998), *J. Neurochem.* **70**(1), 308-15.
132. Dupree, J.L., K. Suzuki, and B. Popko, (1998), *Microsc. Res. Tech.* **41**(5), 431-40.
133. Marcus, J. and B. Popko, (2002), *Biochim. Biophys. Acta.* **1573**(3), 406-13.
134. Dupree, J.L. and B. Popko, (1999), *J. Neurocytol.* **28**(4-5), 271-9.
135. Honke, K., Y. Hirahara, J. Dupree, K. Suzuki, B. Popko, K. Fukushima, J. Fukushima, T. Nagasawa, N. Yoshida, Y. Wada, and N. Taniguchi, (2002), *Proc. Natl. Acad. Sci. U. S. A.* **99**(7), 4227-32.
136. Wang, C., M. Wang, Y. Zhou, J.L. Dupree, and X. Han, (2014), *Mol. Neurobiol.* **50**(1), 88-96.
137. Marcus, J., S. Honigbaum, S. Shroff, K. Honke, J. Rosenbluth, and J.L. Dupree, (2006), *Glia.* **53**(4), 372-81.
138. Honke, K., (2013), *Proceedings of the Japan Academy. Series B, Physical and biological sciences.* **89**(4), 129-38.
139. Ishibashi, T., J.L. Dupree, K. Ikenaka, Y. Hirahara, K. Honke, E. Peles, B. Popko, K. Suzuki, H. Nishino, and H. Baba, (2002), *J. Neurosci.* **22**(15), 6507-14.
140. Hoshi, T., A. Suzuki, S. Hayashi, K. Tohyama, A. Hayashi, Y. Yamaguchi, K. Takeuchi, and H. Baba, (2007), *Glia.* **55**(6), 584-94.
141. Schafer, D.P., R. Bansal, K.L. Hedstrom, S.E. Pfeiffer, and M.N. Rasband, (2004), *J. Neurosci.* **24**(13), 3176-85.
142. Hirahara, Y., R. Bansal, K. Honke, K. Ikenaka, and Y. Wada, (2004), *Glia.* **45**(3), 269-77.
143. Shroff, S.M., A.D. Pomicter, W.N. Chow, M.A. Fox, R.J. Colello, S.C. Henderson, and J.L. Dupree, (2009), *J. Neurosci. Res.* **87**(15), 3403-14.
144. Kajigaya, H., K.F. Tanaka, A. Hayashi, A. Suzuki, T. Ishibashi, K. Ikenaka, and H. Baba, (2011), *Proceedings of the Japan Academy. Series B, Physical and biological sciences.* **87**(7), 415-24.
145. Ozgen, H., W. Schrimpf, J. Hendrix, J.C. de Jonge, D.C. Lamb, D. Hoekstra, N. Kahya, and W. Baron, (2014), *PloS one.* **9**(7), e101834.
146. Debruin, L.S. and G. Harauz, (2007), *Neurochem. Res.* **32**(2), 213-28.
147. DeBruin, L.S., J.D. Haines, L.A. Wellhauser, G. Radeva, V. Schonmann, D. Bienzle, and G. Harauz, (2005), *J. Neurosci. Res.* **80**(2), 211-25.

148. Baron, W., H. Ozgen, B. Klunder, J.C. de Jonge, A. Nomden, A. Plat, E. Trifilieff, H. de Vries, and D. Hoekstra, (2015), *Mol. Cell. Biol.* **35**(1), 288-302.
149. Boggs, J.M., W. Gao, and Y. Hirahara, (2008), *J. Neurosci. Res.* **86**(7), 1448-58.
150. Boggs, J.M., W. Gao, and Y. Hirahara, (2008), *Biochim. Biophys. Acta*. **1780**(3), 445-55.
151. Boggs, J.M., W. Gao, J. Zhao, H.J. Park, Y. Liu, and A. Basu, (2010), *FEBS Lett.* **584**(9), 1771-8.
152. Boggs, J.M., (2014), *Advances in neurobiology*. **9**, 263-91.
153. Aureli, M., S. Grassi, S. Prioni, S. Sonnino, and A. Prinetti, (2015), *Biochim. Biophys. Acta*. **1851**(8), 1006-16.
154. Hamby, M.E. and M.V. Sofroniew, (2010), *Neurotherapeutics : the journal of the American Society for Experimental NeuroTherapeutics*. **7**(4), 494-506.
155. Sofroniew, M.V. and H.V. Vinters, (2010), *Acta Neuropathol.* **119**(1), 7-35.
156. Ullian, E.M., S.K. Sapperstein, K.S. Christopherson, and B.A. Barres, (2001), *Science*. **291**(5504), 657-61.
157. Kessaris, N., N. Pringle, and W.D. Richardson, (2008), *Philos. Trans. R. Soc. Lond. B. Biol. Sci.* **363**(1489), 71-85.
158. Butt, A.M., A. Duncan, and M. Berry, (1994), *J. Neurocytol.* **23**(8), 486-99.
159. Correale, J. and M.F. Farez, (2015), *Frontiers in neurology*. **6**, 180.
160. Nash, B., C.E. Thomson, C. Linington, A.T. Arthur, J.D. McClure, M.W. McBride, and S.C. Barnett, (2011), *J. Neurosci.* **31**(37), 13028-38.
161. Kaneko, J., M.O. Kinoshita, T. Machida, Y. Shinoda, Y. Nagatsuka, and Y. Hirabayashi, (2011), *J. Neurochem.* **116**(5), 840-4.
162. Nagatsuka, Y. and Y. Hirabayashi, (2008), *Biochim. Biophys. Acta*. **1780**(3), 405-9.
163. Murate, M., T. Hayakawa, K. Ishii, H. Inadome, P. Greimel, M. Watanabe, Y. Nagatsuka, K. Ito, Y. Ito, H. Takahashi, Y. Hirabayashi, and T. Kobayashi, (2010), *Biochemistry (Mosc).* **49**(23), 4732-9.
164. Nagatsuka, Y., Y. Horibata, Y. Yamazaki, M. Kinoshita, Y. Shinoda, T. Hashikawa, H. Koshino, T. Nakamura, and Y. Hirabayashi, (2006), *Biochemistry (Mosc).* **45**(29), 8742-50.
165. Kinoshita, M.O., S. Furuya, S. Ito, Y. Shinoda, Y. Yamazaki, P. Greimel, Y. Ito, T. Hashikawa, T. Machida, Y. Nagatsuka, and Y. Hirabayashi, (2009), *Biochem. J.* **419**(3), 565-75.
166. Kim, K.S., J.S. Kim, J.Y. Park, Y.H. Suh, I. Jou, E.H. Joe, and S.M. Park, (2013), *Hum. Mol. Genet.* **22**(23), 4805-17.
167. Wider, C. and Z.K. Wszolek, (2007), *Parkinsonism & related disorders*. **13 Suppl 3**, S229-32.
168. Lev, N., D. Ickowicz, Y. Barhum, N. Blondheim, E. Melamed, and D. Offen, (2006), *Antioxidants & redox signaling*. **8**(11-12), 1987-95.
169. Lev, N., D. Roncevic, D. Ickowicz, E. Melamed, and D. Offen, (2006), *J. Mol. Neurosci.* **29**(3), 215-25.
170. van Horssen, J., J.A. Drexhage, T. Flor, W. Gerritsen, P. van der Valk, and H.E. de Vries, (2010), *Free Radic. Biol. Med.* **49**(8), 1283-9.

171. Hwang, J., H.J. Lee, W.H. Lee, and K. Suk, (2010), *J. Neuroimmunol.* **226**(1-2), 66-72.
172. Tian, G., Q. Kong, L. Lai, A. Ray-Chaudhury, and C.L. Lin, (2010), *J. Neurochem.* **113**(4), 978-89.
173. Hibino, H. and Y. Kurachi, (2007), *Eur. J. Neurosci.* **26**(9), 2539-55.
174. Nimmerjahn, A., F. Kirchhoff, and F. Helmchen, (2005), *Science*. **308**(5726), 1314-8.
175. Soulet, D. and S. Rivest, (2008), *Curr. Biol.* **18**(12), R506-8.
176. Chan, W.Y., S. Kohsaka, and P. Rezaie, (2007), *Brain Res Rev*. **53**(2), 344-54.
177. Prewitt, C.M., I.R. Niesman, C.J. Kane, and J.D. Houle, (1997), *Exp. Neurol.* **148**(2), 433-43.
178. Butovsky, O., E. Hauben, and M. Schwartz, (2001), *FASEB J.* **15**(6), 1065-7.
179. Shaked, I., Z. Porat, R. Gersner, J. Kipnis, and M. Schwartz, (2004), *J. Neuroimmunol.* **146**(1-2), 84-93.
180. Perry, V.H., J.A. Nicoll, and C. Holmes, (2010), *Nature reviews. Neurology*. **6**(4), 193-201.
181. Muzio, L., G. Martino, and R. Furlan, (2007), *J. Neuroimmunol.* **191**(1-2), 39-44.
182. Block, M.L., L. Zecca, and J.S. Hong, (2007), *Nature reviews. Neuroscience*. **8**(1), 57-69.
183. Antonucci, F., E. Turola, L. Riganti, M. Caleo, M. Gabrielli, C. Perrotta, L. Novellino, E. Clementi, P. Giussani, P. Viani, M. Matteoli, and C. Verderio, (2012), *EMBO J.* **31**(5), 1231-40.
184. Indaram, M., W. Ma, L. Zhao, R.N. Fariss, I.R. Rodriguez, and W.T. Wong, (2015), *Scientific reports*. **5**, 9144.
185. Ebert, S., K. Weigelt, Y. Walczak, W. Drobnik, R. Mauerer, D.A. Hume, B.H. Weber, and T. Langmann, (2009), *J. Neurochem.* **110**(6), 1863-75.
186. Jeon, S.B., H.J. Yoon, S.H. Park, I.H. Kim, and E.J. Park, (2008), *J. Immunol.* **181**(11), 8077-87.
187. Park, J.Y., K.S. Kim, S.B. Lee, J.S. Ryu, K.C. Chung, Y.K. Choo, I. Jou, J. Kim, and S.M. Park, (2009), *J. Neurochem.* **110**(1), 400-11.
188. Niesman, I.R., N. Zemke, H.N. Fridolfsson, K.J. Haushalter, K. Levy, A. Grove, R. Schnoor, J.C. Finley, P.M. Patel, D.M. Roth, B.P. Head, and H.H. Patel, (2013), *Mol. Cell. Neurosci.* **56**, 283-97.
189. Frost, J.L. and D.P. Schafer, (2016), *Trends Cell Biol.* **26**(8), 587-97.
190. Yokoyama, A., L. Yang, S. Itoh, K. Mori, and J. Tanaka, (2004), *Glia*. **45**(1), 96-104.
191. Nave, K.A. and H.B. Werner, (2014), *Annu. Rev. Cell Dev. Biol.* **30**, 503-33.
192. Nave, K.A. and B.D. Trapp, (2008), *Annu. Rev. Neurosci.* **31**, 535-61.
193. Edgar, J.M. and J. Garbern, (2004), *J. Neurosci. Res*. **76**(5), 593-8.
194. Devaux, J.J. and S.S. Scherer, (2005), *J. Neurosci.* **25**(6), 1470-80.
195. Kassmann, C.M. and K.A. Nave, (2008), *Curr. Opin. Neurol.* **21**(3), 235-41.
196. Bruce, C.C., C. Zhao, and R.J. Franklin, (2010), *Horm. Behav.* **57**(1), 56-62.

197. Yeung, M.S., S. Zdunek, O. Bergmann, S. Bernard, M. Salehpour, K. Alkass, S. Perl, J. Tisdale, G. Possnert, L. Brundin, H. Druid, and J. Frisen, (2014), *Cell*. **159**(4), 766-74.
198. Crawford, A.H., J.H. Stockley, R.B. Tripathi, W.D. Richardson, and R.J. Franklin, (2014), *Exp. Neurol.* **260**, 50-5.
199. Levine, J.M., R. Reynolds, and J.W. Fawcett, (2001), *Trends Neurosci.* **24**(1), 39-47.
200. Domingues, H.S., C.C. Portugal, R. Socodato, and J.B. Relvas, (2016), *Frontiers in cell and developmental biology*. **4**, 71.
201. Dimou, L. and V. Gallo, (2015), *Glia*. **63**(8), 1429-51.
202. Franklin, R.J. and C. Ffrench-Constant, (2008), *Nature reviews. Neuroscience*. **9**(11), 839-55.
203. Alizadeh, A., S.M. Dyck, and S. Karimi-Abdolrezaee, (2015), *Frontiers in molecular neuroscience*. **8**, 35.
204. Pomeroy, I.M., E.K. Jordan, J.A. Frank, P.M. Matthews, and M.M. Esiri, (2010), *Mult. Scler.* **16**(5), 537-48.
205. Wegner, C., M.M. Esiri, S.A. Chance, J. Palace, and P.M. Matthews, (2006), *Neurology*. **67**(6), 960-7.
206. El Waly, B., M. Macchi, M. Cayre, and P. Durbec, (2014), *Frontiers in neuroscience*. **8**, 145.
207. Blakemore, W.F. and J.A. Murray, (1981), *J. Neurol. Sci.* **49**(2), 273-84.
208. Gledhill, R.F. and W.I. McDonald, (1977), *Ann. Neurol.* **1**(6), 552-60.
209. Powers, B.E., D.L. Sellers, E.A. Lovelett, W. Cheung, S.P. Aalami, N. Zapertov, D.O. Maris, and P.J. Horner, (2013), *Proc. Natl. Acad. Sci. U. S. A.* **110**(10), 4075-80.
210. Zawadzka, M., L.E. Rivers, S.P. Fancy, C. Zhao, R. Tripathi, F. Jamen, K. Young, A. Goncharevich, H. Pohl, M. Rizzi, D.H. Rowitch, N. Kessaris, U. Suter, W.D. Richardson, and R.J. Franklin, (2010), *Cell stem cell*. **6**(6), 578-90.
211. Franklin, R.J. and S.A. Goldman, (2015), *Cold Spring Harbor perspectives in biology*. **7**(7), a020594.
212. Kipp, M., P. van der Valk, and S. Amor, (2012), *CNS & neurological disorders drug targets*. **11**(5), 506-17.
213. Rivera, F.J., C. Steffenhagen, D. Kremer, M. Kandasamy, B. Sandner, S. Couillard-Despres, N. Weidner, P. Kury, and L. Aigner, (2010), *Stem cells and development*. **19**(5), 595-606.
214. Kremer, D., O. Aktas, H.P. Hartung, and P. Kury, (2011), *Ann. Neurol.* **69**(4), 602-18.
215. Redwine, J.M. and R.C. Armstrong, (1998), *J. Neurobiol.* **37**(3), 413-28.
216. Fancy, S.P., C. Zhao, and R.J. Franklin, (2004), *Mol. Cell. Neurosci.* **27**(3), 247-54.
217. Moyon, S., A.L. Dubessy, M.S. Aigrot, M. Trotter, J.K. Huang, L. Dauphinot, M.C. Potier, C. Kerninon, S. Melik Parsadaniantz, R.J. Franklin, and C. Lubetzki, (2015), *J. Neurosci.* **35**(1), 4-20.
218. Shen, S. and P. Casaccia-Bonnefil, (2008), *J. Mol. Neurosci.* **35**(1), 13-22.

219. Noble, M., K. Murray, P. Stroobant, M.D. Waterfield, and P. Riddle, (1988), *Nature*. **333**(6173), 560-2.
220. Raff, M.C., L.E. Lillien, W.D. Richardson, J.F. Burne, and M.D. Noble, (1988), *Nature*. **333**(6173), 562-5.
221. Bogler, O., D. Wren, S.C. Barnett, H. Land, and M. Noble, (1990), *Proc. Natl. Acad. Sci. U. S. A.* **87**(16), 6368-72.
222. Lalive, P.H., R. Paglinawan, G. Biollaz, E.A. Kappos, D.P. Leone, U. Malipiero, J.B. Relvas, M. Moransard, T. Suter, and A. Fontana, (2005), *Eur. J. Immunol.* **35**(3), 727-37.
223. Kotter, M.R., W.W. Li, C. Zhao, and R.J. Franklin, (2006), *J. Neurosci.* **26**(1), 328-32.
224. Lampron, A., A. Larochelle, N. Laflamme, P. Prefontaine, M.M. Plante, M.G. Sanchez, V.W. Yong, P.K. Stys, M.E. Tremblay, and S. Rivest, (2015), *J. Exp. Med.* **212**(4), 481-95.
225. Skripuletz, T., D. Hackstette, K. Bauer, V. Gudi, R. Pul, E. Voss, K. Berger, M. Kipp, W. Baumgartner, and M. Stangel, (2013), *Brain*. **136**(Pt 1), 147-67.
226. Armstrong, R.C., T.Q. Le, E.E. Frost, R.C. Borke, and A.C. Vana, (2002), *J. Neurosci.* **22**(19), 8574-85.
227. Mason, J.L., S. Xuan, I. Dragatsis, A. Efstratiadis, and J.E. Goldman, (2003), *J. Neurosci.* **23**(20), 7710-8.
228. Xin, M., T. Yue, Z. Ma, F.F. Wu, A. Gow, and Q.R. Lu, (2005), *J. Neurosci.* **25**(6), 1354-65.
229. Stidworthy, M.F., S. Genoud, W.W. Li, D.P. Leone, N. Mantei, U. Suter, and R.J. Franklin, (2004), *Brain*. **127**(Pt 9), 1928-41.
230. Shields, S.A., J.M. Gilson, W.F. Blakemore, and R.J. Franklin, (1999), *Glia*. **28**(1), 77-83.
231. Li, W.W., J. Penderis, C. Zhao, M. Schumacher, and R.J. Franklin, (2006), *Exp. Neurol.* **202**(1), 250-4.
232. Bieber, A.J., D.R. Ure, and M. Rodriguez, (2005), *J. Neuropathol. Exp. Neurol.* **64**(1), 46-57.
233. Kuhlmann, T., V. Miron, Q. Cui, C. Wegner, J. Antel, and W. Bruck, (2008), *Brain*. **131**(Pt 7), 1749-58.
234. Boespflug-Tanguy, O., P. Labauge, A. Fogli, and C. Vaurs-Barriere, (2008), *Current neurology and neuroscience reports*. **8**(3), 217-29.
235. Popescu, B.F. and C.F. Lucchinetti, (2012), *Annual review of pathology*. **7**, 185-217.
236. Weinshenker, B.G., (1998), *Semin. Neurol.* **18**(3), 301-7.
237. Pugliatti, M., S. Sotgiu, and G. Rosati, (2002), *Clin. Neurol. Neurosurg.* **104**(3), 182-91.
238. Munzel, E.J. and A. Williams, (2013), *Drugs*. **73**(18), 2017-29.
239. Munzel, E.J., J.Z. Wimperis, and A. Williams, (2013), *BMJ case reports*. **2013**.
240. Cua, D.J., J. Sherlock, Y. Chen, C.A. Murphy, B. Joyce, B. Seymour, L. Lucian, W. To, S. Kwan, T. Churakova, S. Zurawski, M. Wiekowski, S.A. Lira, D. Gorman, R.A. Kastelein, and J.D. Sedgwick, (2003), *Nature*. **421**(6924), 744-8.

241. Tzartos, J.S., M.A. Friese, M.J. Craner, J. Palace, J. Newcombe, M.M. Esiri, and L. Fugger, (2008), *Am. J. Pathol.* **172**(1), 146-55.
242. Frei, K., C. Siepl, P. Groscurth, S. Bodmer, C. Schwerdel, and A. Fontana, (1987), *Eur. J. Immunol.* **17**(9), 1271-8.
243. Pang, Y., L. Campbell, B. Zheng, L. Fan, Z. Cai, and P. Rhodes, (2010), *Neuroscience*. **166**(2), 464-75.
244. Nakahara, J., M. Maeda, S. Aiso, and N. Suzuki, (2012), *Clin. Rev. Allergy Immunol.* **42**(1), 26-34.
245. Alter, M., Z. Zhen-xin, Z. Davanipour, E. Sobel, S. Min Lai, and L. LaRue, (1987), *Ital. J. Neurol. Sci.* **Suppl 6**, 11-6.
246. Rodriguez, M., (2007), *Brain Pathol.* **17**(2), 219-29.
247. Sriram, S. and I. Steiner, (2005), *Ann. Neurol.* **58**(6), 939-45.
248. Lucchinetti, C., W. Bruck, J. Parisi, B. Scheithauer, M. Rodriguez, and H. Lassmann, (2000), *Ann. Neurol.* **47**(6), 707-17.
249. Barnett, M.H. and J.W. Prineas, (2004), *Ann. Neurol.* **55**(4), 458-68.
250. Henderson, A.P., M.H. Barnett, J.D. Parratt, and J.W. Prineas, (2009), *Ann. Neurol.* **66**(6), 739-53.
251. Kantarci, O.H., I. Pirko, and M. Rodriguez, (2014), *Clin. Pharmacol. Ther.* **95**(1), 32-44.
252. Goldschmidt, T., J. Antel, F.B. Konig, W. Bruck, and T. Kuhlmann, (2009), *Neurology*. **72**(22), 1914-21.
253. Patrikios, P., C. Stadelmann, A. Kutzelnigg, H. Rauschka, M. Schmidbauer, H. Laursen, P.S. Sorensen, W. Bruck, C. Lucchinetti, and H. Lassmann, (2006), *Brain*. **129**(Pt 12), 3165-72.
254. Patani, R., M. Balaratnam, A. Vora, and R. Reynolds, (2007), *Neuropathol. Appl. Neurobiol.* **33**(3), 277-87.
255. Bramow, S., J.M. Frischer, H. Lassmann, N. Koch-Henriksen, C.F. Lucchinetti, P.S. Sorensen, and H. Laursen, (2010), *Brain*. **133**(10), 2983-98.
256. Fawcett, J.W. and R.A. Asher, (1999), *Brain Res. Bull.* **49**(6), 377-91.
257. Silver, J. and J.H. Miller, (2004), *Nature reviews. Neuroscience*. **5**(2), 146-56.
258. Nair, A., T.J. Frederick, and S.D. Miller, (2008), *Cell. Mol. Life Sci.* **65**(17), 2702-20.
259. Clemente, D., M.C. Ortega, C. Melero-Jerez, and F. de Castro, (2013), *Frontiers in cellular neuroscience*. **7**, 268.
260. Zamvil, S.S. and L. Steinman, (1990), *Annu. Rev. Immunol.* **8**, 579-621.
261. Steinman, L., (1993), *Proc. Natl. Acad. Sci. U. S. A.* **90**(17), 7912-4.
262. Steinman, L., J.W. Lindsey, S. Alters, and S. Hodgkinson, (1993), *Immunol. Ser.* **59**, 253-60.
263. Steinman, L., (1995), *Nature*. **375**(6534), 739-40.
264. Kerlero de Rosbo, N., R. Milo, M.B. Lees, D. Burger, C.C. Bernard, and A. Ben-Nun, (1993), *J. Clin. Invest.* **92**(6), 2602-8.
265. Jaskiewicz, E., (2004), *Postepy Hig Med Dosw (Online)*. **58**, 472-82.
266. Meinl, E. and R. Hohlfeld, (2002), *Clin. Exp. Immunol.* **128**(3), 395-7.
267. Sela, B.A., G. Konat, and H. Offner, (1982), *J. Neurol. Sci.* **54**(1), 143-8.

268. Lubetzki, C., Y. Thuillier, A. Galli, O. Lyon-Caen, F. Lhermitte, and B. Zalc, (1989), *Ann. Neurol.* **26**(3), 407-9.
269. Bansal, A.S., B. Abdul-Karim, R.A. Malik, P. Goulding, R.S. Pumphrey, A.J. Boulton, P.L. Holt, and P.B. Wilson, (1994), *J. Clin. Pathol.* **47**(4), 300-2.
270. Endo, T., D.D. Scott, S.S. Stewart, S.K. Kundu, and D.M. Marcus, (1984), *Adv. Exp. Med. Biol.* **174**, 455-61.
271. Ilyas, A.A., Z.W. Chen, and S.D. Cook, (2003), *J. Neuroimmunol.* **139**(1-2), 76-80.
272. Marconi, S., L. De Toni, L. Lovato, E. Tedeschi, L. Gaetti, M. Acler, and B. Bonetti, (2005), *J. Neuroimmunol.* **170**(1-2), 115-21.
273. Kanter, J.L., S. Narayana, P.P. Ho, I. Catz, K.G. Warren, R.A. Sobel, L. Steinman, and W.H. Robinson, (2006), *Nat. Med.* **12**(1), 138-43.
274. Quintana, F.J., M.F. Farez, V. Viglietta, A.H. Iglesias, Y. Merbl, G. Izquierdo, M. Lucas, A.S. Basso, S.J. Khoury, C.F. Lucchinetti, I.R. Cohen, and H.L. Weiner, (2008), *Proc. Natl. Acad. Sci. U. S. A.* **105**(48), 18889-94.
275. Moyano, A.L., K. Pituch, G. Li, R. van Breemen, J.E. Mansson, and M.I. Givogri, (2013), *J. Neurochem.* **127**(5), 600-4.
276. Haghighi, S., A. Lekman, S. Nilsson, M. Blomqvist, and O. Andersen, (2012), *Acta Neurol. Scand.* **125**(1), 64-70.
277. Haghighi, S., A. Lekman, S. Nilsson, M. Blomqvist, and O. Andersen, (2013), *J. Neurol. Sci.* **326**(1-2), 35-9.
278. Rodriguez, M., A.E. Warrington, and L.R. Pease, (2009), *Neurology.* **72**(14), 1269-76.
279. Kremer, D., P. Gottle, H.P. Hartung, and P. Kury, (2016), *Trends Neurosci.* **39**(4), 246-63.
280. Chang, A., S.M. Staugaitis, R. Dutta, C.E. Batt, K.E. Easley, A.M. Chomyk, V.W. Yong, R.J. Fox, G.J. Kidd, and B.D. Trapp, (2012), *Ann. Neurol.* **72**(6), 918-26.
281. Ingwersen, J., O. Aktas, P. Kuery, B. Kieseier, A. Boyko, and H.P. Hartung, (2012), *Clin. Immunol.* **142**(1), 15-24.
282. Healy, L.M., M.A. Michell-Robinson, and J.P. Antel, (2015), *Seminars in immunopathology.* **37**(6), 639-49.
283. Choi, J.W., S.E. Gardell, D.R. Herr, R. Rivera, C.W. Lee, K. Noguchi, S.T. Teo, Y.C. Yung, M. Lu, G. Kennedy, and J. Chun, (2011), *Proc. Natl. Acad. Sci. U. S. A.* **108**(2), 751-6.
284. Miron, V.E., C.G. Jung, H.J. Kim, T.E. Kennedy, B. Soliven, and J.P. Antel, (2008), *Ann. Neurol.* **63**(1), 61-71.
285. Miron, V.E., S.K. Ludwin, P.J. Darlington, A.A. Jarjour, B. Soliven, T.E. Kennedy, and J.P. Antel, (2010), *Am. J. Pathol.* **176**(6), 2682-94.
286. Duncan, I.D., A.J. Aguayo, R.P. Bunge, and P.M. Wood, (1981), *J. Neurol. Sci.* **49**(2), 241-52.
287. Blakemore, W.F. and A.J. Crang, (1985), *J. Neurol. Sci.* **70**(2), 207-23.
288. Jadasz, J.J., L. Aigner, F.J. Rivera, and P. Kury, (2012), *Cell Tissue Res.* **349**(1), 331-47.

289. Ben-Hur, T. and S.A. Goldman, (2008), *Ann. N. Y. Acad. Sci.* **1142**, 218-49.
290. Wang, Z., H. Colognato, and C. Ffrench-Constant, (2007), *Glia*. **55**(5), 537-45.
291. Franklin, R.J., (2002), *Nature reviews. Neuroscience*. **3**(9), 705-14.
292. Franklin, R.J., (2002), *Brain Res. Bull.* **57**(6), 827-32.
293. Mi, S., R.B. Pepinsky, and D. Cadavid, (2013), *CNS Drugs*. **27**(7), 493-503.
294. Fredman, P., J.L. Magnani, M. Nirenberg, and V. Ginsburg, (1984), *Arch. Biochem. Biophys.* **233**(2), 661-6.
295. Dubois, C., J.C. Manuguerra, B. Hauttecoeur, and J. Maze, (1990), *J. Biol. Chem.* **265**(5), 2797-803.
296. Bansal, R., A.E. Warrington, A.L. Gard, B. Ranscht, and S.E. Pfeiffer, (1989), *J. Neurosci. Res.* **24**(4), 548-57.
297. Bansal, R., K. Stefansson, and S.E. Pfeiffer, (1992), *J. Neurochem.* **58**(6), 2221-9.
298. Burger, D., G. Perruisseau, M. Simon, and A.J. Steck, (1992), *J. Neurochem.* **58**(3), 854-61.
299. Burger, D., M. Simon, G. Perruisseau, and A.J. Steck, (1990), *J. Neurochem.* **54**(5), 1569-75.
300. Paz Soldan, M.M., A.E. Warrington, A.J. Bieber, B. Ciric, V. Van Keulen, L.R. Pease, and M. Rodriguez, (2003), *Mol. Cell. Neurosci.* **22**(1), 14-24.
301. Dimopoulos, M.A., E. Kastritis, and I.M. Ghobrial, (2016), *Ann. Oncol.* **27**(2), 233-40.
302. Warrington, A.E., A.J. Bieber, B. Ciric, L.R. Pease, V. Van Keulen, and M. Rodriguez, (2007), *J. Neurosci. Res.* **85**(5), 967-76.
303. Mitsunaga, Y., B. Ciric, V. Van Keulen, A.E. Warrington, M. Paz Soldan, A.J. Bieber, M. Rodriguez, and L.R. Pease, (2002), *FASEB J.* **16**(10), 1325-7.
304. Watzlawik, J., E. Holicky, D.D. Edberg, D.L. Marks, A.E. Warrington, B.R. Wright, R.E. Pagano, and M. Rodriguez, (2010), *Glia*. **58**(15), 1782-93.
305. Watzlawik, J.O., A.E. Warrington, and M. Rodriguez, (2013), *PloS one*. **8**(2), e55149.
306. Watzlawik, J.O., B. Wootla, M.M. Painter, A.E. Warrington, and M. Rodriguez, (2013), *Expert review of neurotherapeutics*. **13**(9), 1017-29.
307. Scandroglio, F., J.K. Venkata, N. Loberto, S. Prioni, E.H. Schuchman, V. Chigorno, A. Prinetti, and S. Sonnino, (2008), *J. Neurochem.* **107**(2), 329-38.
308. McCarthy, K.D. and J. de Vellis, (1980), *J. Cell Biol.* **85**(3), 890-902.
309. Norton, W.T. and S.E. Poduslo, (1973), *J. Neurochem.* **21**(4), 749-57.
310. Scandroglio, F., N. Loberto, M. Valsecchi, V. Chigorno, A. Prinetti, and S. Sonnino, (2009), *Glycoconj. J.* **26**(8), 961-73.
311. Ishizuka, I., (1997), *Prog. Lipid Res.* **36**(4), 245-319.
312. Iwabuchi, K., H. Masuda, N. Kaga, H. Nakayama, R. Matsumoto, C. Iwahara, F. Yoshizaki, Y. Tamaki, T. Kobayashi, T. Hayakawa, K. Ishii, M. Yanagida, H. Ogawa, and K. Takamori, (2015), *Glycobiology*. **25**(6), 655-68.
313. Emery, B., (2010), *Science*. **330**(6005), 779-82.
314. Taylor, C.M., C.B. Marta, R.J. Claycomb, D.K. Han, M.N. Rasband, T. Coetzee, and S.E. Pfeiffer, (2004), *Proc. Natl. Acad. Sci. U. S. A.* **101**(13), 4643-8.

315. Blomqvist, M., V. Gieselmann, and J.E. Mansson, (2011), *Lipids in health and disease*. **10**, 28.
316. Rosengren, B., P. Fredman, J.E. Mansson, and L. Svennerholm, (1989), *J. Neurochem.* **52**(4), 1035-41.
317. Toda, K., T. Kobayashi, I. Goto, K. Ohno, Y. Eto, K. Inui, and S. Okada, (1990), *J. Neurochem.* **55**(5), 1585-91.
318. O'Brien, J.S. and E.L. Sampson, (1965), *Science*. **150**(3703), 1613-4.
319. Nair, S., A.R. Branagan, J. Liu, C.S. Boddupalli, P.K. Mistry, and M.V. Dhodapkar, (2016), *N. Engl. J. Med.* **374**(6), 555-61.
320. Guy, A.T., Y. Nagatsuka, N. Ooashi, M. Inoue, A. Nakata, P. Greimel, A. Inoue, T. Nabetani, A. Murayama, K. Ohta, Y. Ito, J. Aoki, Y. Hirabayashi, and H. Kamiguchi, (2015), *Science*. **349**(6251), 974-7.
321. Bjorkqvist, Y.J., S. Nybond, T.K. Nyholm, J.P. Slotte, and B. Ramstedt, (2008), *Biochim. Biophys. Acta*. **1778**(4), 954-62.
322. Stewart, R.J. and J.M. Boggs, (1990), *Biochemistry (Mosc)*. **29**(15), 3644-53.
323. Vaskovsky, V.E. and E.Y. Kostetsky, (1968), *J. Lipid Res.* **9**(3), 396.
324. Eisenbarth, G.S., F.S. Walsh, and M. Nirenberg, (1979), *Proc. Natl. Acad. Sci. U. S. A.* **76**(10), 4913-7.
325. Bansal, R. and S.E. Pfeiffer, (1989), *Proc. Natl. Acad. Sci. U. S. A.* **86**(16), 6181-5.
326. Schachner, M., (1982), *J. Neurochem.* **39**(1), 1-8.
327. Singh, H. and S.E. Pfeiffer, (1985), *J. Neurochem.* **45**(5), 1371-81.
328. Noseworthy, J.H., C. Lucchinetti, M. Rodriguez, and B.G. Weinshenker, (2000), *N. Engl. J. Med.* **343**(13), 938-52.
329. Lassmann, H., W. Bruck, and C.F. Lucchinetti, (2007), *Brain Pathol.* **17**(2), 210-8.
330. Maggio, B., (1997), *Neurochem. Res.* **22**(4), 475-81.
331. Maggio, B., J.M. Sturtevant, and R.K. Yu, (1987), *J. Biol. Chem.* **262**(6), 2652-9.
332. Viani, P., G. Cervato, P. Gatti, and B. Cestaro, (1992), *Biochim. Biophys. Acta*. **1106**(1), 77-84.
333. Wu, X. and Q.T. Li, (1999), *Biochim. Biophys. Acta*. **1416**(1-2), 285-94.
334. Wu, X., K.H. Lee, and Q.T. Li, (1996), *Biochim. Biophys. Acta*. **1284**(1), 13-9.
335. Wu, X. and Q.T. Li, (1999), *J. Lipid Res.* **40**(7), 1254-62.
336. Rintoul, D.A. and R. Welti, (1989), *Biochemistry (Mosc)*. **28**(1), 26-31.